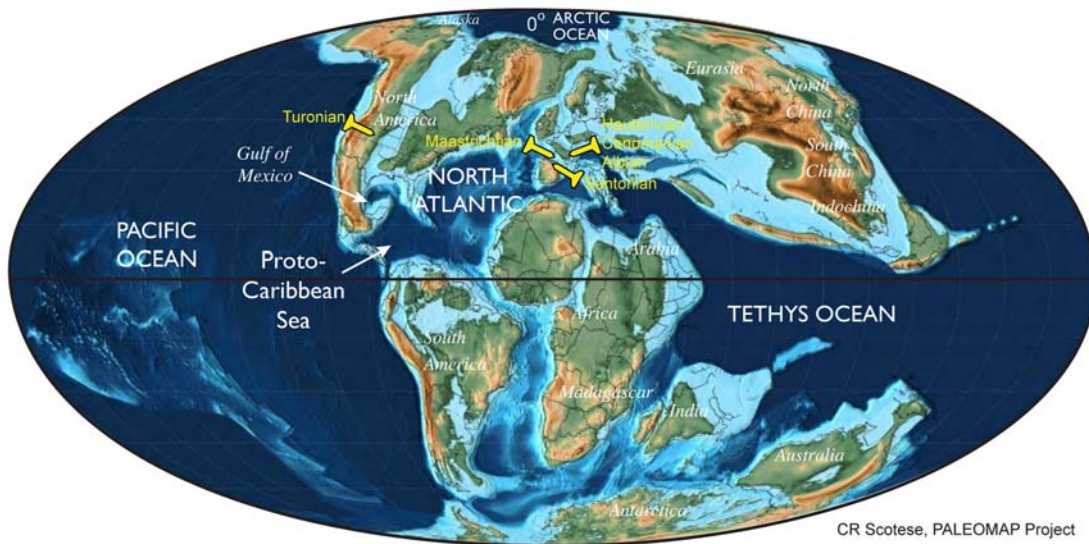


The Cretaceous Period

96.6 Ma Cretaceous



Chapter outline

27.1 History and subdivisions	1023	27.2.3 Physical stratigraphy	1051
27.1.1 Subdivisions of the Lower Cretaceous	1024	27.3 Cretaceous time scale	1058
27.1.2 Subdivisions of the Upper Cretaceous	1034	27.3.1 Previous scales	1059
27.2 Cretaceous stratigraphy	1043	27.3.2 Cretaceous numerical age model of GTS2020	1061
27.2.1 Marine biostratigraphy	1043	Bibliography	1068
27.2.2 Terrestrial biostratigraphy	1051		

Abstract

The breakup of the former Pangea supercontinent culminated in the modern drifting continents. Increased rifting caused the establishment of the Atlantic Ocean in the middle Jurassic and significant widening in Cretaceous. An explosion of calcareous nannoplankton and foraminifers in the warm seas created massive chalk deposits. A surge in submarine volcanic activity enhanced supergreenhouse conditions in the middle Cretaceous with high CO₂ concentrations. Angiosperm plants bloomed on the dinosaur-dominated land during late Cretaceous. The Cretaceous dramatically ended with an asteroid impact, which resulted in a mass extinction.

27.1 History and subdivisions

The stratigraphic unit of the “Terrain Crétacé” was established by d’Omalius d’Halloy (1822) to encompass the Chalk (*creta* in Latin) that characterizes a major unit of strata in the Paris Basin and across much of northern Europe. Smith (1815) had already mapped four stratigraphic units between the “lower clay” (Eocene) and the “Portland Stone” (Jurassic). These units were grouped by Conybeare and Phillips (1822) into two main divisions—a higher Chalk and the dominantly clastic formations beneath. This twofold division, adopted in England and France at an early

stage, has persisted as the two Cretaceous series and epochs, Lower and Upper. Attempts to introduce a Middle Cretaceous in the 1980s were unsuccessful.

D'Orbigny (1840) divided the Cretaceous fossil assemblages of France into five divisions, which were termed “étages” (stages): Neocomian, Aptian, Albian, Turonian and Senonian. Later D'Orbigny (1849–1850) added “Urgonian” between the Neocomian and Aptian and “Cenomanian” stage between the Albian and Turonian. The term “Neocomian” had been coined by [Thurmann \(1836\)](#) for strata in the vicinity of Neuchâtel, Switzerland. This Neocomian interval has subsequently been subdivided into three stages—the Berriasian, Valanginian and Hauterivian—following the recommendation of [Barbier and Thieuloy \(1965\)](#), and the term Neocomian abandoned. In this definition the “Urgonian” stage has been replaced by a “Barremian” and an expanded Aptian stage. The “Senonian,” named by [d'Orbigny \(1842\)](#) after the town of Sens in the Départments of Yonne and Seine et Marne is also no longer used, being replaced by four stages, the Coniacian, Santonian, Campanian and Maastrichtian.

The uppermost units of the chalk of Denmark, which had traditionally been included in the Cretaceous, are now classified as a Danian Stage of the lowermost Paleogene (Cenozoic). The termination of the Cretaceous is now defined by a major mass extinction and impact-generated iridium anomaly horizon at the base of the Danian Stage.

The boundaries of the 12 historical Cretaceous stages were primarily defined by ammonites in France ([Birkelund et al., 1984](#); [Kennedy, 1984](#)). Refined recognition or proposed definitions of the basal boundaries of these stages have encompassed other globally identifiable criteria, including geomagnetic reversals, carbon-isotope excursions, and microfossil levels ([Fig. 27.1](#); and also [Fig. 27.12](#) later in this chapter).

Historical usage, coupled with the expertise of members of the various boundary working groups, has dictated a preferential selection of boundary stratotypes [Global Boundary Stratotype Section and Points (GSSPs)] for most stages and substages to be within Western European basins. A major problem in Cretaceous chronostratigraphy was, and still is, the correlation of regional biostratigraphic events and associated stage boundary definitions to other paleogeographic and paleoceanographic areas. At the time of completion of this chapter (October 2019) only 6 of the 12 Cretaceous stages had ratified GSSPs (Hauterivian, Albian, Cenomanian, Turonian, Santonian, and Maastrichtian).

27.1.1 Subdivisions of the Lower Cretaceous

The subdivisions of the Berriasian through Aptian stages of the Lower Cretaceous are based on exposures in southeast France and adjacent northwest Switzerland. The Vocontian

Basin preserves a nearly continuous record, either as clay and limestone–marl successions (basin center) or carbonate dominated deposits (basin margin). The marine fauna and microflora thriving in the warm ocean of the northern Tethyan Realm only rarely extended into the Boreal Realm of Northwest Europe, Greenland, Siberia, and other northern regions. The northern higher latitudes were characterized by taxonomically different organisms, causing a distinctive faunal and floral provincialism throughout most of the Early Cretaceous. The segregation, which culminated in the latest Jurassic to earliest Cretaceous, was exacerbated by a global sea-level low stand and resulted in the application of different stage names for the Jurassic/Cretaceous boundary interval in the two realms. The ongoing discussion on the positioning of the Jurassic/Cretaceous boundary at global scale is related to this strong provincialism. A subsequent transgression in the Valanginian allowed a limited exchange of marine biota via marine gateways during certain short-lived periods, but the Tethyan and Boreal Realms persisted through the Cretaceous.

Traditionally, the primary markers that were considered for defining stage and substage boundaries of the Berriasian through Aptian were lowest or highest occurrences of ammonite species. In an effort to achieve global correlation, these macrofossil datums have been replaced or enhanced by magnetostratigraphic, geochemical, or microfossil events. For example, the base of the Albian stage is now taken at the first occurrence of a planktonic foraminifer and the proposed base of the Aptian Stage will probably be a magnetic reversal. The base of the Berriasian Stage (base of the Cretaceous) is a microfossil level. [Fig. 27.2](#) shows a probable correlation between western Tethys and the Boreal realm, using this information.

27.1.1.1 The Jurassic/Cretaceous boundary and the Berriasian Stage

The Cretaceous is the only Phanerozoic system that does not yet have an accepted global boundary definition, despite over a dozen international conferences and working group meetings dedicated to the issue since the 1970s (e.g., reviews by [Zakharov et al., 1996](#); [Cope, 2007](#); [Wimbledon, 2017](#)). Difficulties in assigning a global Jurassic/Cretaceous boundary are the product of historical usage, the lack of any major faunal change between the latest Jurassic and earliest Cretaceous, a pronounced provincialism of marine fauna and flora and a concentration of previous studies on often endemic ammonites ([Fig. 27.2](#)). Another problem is the occurrence of widespread hiatuses or condensations in many European and Russian epicontinental successions caused by the long-term “Purbeckian regression.”

The Tithonian Stage of the latest Jurassic was defined by [Oppel \(1865\)](#) to include all deposits in the Mediterranean area that lie between a restricted Kimmeridgian and

“Valanginian,” but no representative section or upper limit were designated. Coquand (1871) coined the “Berriasian” for a limestone succession near the village of Berrias (Ardèche, southeast France) (reviewed in Rawson, 1983). This unit was originally conceived as a subdivision of the Valanginian, subsequently often referred to as “Infra-Valanginian.” It was only during a colloquium in Lyon during 1963 that the Berriasian was formally established as a stage below the Valanginian. This Berriasian Stage overlapped to some degree with the original concept of the Tithonian Stage. The historical lower boundary of the Berriasian Stage lacks any significant faunal change, indeed the basal part of the Berrias stratotype lacks any diagnostic ammonites (Cope, 2007). The *Colloque sur la limite Jurassique-Crétacé* (1975) voted to define the base of the Berriasian at the base of the *Berriasella jacobi* ammonite subzone. This was a shift downward from the 1963 vote to use the base of the *Pseudosubplanites grandis* ammonite subzone (reviewed in Wimbledon et al., 2011).

Some workers raised the Jurassic/Cretaceous boundary to the beginning of the current Valanginian Stage (e.g., Zakharov et al., 1996). An alternative suggestion assigns the lower part of the historical Berriasian Stage to the Jurassic, and defines the Jurassic/Cretaceous boundary at the base of the “middle Berriasian” *Subthurmannia occitana* ammonite zone (Remane, 1991). This proposal takes intervals with reworked sediments below that zone into account (Hoedemaeker et al., 2003). Using the *S. occitana* zone has the advantage in that it can be correlated to the southern part of the Boreal Realm where it approximately coincides with the base of the *Runctonia runctoni* ammonite zone.

The current Berriasian Working Group of the International Commission on Cretaceous Stratigraphy has worked to integrate regional ammonite zonations, calpionellid zones, calcareous nannofossil datums, paly-nomorphs, and magnetostratigraphy (e.g., Schnabl et al., 2015; Wimbledon, 2017; summarized in Fig. 27.2). Their emphasis is on identifying a GSSP level near markers of both regional and global significance.

The absence of the ammonite species *B. jacobi* (= *Strambergella jacobi*) in the lower part of the nominal *B. jacobi* Subzone rules this taxon out as a GSSP marker (Frau et al., 2016; Wimbledon, 2017). It further appears that there are no ammonite-zone boundaries that are synchronous among the main European regions within the basal Cretaceous transition interval.

The lowest occurrence of the small, globular calpionellid species *Calpionella alpina*, which marks the base of the *C. alpina* Subzone, has been documented as a useful event for dating deep-shelf to pelagic limestone sequences. This event, which falls into the middle of magnetozones M19n.2n, has been recorded from southern Europe, Arabia, Iran, and Argentina. The base of the *C. alpina* Subzone has therefore been proposed as

the primary Tithonian–Berriasian boundary marker (Wimbledon, 2017).

Calcareous nannofossils underwent a rapid diversification in the interval under discussion. The lowest occurrences of several species bracket the base of the *C. alpina* Subzone. *Hexalithus strictus* (= *H. geometricus*) predates and *Nannoconus steinmannii minor* postdates the base of the *C. alpina* Subzone. Other nannofossils taxa can be used as secondary markers (Casellato, 2010).

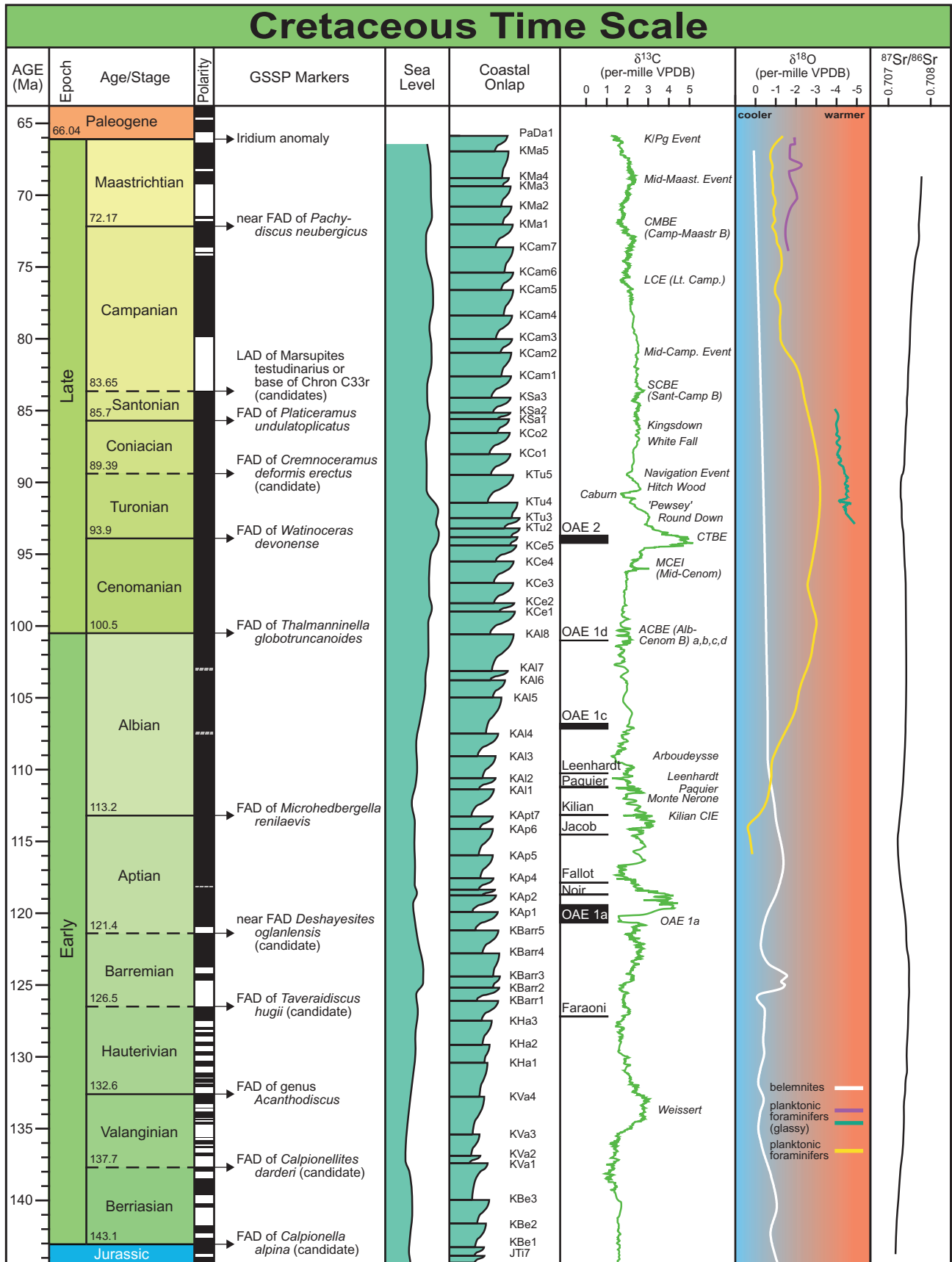
Magnetostratigraphy has proven to be a reliable method for placing biostratigraphic events into a common framework (e.g., Channell et al., 2010). In the GTS2012, the base of Chron M18r was used as a temporary assignment for the Jurassic/Cretaceous boundary. However, this datum, even though it can be recognized in both marine and terrestrial deposits in tropical to boreal settings, does not coincide with any consistent biotic marker, and the same is true of the base of M19n.2n. The Berriasian Working Group therefore voted to adopt the turnover in calpionellids from *Crassicollaria* to *Calpionella* as the primary marker for the base of the Berriasian Stage. This datum coincides with the base of the *C. alpina* Subzone, which falls in the middle of Chron M19n.2n and may correspond to the base of the *Arctoteuthis tehamaensis* belemnite zone of Siberia. U–Pb radioisotopic dates zircons in volcanic ash beds from Argentina and Mexico suggested an age of 140.2 ± 0.1 Ma for the base of the Berriasian (Lena et al., 2019). However, this does not fit with regional magnetostratigraphy and with the duration of the Berriasian Stage as indicated by cyclostratigraphy (see later).

In October 2019, following a decade of international collaboration, the Berriasian Working Group of ICS submitted a proposal to define the GSSP for the Berriasian Stage and the Cretaceous System at Bed 14 in the lower section at Tré Maroua (Le Saix, Hautes-Alpes), which is about 30 km southeast of Gap in southern France (Wimbledon et al., 2019, 2020). The GSSP level would coincide with the appearance of small, orbicular *C. alpina* calpionellids (base of the *Calpionella* Zone). This section yielded macrofossils (mainly ammonites) and abundant, well-preserved microfossils in the context of magnetozones M20n–M17n. As of April 2020, this formal proposal was still under consideration by the ICS and IUGS.

27.1.1.1 Portlandian–Purbeckian and Volgian–Ryazanian

d’Orbigny (1849–1850) introduced the Portlandian and Purbeckian stages for the Portland Limestone and the nonmarine Purbeck facies of England and northern France. This usage has been largely discontinued, as both facies types are of only regional relevance (Cope, 2007).

The marked provinciality found across the Jurassic/Cretaceous boundary interval lead to the establishment of



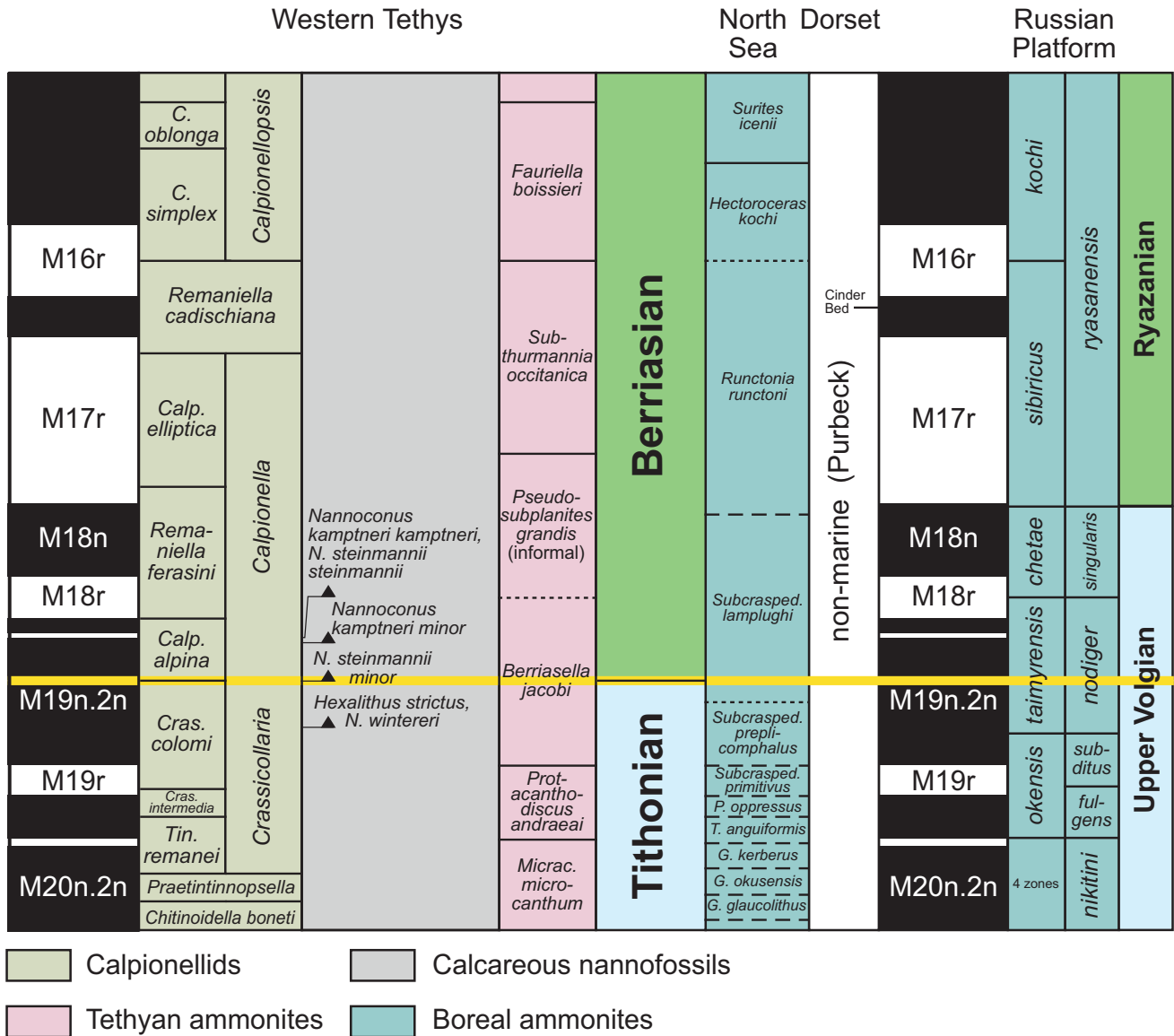


FIGURE 27.2 Possible correlation of the Jurassic–Cretaceous boundary from Western Tethys into the Boreal Realm. Relative placement of selected index fossils for defining the Jurassic–Cretaceous boundary among different paleogeographic regions of the Western Tethys, the Sub-Boreal (North Sea, Dorset), the Boreal (Nordvik, Russian Platform). Yellow line is the proposed GSSP (Global Boundary Stratotype Section and Point). Modified from Wimbledon (2017) and Wimbledon et al. (2019).

FIGURE 27.1 Cretaceous overview. Main markers or candidate markers for GSSPs of Cretaceous stages are currently a combination of calpionellids (Berriasian, Valanginian), ammonites (Hauterivian, Barremian, Aptian, Turonian, Maastrichtian), polarity chron (alternate candidates for Aptian and Campanian), planktonic foraminifers (Albian, Cenomanian), inoceramus bivalve (Coniacian, Santonian), and microcrinoids (Campanian); details are in text and Fig. 27.12. (“Age” is the term for the time equivalent of the rock-record “Stage.”) Magnetic polarity column is the C- and M-sequence pattern as scaled in GTS2020 (Ogg, 2020, Ch. 5: Geomagnetic polarity time scale, this book). Schematic sea-level, coastal onlap curves, and sequence nomenclature are modified from Haq (2014). See also review in Simmons et al. (2020, Ch. 13: Phanerozoic eustasy, this book). The $\delta^{13}\text{C}$ curve with major named-excursions (and widespread anoxic events) from Cramer and Jarvis (2020, Ch. 11: Carbon isotope stratigraphy, this book) had compiled numerous studies, including Sprovieri et al. (2006, 2013), Herrle et al. (2004, 2015), Gale et al. (2011), Thibault et al. (2012, 2016), and Jarvis et al. (2006). The oxygen isotope curve and implied sea-surface temperature trends is the statistical mean curve from a synthesis of numerous belemnite and planktonic foraminifera studies (see Grossman and Joachimski, 2020, Ch. 10: Oxygen isotope stratigraphy, this book), although some temperature trends derived from other proxies have more detailed excursions. Strontium isotope curve is modified from McArthur et al. (2020, Ch. 7: Strontium isotope stratigraphy, this book). The vertical scale of this diagram is standardized to match the vertical scales of the period-overview figure in all other Phanerozoic chapters. GSSP, Global Boundary Stratotype Section and Point; VPDB, Vienna PeeDee Belemnite $\delta^{13}\text{C}$ standard; VSMOW, Vienna Standard Mean Ocean Water $\delta^{18}\text{O}$ standard.

two biogeographic units, the Tethyan and the Boreal Realms. This has resulted in the application of different stage names for the two realms. The Tithonian and Berriasian stages of the Tethys correspond approximately with the Volgian and Ryazanian stages of the Boreal Realm. The ongoing discussion on the positioning of the Jurassic/Cretaceous boundary at global scale is a result of this strong provincialism. The Volgian Stage was defined by Nikitin (1881) and later extended downward to approximately coincide with the base of the Tithonian (see Cope, 2007). On the Russian Platform and in Siberia, the Volgian is followed by a Ryazanian regional stage (Sazonov, 1951); subsequently the use of a “Volgian–Ryazanian” interval has been applied to the North Sea and high northern latitude regions. At Nordvik (North Siberia), magnetozone M19n.2n is situated in the *Taimyroceras taimyrensis* ammonite zone, which corresponds to the Late Volgian *Craspedites nodiger* ammonite zone of the Volgian type area on the Russian Platform (Schnabl et al., 2015; Wierzbowski et al., 2017). Accordingly, the Tithonian/Berriasian boundary in North Siberia is positioned in the middle part of the *T. taimyrensis* Zone, in the upper Volgian (Dzyuba et al., 2013). The top of the regional Ryazanian is probably close to the base of the Valanginian Stage, as revised by Hoedemaeker et al. (2003).

The Berriasian Working Group of the Cretaceous Subcommittee recommends the lowest occurrence of *C. alpina* in a section at Tré Maroua in the Vocontian Basin, southeast France, as the GSSP for the base of the stage, and the base of the Cretaceous (Wimbledon et al., 2019, 2020).

The base of the Berriasian is taken at 143.1 Ma, by extrapolation from the probable cyclostratigraphic duration of the stage and spline-fitting (Section 27.3.2).

27.1.1.1.2 Berriasian substages

No formal substages or boundary stratotypes have yet been recommended for the Berriasian Stage. The four ammonite zones of the Berriasian of the Mediterranean area have been used as informal substages (e.g., Reboulet and Atrops, 1999).

The base of the Middle Berriasian *S. occitanica* ammonite zone correlates to the middle portion of polarity-Chron M17r. This level falls near the base of the *Chetaites sibiricus* ammonite zone of North Siberia (Dzyuba et al., 2013).

The base of the Upper Berriasian Substage is currently placed at the base of the *Subthurmannia boissieri* ammonite zone. This event approximates the base of Zone D of the calpionellid zonation and lies in the middle of magnetic polarity zone M16r (M16r.5). It falls amidst the *Heteroceras kochi* ammonite zone of the Russian Platform and North Siberia (Dzyuba et al., 2013).

27.1.1.2 Valanginian

27.1.1.2.1 History, definition, and boundary stratotype

The original type section of the Valanginian stage is the Seyon Gorge near Valangin (Neuchâtel, Switzerland). Desor (1854) included all post–Jurassic strata up to the base of the “Marnes d’ Hauterive” in this definition. The “Marnes à *Astieria*,” which were either attributed to the uppermost Valanginian or to the lowermost Hauterivian, were finally included in the Upper Valanginian by Baumberger (1901; reviewed in Rawson, 1983). Because the shallow-water carbonates of the Seyon Gorge are poor in ammonites, two “hypostratotypes” at Angles (Alpes-de-Haute-Provence) and Barret-le-Bas (Hautes-Alpes) in southeast France have been proposed as reference sections (Busnardo et al., 1979). The base of the Valanginian was placed at the lowest occurrence of the ammonite *Thurmanniceras otopeta* (Busnardo et al., 1979; Birkelund et al., 1984).

Taxonomic and correlation problems with the ammonites led the Valanginian Working Group (Hoedemaeker et al., 2003) to move the base of the Valanginian stage upward to the base of Calpionellid Zone E, defined by the lowest occurrence of *Calpionellites darderi* (Bulot et al., 1996; Aguado et al., 2000). The *C. darderi* level can be traced from France to Mexico (López-Martínez et al., 2017). This transfers the *T. otopeta* ammonite zone into the Berriasian stage. The potential GSSP section near Caravaca in southern Spain has integrated ammonoid, nannofossil, and magnetostratigraphy, but poor preservation of calpionellids (Aguado et al., 2000).

Cyclostratigraphic studies based in the Vocontian Basin suggest a 5.1 Ma duration of the Valanginian (Table 27.2), with anchoring points for the base of the Valanginian near the base of Chron M14r (Martinez et al., 2013). The previous estimate that the top of the Valanginian was near the base of Chron M10n (e.g., Weissert et al., 1998) as used in GTS2012 is not consistent with this astronomical-tuned duration, therefore is no longer used as a constraint. Corresponding absolute ages are 137 ± 1 Ma for the base of the Valanginian and 131.3 ± 0.25 Ma for the base of the Hauterivian, based on U–Pb ages (Aguirre-Urreta et al., 2015, 2017, 2019).

Correlation of the base of Valanginian from the Tethys into the Boreal Realm is problematic, both areas are characterized by a distinctive faunal and floral provincialism. In the Tethys the interval of the *Tirnovella pertransiens* Zone is marked by the presence of the ammonite genus *Platylenticeras*, which is quite common in northern Europe. The base of the *T. pertransiens* Zone is therefore correlated with the lowest occurrence of the genus *Platylenticeras* in northern Europe (England, Germany; Mutterlose et al., 2014). $^{87}\text{Sr}/^{86}\text{Sr}$ values of 0.707300–0.707355 are typical for the Lower Valanginian of both realms.

The base of the Valanginian is taken at 137.7 Ma based on cyclostratigraphical tuning of the duration of the stage anchored to the base of the Barremian (Martinez et al., 2015).

27.1.1.2.2 Upper Valanginian substage

In the Tethys the base of the Upper Valanginian is traditionally placed at the base of the distinctive *Saynoceras verrucosum* ammonite zone. Rare specimens of *S. verrucosum* have also been recognized in the West European Province of the Boreal Realm, allowing for correlation. In the Boreal Realm *S. verrucosum* first appears in the upper part of the *Prodichotomites hollwedensis* Zone. This observation and the record of earliest specimens of boreal *Prodichotomites* from the top of the Lower Valanginian in southeast France (Thieuloy, 1977; Kemper et al., 1981) support a placement of the base of the upper Valanginian in northern Europe in the middle of the *P. hollwedensis* ammonite zone.

The Weissert isotope excursion started and peaked in the *S. verrucosum* Zone (135–134 Ma; Martinez et al., 2013, 2015). $^{87}\text{Sr}/^{86}\text{Sr}$ values increase from 0.707355 to 0.707379 near the Valanginian/Hauterivian boundary.

Potential boundary stratotypes in southeast France (section at Vergol) and in the Betic Cordillera of Spain are being considered (Bulot et al., 1996; Subcommittee on Cretaceous Stratigraphy, 2009).

27.1.1.3 Hauterivian

27.1.1.3.1 History, definition, and boundary stratotype

The original definition of the Hauterivian Stage in the area of Hauterive (Neuchâtel, Switzerland) by Renevier (1874) includes from bottom to top three lithological units: the “Marnes à *Astieria*” (later transferred to the Valanginian), the “Marnes d’ Hauterive à *Ammonites Radiates*,” and the “Pierre Jaune de Neuchâtel” (see Rawson, 1983). In the Tethys the base of the Hauterivian is recognized by the lowest occurrence of the ammonite species *Acanthodiscus radiatus* (Reboulet, 1996; Mutterlose et al., 1996). This event coincides with the lowest occurrence of the ammonite genus *Acanthodiscus*, which accordingly marks the base of the Hauterivian. In the La Charce GSSP section (southeast France, Fig. 27.3), the presence of *Acanthodiscus* in bed number 189 marks the base of the Hauterivian Stage (Mutterlose et al., in press).

In the Boreal Realm the early Hauterivian shows major influxes of ammonite faunas from the Tethys, events which can be used for correlation. These indicate that the traditional definition of the base of the Hauterivian in the Boreal Realm by the lowest occurrence of *Endemoceras*

amblygonium is nearly coeval with the suggested GSSP level in the Tethyan Realm (Mutterlose et al., 1996). The lowermost part of the boreal *E. amblygonium* Zone corresponds to the uppermost part of the *Criosarasinella furcillata* ammonite zone of the La Charce section. The characterization of the base of the Hauterivian by ammonites is extremely difficult outside Europe and North Africa. In Argentina the base of the *Holcoptychites neuquensis* ammonite zone is correlated with the base of the *A. radiatus* Zone, based on rare ammonite taxa occurring both in Europe and Argentina (Aguirre-Urreta et al., 2005). Magnetostratigraphy had suggested that the base of the Hauterivian was near the top of Chron M10Nn (e.g., Weissert et al., 1998; Sprovieri et al., 2006), but those studies were not directly calibrated to the bases of ammonite zones. The cycle-scaled duration of the Hauterivian was calculated at 5.9 ± 0.4 Ma (Martinez et al., 2015), attributing the base of the Hauterivian an absolute age of 132 ± 1 Ma and the top an age of 126 ± 1 Ma (Table 27.2). Published $^{87}\text{Sr}/^{86}\text{Sr}$ data (McArthur et al., 2007; Meissner et al., 2015) suggest Sr-values of >0.707380 for the lowermost Hauterivian for the Tethys and the Boreal Realm.

The base of the Hauterivian is taken at 132.6 Ma based on cyclostratigraphic projection down from the base of the Berriasian (Martinez et al., 2015) and spline fitting. For details see Section 27.3.2.

27.1.1.3.2 Upper Hauterivian substage

The base of the Upper Hauterivian substage in the Tethyan Realm is defined by the highest occurrence of Neocomitinae ammonites and the lowest occurrence of the ammonite species *Subsaynella sayni*. None of these events can be recognized in the Boreal Realm, where the base of the Upper Hauterivian is approximated by the lowest occurrence of the ammonite *Simbirskites*. A correlation tie-point is provided by the Tethyan ammonite *Crioceratites duvali*. Its presence in both realms correlates the base of the Upper Hauterivian of the Tethyan Realm to the upper part of the Boreal *Simbirskites inversum* ammonite zone of the Boreal Realm. The highest occurrence of the calcareous nannofossil species *Cruciellipsis cuvillieri* may serve as an alternative marker for the base of the Upper Hauterivian (Mutterlose et al., 1996). It has been reported from the middle part of the *S. sayni* ammonite zone (Bergen, 1994) and is near the base of magnetic polarity zone M8r in Italy (Channell et al., 1995a). In the Boreal Realm this datum equates the middle part of the *Simbirskites staffi* ammonite zone (Möller et al., 2015).

The La Charce section has also been proposed as a candidate for the Lower/Upper Hauterivian substage boundary section.

Base of the Hauterivian Stage of the Cretaceous System, La Charce Section, Drôme, France

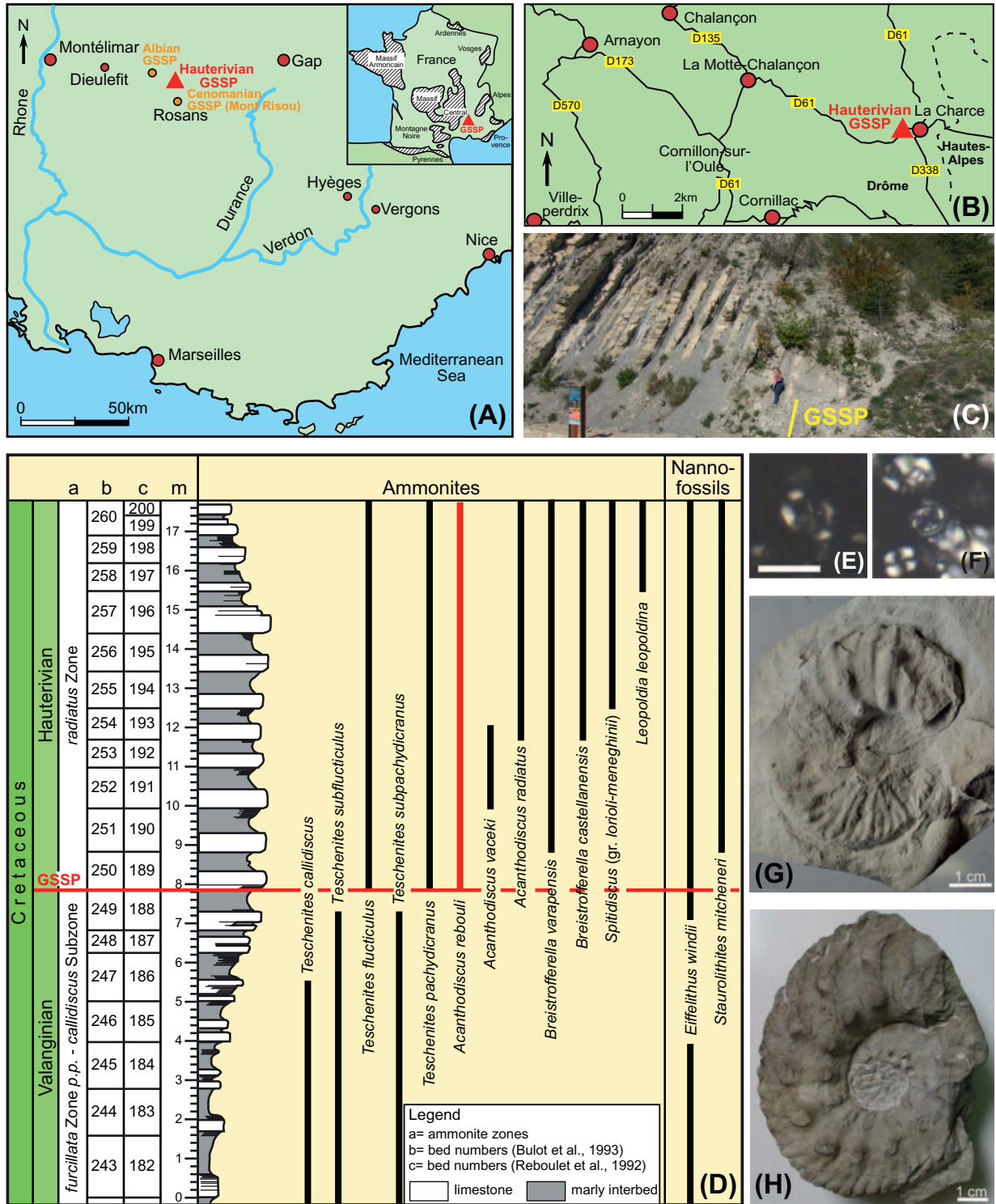


FIGURE 27.3 GSSP for the Hauterivian Stage, in the commune of La Charce, Drôme, southern France. (A and B) Location maps. (C) Photograph of outcrop, with GSSP marked at the base of Bed 189 (photograph by Andy Gale). (D) Stratigraphy and distribution of key ammonites and nannofossils. (E) *Eifelithus windii*, (F) *Stauroolithes mitcheneri*, (G and H) *Acanthodiscus radiatus*. Genus *Acanthodiscus* is the GSSP marker for the base of the Hauterivian. GSSP, Global Boundary Stratotype Section and Point.

27.1.1.4 Barremian

27.1.1.4.1 History, definition, and boundary stratotype

The original concept for the Barremian stage is based on marine strata cropping out in the area near Barrême (Alpes-de-Haute-Provence, southeast France). Without giving a specific type locality, [Coquand \(1861\)](#) quoted various belemnites and ammonites for the Barremian, which also encompass parts of the current Upper Hauterivian substage. A more precise definition of the Barremian Stage goes back to [Kilian \(1888\)](#), which has later been redefined by [Busnardo \(1965\)](#) who used the roadside exposures of Angles in south-east France as the type locality.

In the Tethys the base of the Barremian is marked by the lowest occurrence of the ammonite species *Taveraiidiscus hugii* ([Reboulet and Atrops, 1999](#)). A candidate for the global boundary stratotype is at Río Argos near Caravaca, Spain ([Company et al., 1995](#); [Rawson et al., 1996a](#)). Correlation to the Boreal Realm by dinoflagellate cysts indicates that the base of the Barremian Stage approximates the base of the *Hoplocrioceras rarocinctum* ammonite zone ([Leereveld, 1995](#); [Rawson et al., 1996a](#)). This correlation is supported by belemnite based $^{87}\text{Sr}/^{86}\text{Sr}$ -isotope data, which show values of ~ 0.707475 for the lowermost Barremian of both realms ([Mutterlose et al., 2014](#)).

In Italy the boundary interval falls in the uppermost part of magnetic polarity zone M4n (at approximately Chron M4n.8 = “M5n.8”; [Channell et al., 1995a](#)). Absolute ages for the base of the Barremian of 126 ± 1 Ma and of 121.2 ± 0.5 Ma for the base of the Aptian ([Table 27.2](#)) are based on U–Pb zircons ([Aguirre-Urreta et al., 2015](#)) resp. $\text{Ar}^{40}/\text{Ar}^{39}$ sanidines ([He et al., 2008](#)). [Bodin et al. \(2006\)](#) calculated a duration of 4.5 Ma for the Barremian, based on phosphorous burial rates.

The base of the Barremian is taken at 126.5 Ma, based on intercalibration of radioisotopic dates from Argentina and cyclostratigraphy ([Martinez et al., 2015](#)). For details see [Section 27.3.2](#).

27.1.1.4.2 Upper Barremian substage

In the Tethys region the boundary between the Lower and Upper Barremian is placed at the lowest occurrence of the ammonite *Toxancyloceras vandenheckei* ([Rawson et al., 1996a](#); [Reboulet and Atrops, 1999](#)). The proposed substage GSSP is near Caravaca, Spain ([Company et al., 1995](#)). This substage boundary level is within the uppermost part of magnetic polarity zone M3r (at approximately Chron M3r.8) in Italy ([Channell et al., 1995a](#)). $^{87}\text{Sr}/^{86}\text{Sr}$ -isotope data suggest that in the Boreal Realm the base of the Upper Barremian lies in the upper third of the *Paracrioceras elegans* ammonite zone.

27.1.1.5 Aptian

27.1.1.5.1 History, definition, and boundary stratotype

The Aptian Stage was a vague designation by [d’Orbigny \(1840\)](#) for strata containing “Upper Neocomian” fauna and named after the village of Apt (Vaucluse province, southeast France). The extent and nomenclature of the Aptian and underlying stages have undergone major revisions (reviewed by [Moullade et al., 2011](#)). The French sections are poor in ammonites; therefore the classical marker for the base of the Aptian was the lowest occurrence of the deshayesitid ammonite *Prodeshayesites* in northwest Europe ([Rawson, 1983](#); [Moullade et al., 1998a,b](#); [Hoedemaeker et al., 2003](#)). However, the local lowest occurrence of this ammonite genus is commonly associated with a major transgression in earliest Aptian and virtually no ammonite-bearing section exists which represents a continuous and complete Barremian–Aptian boundary interval ([Erba et al., 1996](#)). Therefore the proposed primary marker for base of the Aptian Stage is the beginning of magnetic polarity-Chron M0r. A quite different boundary concept was proposed by [Moullade et al. \(2011\)](#), who on historical grounds recommended converting the lower three ammonite zone of the current Aptian into a Bedoulian Stage, and beginning the Aptian at the base of *Dufrenoyia furcata* zone (marked by lowest occurrence of *Dufrenoyia* ammonite genus) with a GSSP near Roquefort-La-Bédoule in southeastern France. [Reboulet et al. \(2011\)](#) reject the usage of Bedoulian (see [Section 27.1.1.5.2](#)). The GTS2020 scale retains the current Aptian/Barremian usage with its working boundary definition as the base of Chron M0r.

The proposed global boundary stratotype in pelagic limestone at Gorgo a Cerbara in central Italy has an integrated stratigraphy of paleomagnetism, biostratigraphy (calcareous nannofossils, planktonic foraminifers, radiolarians, dinoflagellates) carbon-isotope chemostratigraphy, and cycle stratigraphy ([Erba et al., 1996, 1999](#); [Channell et al., 2000](#); [Jenkyns, 2017](#)). However, recently [Frau et al. \(2018\)](#) have reidentified ammonites found beneath, within, and above magnetochron M0r as belonging to the *Martelites sarasini* Zone, traditionally placed within the Barremian, rather than Aptian *Prodeshayesites* as previously recorded.

An important event about 1 Myr after the boundary is Oceanic Anoxic Event 1a (OAE1a), marked by widespread organic-rich shale (e.g., Selli Level in Italy, Goguel level in southeast France, Fischschiefer in northwestern Germany) and the initial, sharp, negative excursion at the base of a longer positive carbon-13 isotopic excursion ([Weissert and Lini, 1991](#); [Mutterlose and Böckel, 1998](#); [Li et al., 2008](#); [Jenkyns 2017](#)).

The Aptian Working Group of the Cretaceous Subcommittee is likely to recommend taking the maximum

negative value of the basal excursion of OAE1a in the Gorgo a Cerbara section in central Italy as GSSP for base of the Aptian Stage (STRATI meeting, Milan, July 2019). However, for our study, the base of the Aptian is taken at 121.4 Ma, at the base of Chron M0, on the basis of dates from Svalbard (Zhang et al. 2019). A modified version of the proposed calibrations and durations of latest Barremian through earliest Aptian Tethyan and Boreal ammonite zones relative to Chron M0r and carbon-isotope excursions (Frau et al., 2018; Lubert et al., 2019; Martinez et al., 2020; C. Frau, pers. commun., June 2020) is used the GTS2020 summary diagrams of that interval. For details see Section 27.3.2.

27.1.1.5.2 Substages of Aptian

Two substages are recommended for subdividing the Aptian Stage. The Lower Aptian has traditionally been subdivided using the ammonite lineage *Deshayesites*–*Dufrenoyia*, but there is currently considerable disagreement as to the application of species names to *Deshayesites*, such that the zonation provided here is provisional (Reboulet and Atrops, 1999; Bersac and Bert, 2012). The Lower/Upper substage boundary is taken at the base of the *Epicheloniceras martinoides* ammonite zone in the standard Tethyan zonation which is approximately equivalent to the base of the *Tropaeum bowerbanki* ammonite zone of the Boreal zonations (Reboulet et al., 2011). At this level, there is an important change in ammonite fauna in both the Tethyan and Sub-Boreal realms.

This level coincides with a traditional boundary between a lower “Bedoulian” and an upper “Gargasian” stage, which were based on sections at Cassis-La Bédoule (Bouches du Rhône province; near Marseilles) and at Gargas (near Apt) in southern France, although historical usage of “Bedoulian” was only for the lower portion of this Lower Aptian (Moullade et al., 2011). A comprehensive synthesis has been compiled for the integrated stratigraphy of the type Bedoulian (Moullade et al., 1998a,b; Ropolo et al., 1998) and type Gargasian (Moullade et al., 2004, 2005; and later articles in *Notebooks on Geology*). The lowest occurrence of planktonic foraminifer *Praehedbergella luterbacheri* is just above the substage boundary followed by the lowest *Globigerinoides ferreolensis* (Moullade et al., 2005), and the lowest calcareous nannofossil *Eprolithus floralis* (base of Zone NC7) slightly precedes the boundary (Moullade et al., 1998b).

In France, an additional uppermost substage of “Clansayesian” was added when Breistroffer (1947) moved the thin “Clansayes” horizon from Albian into the underlying Aptian. However, this substage was not considered useful because (1) the reference sections at Gargas (near Apt) and Clansayes are not suitable for correlation purposes (Rawson, 1983); (2) the rationale for a separate “Clansayesian” substage is questioned (e.g., Owen, 1996a; Casey et al., 1998); and (3) the newly

defined Albian GSSP boundary probably includes part of the Clansayesian interval (Kennedy et al., 2017).

The IUGS Lower Cretaceous Ammonite Working Group or “Kilian Group” voted to “abandon the terms Bedoulian, Gargasian and Clansayesian as they are not recognized internationally, but mainly used in France . . . Moreover, the type sections of these French substages do not offer good prospects (low number and/or bad preservation of ammonoids) . . .” (reported in Reboulet et al., 2011; see also Reboulet and Atrops, 1999).

27.1.1.6 Albian

27.1.1.6.1 History, definition, and boundary stratotype

The Albian Stage was named after the Aube region (the Roman name was *Alba*) in northeast France (d’Orbigny, 1842). Exposures of Albian clays still exist in the Aube, and the stratigraphy and paleontology of the stratotype has been thoroughly reviewed (Amédro and Matrimon, 2007; Amédro et al., 2019; Colleté, 2010).

Prior to 1947, the base of the Albian was assigned as the base of the *Nolaniceras nolani* ammonite zone. Breistroffer (1947) moved this zone and the overlying *Hypacanthoplites jacobi* ammonite zone into an expanded uppermost Aptian, thereby placing the base of the Albian in the Northwest European faunal province of the Boreal realm at the base of the *Leymeriella tardefurcata* ammonite zone with a basal level characterized by *Leymeriella schrammeni*. However, this boundary interval in Western Europe is marked by endemic ammonites, and the occurrences of the earliest *Leymeriella* ammonite species (e.g., *L. schrammeni*) are restricted to northern Germany (Casey, 1996; Hart et al., 1996; Kennedy et al., 2000a; Mutterlose et al., 2003). The successive species *Leymeriella germanica* and *L. tardefurcata* provide an excellent Boreal–Tethyan correlation, because they occur both in northern Germany and the Vocontian Basin in southeast France (Kennedy et al., 2000a), but occur significantly higher than the Aptian–Albian boundary as now defined.

The ratified GSSP for the base of the Albian is the lowest occurrence of the planktonic foraminifer *Microhedbergella miniglobularis* within the thin organic-rich Kilian level, at Pre-Guittard, Arnayon, Drôme, France (Pettrizzo et al., 2012; Kennedy et al., 2014, 2017; Fig. 27.4). This marks a major turnover in planktonic foraminiferans, with the extinction of larger *Hedbergella* and *Paraticinella*, and their replacement by small, smooth *Microhedbergella* species. This same turnover has been recorded in the Atlantic and Indian Oceans (Pettrizzo et al., 2011). The GSSP falls some meters above the first occurrence of circular *Praediscosphaera columnata* (nannofossil) and coincides with a small negative excursion in $\delta^{13}\text{C}$. The GSSP falls within the ammonite zone of *H.*

Base of the Albian Stage of the Cretaceous System, Col de Pré-Guittard Section, Arnanon, Drôme, France.

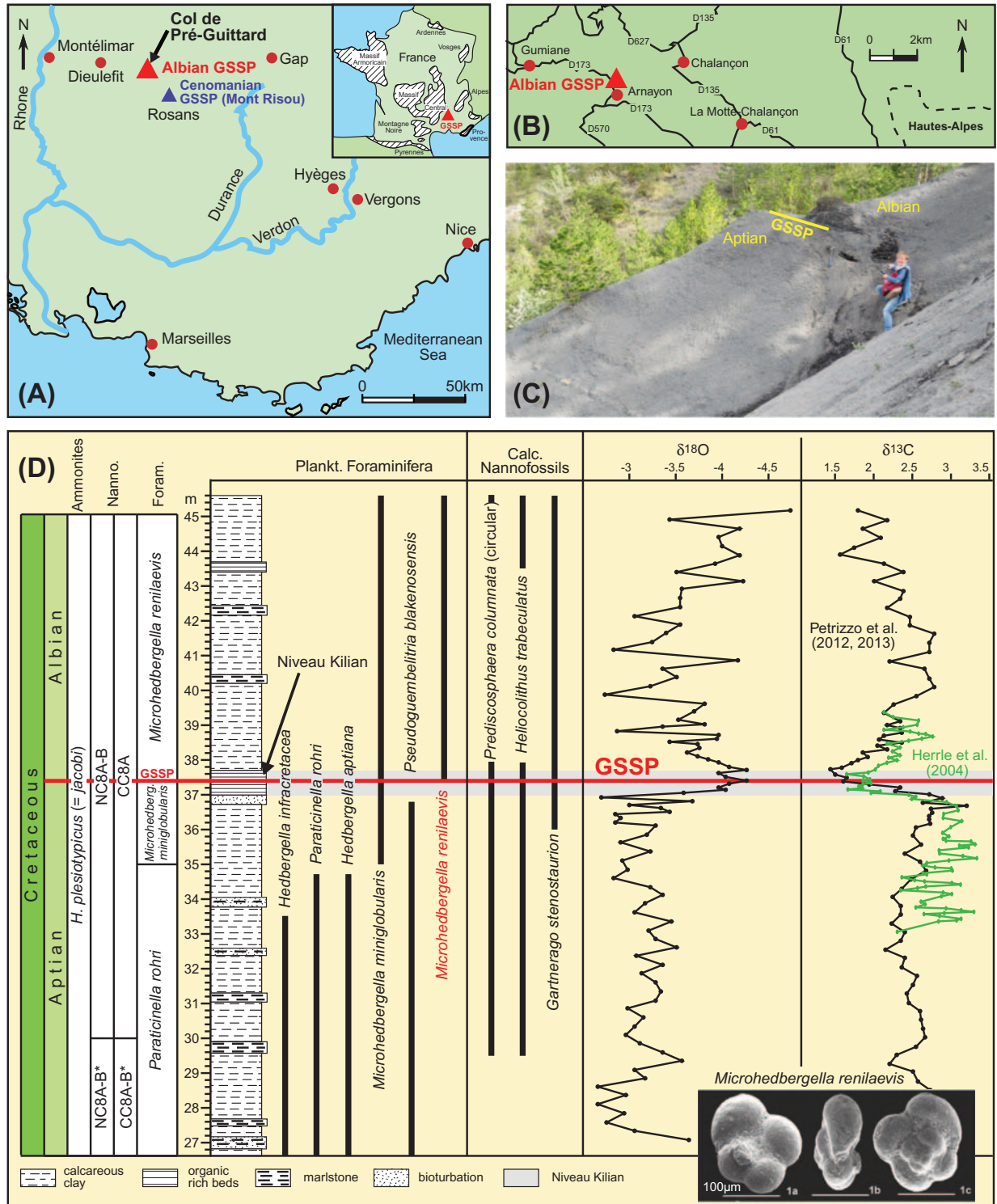


FIGURE 27.4 GSSP for the base of the Albian Stage, Col de Pré-Guittard, Arnanon, Drôme, southeast France. (A and B) Location maps. (C) Photograph of the outcrop, indicating the GSSP within the organic-rich Niveu Kilian. (D) Stratigraphy of the outcrop, and the GSSP marker, the planktonic foraminifer *Microhedbergella renilaevis*. Note also the minor negative carbon isotope excursion at this level. Photograph by Andy Gale. GSSP, Global Boundary Stratotype Section and Point.

jacobi. Correlation to the northern German succession at Vohrum, where a dateable ash lies beneath the first occurrence of *L. schrammeni* (Selby et al., 2009), is guided by the first occurrence of circular *P. columnata*.

Detailed correlation of the Middle and Upper Albian is partly constrained by provinciality of ammonite faunas, with a Boreal province dominated entirely by the Hoplitaceae, and a Tethyan one where keeled ammonites of the family Brancoceratidae predominate. Periodic excursions of the Tethyan Ammonites into the Boreal Realm result in the intercalation of the two faunas at some levels, providing valuable evidence for interregional correlation (Owen, 1996a). Thus the basal Upper Albian species brancoceratid species *Dipoloceras cristatum* extends far northwards from the Tethys into the Boreal Realm, and provides an important marker (Gale et al., 2011). Inoceramid bivalves of the genus *Actinoceramus* underwent rapid evolution in the Middle and Upper Albian and, because the species are global in distribution, provide high-resolution correlation (Crampton and Gale, 2005, 2009).

The base of the Albian is taken at 113.2 Ma, based on the radioisotopic date from an ash at Vohrum, northern Germany (Selby et al., 2009), correlated to the GSSP in SE France by means of the nannofossil datum of the FO of circular *P. columnata*.

27.1.1.6.2 Substages of Albian

The traditional base of the Middle Albian is placed at the lowest occurrence of the ammonite *Lyelliceras lyelli* (Reboulet and Atrops, 1999). The appearance of this ammonite in the European marginal basins marks a temporary incursion of more Tethyan and cosmopolitan forms (Amédéo et al., 2014) although some authors place the *L. lyelli* Subzone within a zone of *Hoplites* (*Hoplites*) *benettianus*. A proposed boundary stratotype within clays near St-Dizier, northern France (Hart et al., 1996; Hancock, 2001) is certainly unsuitable, because it is in a poorly accessible river cliff.

The base of the Upper Albian is assigned to the lowest occurrence of the ammonite *D. cristatum* (Hart et al., 1996; Gale et al., 2011), a species which is widespread in both Tethyan and Boreal Realms. This event commonly coincides with or shortly predates a transgression following a major sequence boundary (e.g., Hesselbo et al., 1990; Amédéo, 1992; Hardenbol et al., 1998), thereby causing the Middle/Upper Albian substage boundary interval to be condensed and incomplete at the key sections along the English Channel/La Manche at Wissant (Pas-de-Calais province, northwest France) and at Folkestone (Kent, United Kingdom) (Hart et al., 1996; Gale and Owen in Young et al., 2010). Therefore an expanded basinal clay-rich section at Col de Palluel in

southeast France was extensively studied as a substage GSSP candidate and tied to cyclostratigraphy, nannofossil, and carbon-isotope stratigraphy (Gale et al., 2011).

27.1.2 Subdivisions of the Upper Cretaceous

The majority of the Late Cretaceous subdivisions were derived from facies successions in marginal-marine to deeper chalk facies in western France (Cenomanian, Turonian, Coniacian, Santonian, Campanian) and the Netherlands (Maastrichtian). The original Turonian and Senonian stages of d'Orbigny (1847) were progressively subdivided into the current six stages. However, none of the classical stratotypes are suitable for placing the limits of the stages, because all are strongly condensed or incomplete.

A diverse array of primary markers are used or under consideration for defining stage and substage boundaries, including ammonoids, inoceramid bivalves, planktonic foraminifers, crinoids, and magnetic polarity chrons.

27.1.2.1 Cenomanian

27.1.2.1.1 History, definition, and boundary stratotype

d'Orbigny (1847) converted the lower portion of his original Turonian into a Cenomanian Stage and assigned the type region as the vicinity of the former Roman town of Cenomanum, now called Le Mans (Sarthe region, northern France). A recently published volume provides a detailed account of the Cenomanian stratotype (Morel, 2015). There is a dramatic turnover in ammonites between the Albian and Cenomanian (Gale et al., 1996). The conventional ammonite marker for the base of the Cenomanian was the lowest occurrence of the acanthoceratid genus *Mantelliceras* (Hancock, 1991).

Because ammonites are relatively rare in many regions, and absent in the ocean basins, the Cenomanian Working Group selected the lowest occurrence of the planktonic foraminifer, "*Rotalipora*" *globotruncanoides* (= *R. brotzeni* of some studies) and now classified as *Thalmaninella globotruncanoides*, as the basal boundary criterion for Cenomanian Stage. This foraminifer level is slightly lower (6 m) than the lowest occurrence of the Cenomanian ammonite marker *Mantelliceras mantelli*, and other typically Cenomanian taxa. The Mont Risou section in southeast France (Fig. 27.5) was chosen as the GSSP section (Tröger and Kennedy, 1996; Gale et al., 1996) and ratified in 2002 (Kennedy et al., 2004). Petrizzo et al. (2015) investigated the taxonomy and distribution of planktonic foraminifera around the Albian–Cenomanian boundary. In many regions, the Albian–Cenomanian boundary interval is coincident with a widespread hiatus and condensation associated with a major sequence boundary (e.g., Tröger and Kennedy, 1996; Hardenbol et al., 1998; Robaszynski, 1998; Gale et al.,

Base of the Cenomanian Stage of the Cretaceous System, Mont Risou, Hautes-Alpes, France.

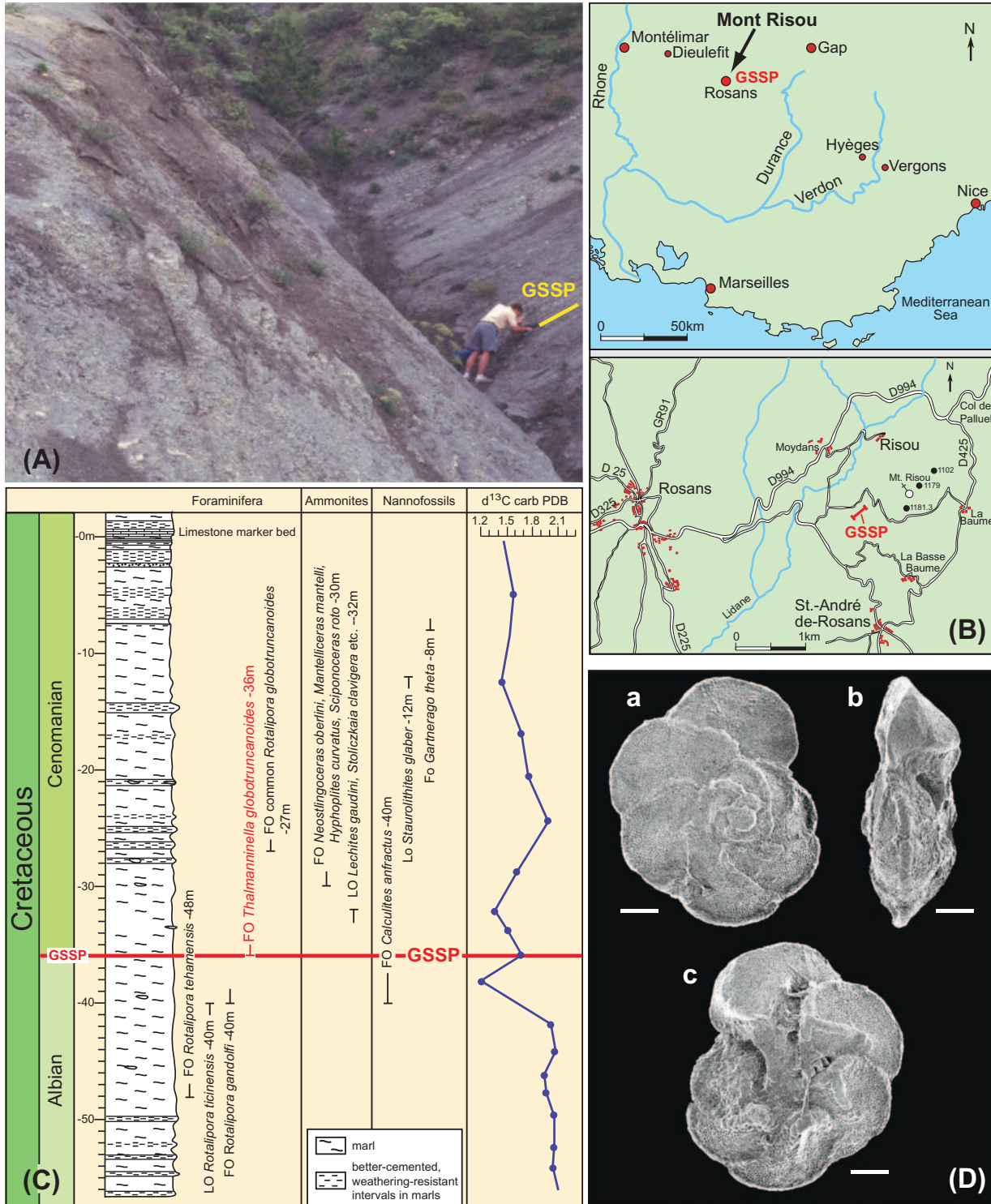


FIGURE 27.5 GSSP for base of the Cenomanian Stage at Mont Risou, Haute Alpes, southeast France. (A) Photo of section. (B) Location maps. (C) Log of section, to show upper part of Marnes Bleues Formation. The GSSP level is the lowest occurrence of the planktonic foraminifer *Thalmaninella globotruncanoides*. (D) Photograph of the marker foraminifer (provided by Atsushi Ando) is the metatype of *T. globotruncanoides* from the type locality (Ando and Huber, 2007). GSSP, Global Boundary Stratotype Section and Point.

2019b). Cenomanian ammonites show relatively little endemism (Wright et al., 2017), and most of the standard zones for the Lower and Middle Cenomanian can be recognized globally; an exception is the Western Interior Basin (see below). However, the Late Cenomanian ammonite faunas are very widespread, extending into the WI Basin, across Tethys, into the Pacific Realm and in South Africa and India (Wright et al., 2017).

The base of the Cenomanian is taken at 100.5 Ma, based on extrapolation from dated tuffs from Hokkaido, Japan (99.7 Ma; 100.8 Ma—Obradovich et al., 2002; Quidelleur et al., 2011; Takashima et al., 2019), which fall at the base of the *Mantelliceras saxbii* Subzone, significantly above the FO of *T. globotruncanoides* which marks the base of the stage.

27.1.2.1.2 Substages of Cenomanian

The sudden entry of the ammonite genera *Cunningtoniceras* and *Acanthoceras* is a major biostratigraphic event in Europe, northern Africa, India, and elsewhere (Kennedy and Gale, 2015, 2017a,b; Gale et al., 2019b; Wright et al., 2017). The base of the Middle Cenomanian is currently placed at the lowest occurrence of the ammonite *Cunningtoniceras inerme* at the Southerham Grey Quarry near Lewes, Sussex, United Kingdom (Tröger and Kennedy, 1996; Kennedy and Gale, 2017a). The lowest occurrences of ammonite *Acanthoceras rhotomagense* and the beginning of a double positive $\delta^{13}\text{C}$ excursion are approximately five couplets higher (~ 100 kyr) (Gale, 1995; Gale et al., 2007). This Lower/Middle Cenomanian boundary interval is missing over large regions due to its coincidence with a major sequence boundary (Gale, 1995; Hardenbol et al., 1998; Robaszynski, 1998). The base of the Middle Cenomanian can be identified in the Western Interior Basin from the FO of the ammonite *Conlinoceras*, associated with the Mid-Cenomanian carbon-isotope excursion (Gale et al., 2007).

The replacement of ammonites of the genus *Acanthoceras* by the genus *Calycoceras* is commonly used to mark the base of the Upper Cenomanian (Hancock, 1991). A marker for the base of the Upper Cenomanian has not yet been selected, but the placement will probably be at the base of the *Calycoceras guerangeri* Zone (Wright et al., 2017). This zone is approximately coeval with *Dunveganoceras pondi* Zone of the Western Interior, of which the base is used by Cobban et al. (2006) for their Upper/Middle substage boundary.

27.1.2.2 Turonian

27.1.2.2.1 History, definition, and boundary stratotype

The concept of the Turonian Stage has undergone continual redefinitions (reviewed in Bengtson et al., 1996). The Turonian proposed by d'Orbigny (1847) in 1842 was later divided by him into a lower Cenomanian Stage and an

upper Turonian Stage. The name is derived from the Touraine region of France (Turonos and Turonia of the Romans), and d'Orbigny (1852) clarified his later definition by selecting a type region lying between Saumur (on the Loire river) and Montrichard (on the Cher river). A detailed stratigraphical and paleontological account of the Turonian stratotype is provided by Amédéo et al. (2018). In this region the lower part of the Turonian contains the ammonite *Mammites nodosoides*, and its lowest occurrence was formerly considered to be the marker for the base of the Turonian Stage (e.g., Harland et al., 1990). After considering several potential placements, the Turonian Working Group placed the base of the Turonian at the lowest occurrence of the ammonite *Watinoceras devonense* (two ammonite zones below the *M. nodosoides* Zone) near the global OAE2 (Bengtson et al., 1996). The GSSP is at Rock Canyon Anticline, east of Pueblo (Colorado, west-central United States) (Kennedy and Cobban, 1991; Bengtson et al., 1996; Kennedy et al., 2000b, 2005) and was ratified in 2003 (Fig. 27.6). The maximum major carbon-isotope peak associated with the OAE2 occurs 0.5 m above the boundary.

The age of the Cenomanian–Turonian boundary is well-constrained by $^{40}\text{Ar}/^{39}\text{Ar}$ ages from bentonites as 94 Ma (Obradovich, 1993; Meyers et al., 2010; Batenburg et al., 2016). Detailed study of the cyclostratigraphy suggests that this falls within long-eccentricity (405 kyr) cycle 232 of the Laskar et al. (2011) numbering system. Gale (2019a) used ammonite biostratigraphy to correlate Turonian radioisotopic dates from the Western Interior Basin into the northwest European succession, and using this information, identified regularly spaced clay-rich levels as representing long-eccentricity maxima.

27.1.2.2.2 Substages of Turonian

The base of the Middle Turonian is marked by the lowest occurrence of the ammonite *Collignoniceras woollgari*. The candidate for the Global Boundary Stratotype Section and Point is the base of Bed 120 in the Rock Canyon Anticline section, approximately 5 m above the GSSP defining the base of the Turonian Stage in the same section (Bengtson et al., 1996; Kennedy et al., 2000b).

The base of the Upper Turonian is not yet formalized, but potential datums are the lowest occurrences of the ammonite *Subprionocyclus neptuni* in the Sub-Boreal realm (e.g., Germany, England), of the ammonite *Romaniceras deverianum* in the Tethys realm (e.g., southern France, Spain), of the ammonite *Scaphites whitfieldi* in the North American Western Interior (as used by Cobban et al., 2006, or of an inoceramid bivalve, *Inoceramus perplexus* (= *Mytiloides costellatus* in some studies) (Bengtson et al., 1996; Wiese and Kaplan, 2001). The best of these suggestions is probably the first

Base of the Turonian Stage of the Cretaceous System at Pueblo, Colorado, USA.

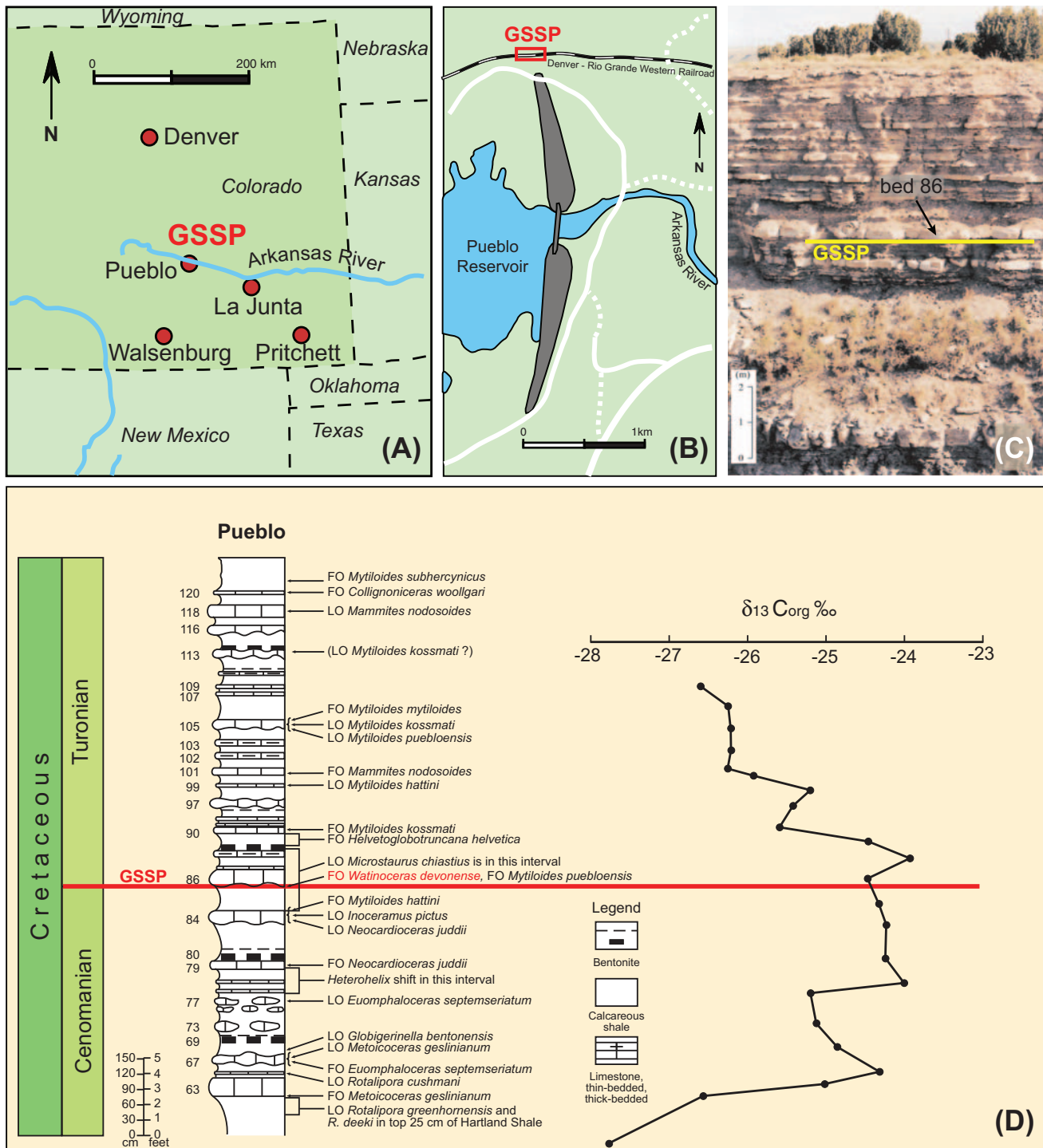


FIGURE 27.6 GSSP for base of the Turonian Stage near Pueblo, Colorado, United States. (A and B) Location maps. (C) Photograph of outcrop. (D) Stratigraphic log of the lower Bridge Creek Limestone Formation. The GSSP level coincides with the lowest occurrence of the ammonite *Watinoceras devonense*. Photograph provided by Jim Kennedy. *GSSP*, Global Boundary Stratotype Section and Point.

occurrence of the widespread species *I. perplexus*, which is close to a small positive carbon-isotope positive excursion, the Caburn Event (Jarvis et al., 2006) identified widely (Joo and Sageman, 2014; Takashima et al., 2019).

27.1.2.3 Coniacian

27.1.2.3.1 History, definition, and boundary stratotype

Coquand (1857a,b) defined the Coniacian Stage with the type locality at Richemont Seminary near Cognac (Charente province, northern part of the Aquitaine Basin, western France). In this region, basal Coniacian glauconitic sands overlie Turonian rudistid-bearing limestones. The entry of ammonoid *Forresteria* (*Harleites*) *petrocoriensis* was taken to mark the base of the Coniacian Stage, but this species is now taken to occur within the highest zone of the Turonian. However, there can be problems in identifying this species, and ammonites are rare or absent in important Coniacian sections (Hancock, 1991; Kauffman et al., 1996). Therefore the Coniacian Working Group proposes to define the Coniacian Stage and its substage boundaries using lowest occurrences of widespread and frequently abundant inoceramid bivalves.

The proposed marker for the base of the Coniacian is the lowest occurrence of inoceramid bivalve *Cremnoceramus deformis erectus* [= *Cremnoceramus rotundatus* (*sensu* Tröger *non* Fiege)], which is above the occurrence of *F. (H.) petrocoriensis* in Europe. This inoceramid is present throughout the Europe–American biogeographic province and in the Tethyan realm and can be easily correlated to the North Pacific and southern hemisphere (Walaszczyk et al., 2010).

A candidate boundary stratotype is the active Salzgitter-Salder Quarry, southwest of Hannover (Lower Saxony province, northern Germany) with an extensive upper Turonian through Lower Coniacian succession with macrofossils, microfossils, and geochemistry (Kauffman et al., 1996; Walaszczyk and Wood, 1998; Walaszczyk et al., 2010). However, at Salzgitter-Salder, the boundary interval is very slightly condensed and may contain a minor hiatus in uppermost Turonian. The most complete succession across the actual boundary is at Słupia Nadbrzeżna in central Poland (Walaszczyk and Wood, 1998; Walaszczyk et al., 2010), but it is limited to only a very brief interval spanning the latest Turonian and earliest Coniacian and is poorly exposed. Therefore a composite GSSP is being proposed that will use both of these reference sections.

The lowest occurrence of inoceramid bivalve *C. deformis erectus* correlates approximately to the base of the *Scaphites preventricosus* ammonite zone of the North American Western Interior basin (Cobban et al., 2006). Bentonites from this ammonite zone and the uppermost Turonian zone have yielded $^{40}\text{Ar}/^{39}\text{Ar}$ ages indicating a

boundary age of approximately 89.8 Ma (Obradovich, 1993; Siewert, 2011; Sageman et al., 2014). The boundary falls close to or within the 405-kyr eccentricity cycle 221, therefore an age of 89.4 Ma is used in GTS2020.

27.1.2.3.2 Substages of Coniacian

The base of the Middle Coniacian is placed at the lowest occurrence of the inoceramid bivalve genus *Volviceramus*, which is at or near the lowest occurrence of ammonoid *Peroniceras* (*Peroniceras*) *tridorsatum* (Kauffman et al., 1996). Potential boundary stratotypes are in the Austin Chalk near Dallas-Fort Worth (Texas, southern United States) or possibly in the chalk succession of southern England.

The base of the Upper Coniacian is placed at the lowest occurrence of the inoceramid bivalve *Magadiceramus subquadratus* (Kauffman et al., 1996). No stratotypes have yet been proposed for this substage boundary.

27.1.2.4 Santonian

27.1.2.4.1 History, definition, and boundary stratotype

The Santonian Stage was named after Saintes (Aquitaine, southwest France) by Coquand (1857b), who placed the lower boundary at a strongly lithified glauconitic hardground.

The sudden turnover from inoceramid bivalves of the genus *Magadiceramus* to the lowest occurrence of the widespread inoceramid *Cladoceramus* (= *Platyceramus*) *undulatopticatus* has been selected as the marker for the base of the Santonian (Lamolda et al., 2014). No other significant calcareous microfossil or nannofossil datums occur near this level—significantly below are the lowest *Lucianorhabdus cayeuxii* nannoplankton (base of Zone UC11c) and lowest rare *Dicarinella asymetrica* planktonic foraminifers (base of *D. asymetrica* zone) (Lamolda et al., 2014; Gale et al., 2007). (The FAD of *D. asymetrica* planktonic foraminifers had been a competing candidate marker for the boundary.) There are lesser known and some newly described calcareous nannofossils that may provide correlation to other facies (Blair and Watkins, 2009). Recently, Petrizzo (2019) identified the lowest occurrence of *Costellagerina pilula* as a useful and widespread proxy for the base of the Santonian.

The GSSP for the Santonian is now fixed at a quarry to the south of Olazagutia in the Navarra region of Spain (Fig. 27.7; Lamolda and Paul, 2007; Lamolda et al., 1996, 2007, 2014). The Olazagutia section is not ideal—the sediment is strongly lithified and the biostratigraphic record may be incomplete. The Olazagutia section was however ratified as the GSSP in 2012 by the Subcommittee on Cretaceous Stratigraphy.

The lowest occurrence of the inoceramid *C. undulatopticatus* boundary marker is just below the base of the *Clioscapites saxitonianus* ammonite zone of the North

Base of the Santonian Stage of the Cretaceous System in the Olazagutia Section, Spain

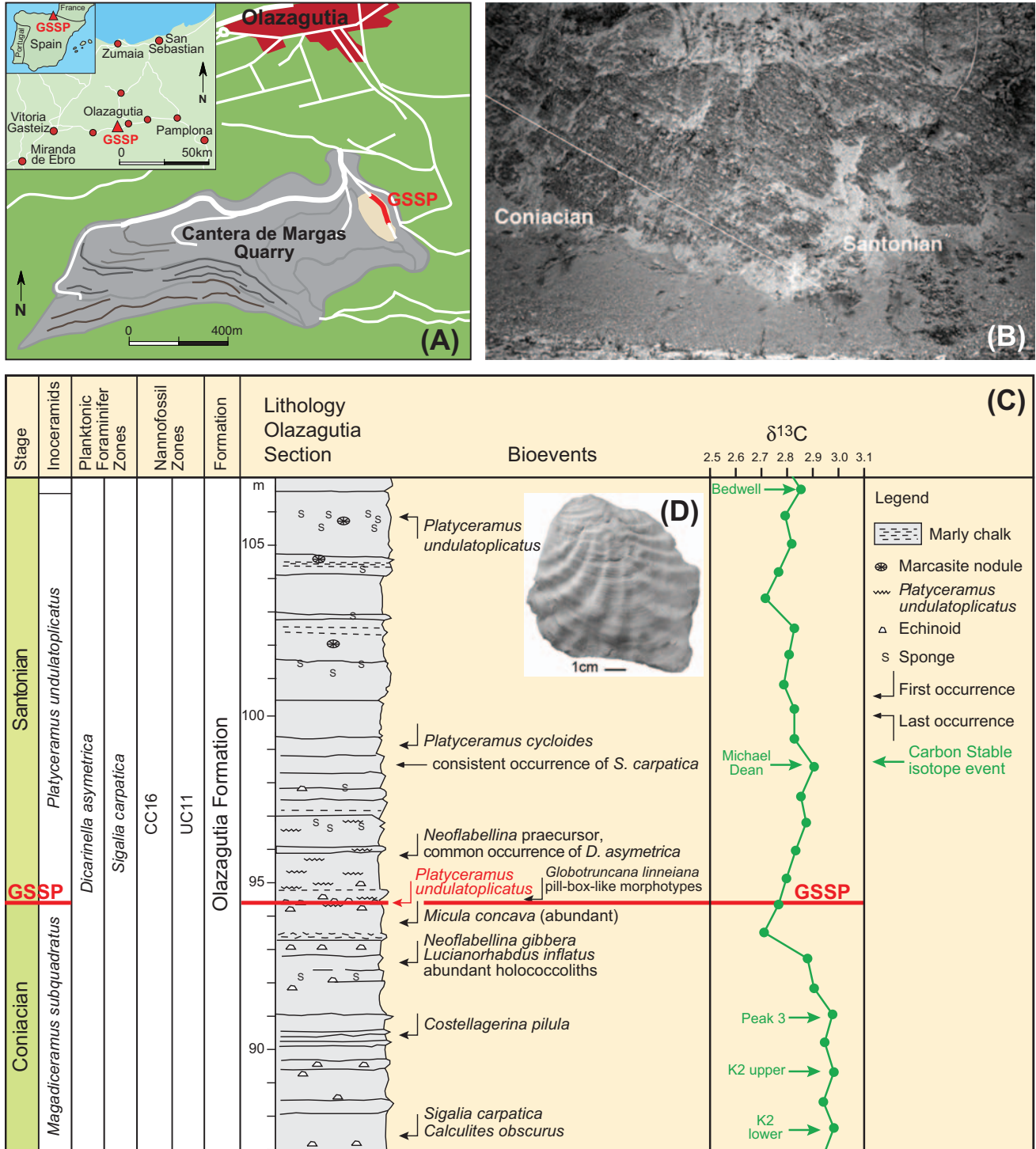


FIGURE 27.7 GSSP for the base of the Santonian Stage, Olazagutia, Navarra, north Spain. (A) Map of region. (B) Photograph of GSSP section in quarry face. (C) Log of section, with GSSP marked, at level of lowest occurrence of the inoceramid bivalve *Platyceramus undulatoplicatus* (D). GSSP, Global Boundary Stratotype Section and Point.

American Western Interior (Walaszczyk and Cobban, 2007). A set of $^{40}\text{Ar}/^{39}\text{Ar}$ ages from bracketing bentonites indicate a boundary age near 86 Ma (Obradovich, 1993; Siewert, 2011; Sageman et al., 2014). A high-resolution $\delta^{13}\text{C}$ record from Seaford Head in Sussex, United Kingdom, provided an orbital tuning for the Santonian (Thibault et al., 2016) and permits detailed correlation to the standard Tethyan succession at Gubbio. The base of the stage is taken at 85.7 Ma, based upon radioisotopic dates from beds yielding *C. undulatopticatus* in Texas and the Western Interior Basin of the United States (Appendix 2), approximately at the level of eccentricity cycle 221, equivalent to cycle Sa1 of Thibault et al. (2016).

27.1.2.4.2 Substages of Santonian

The traditional Santonian has three substages, but no markers for boundary stratotypes have yet been formalized. A possible datum for the base of the Middle Santonian is the extinction of the same *C. undulatopticatus* inoceramid bivalve that marks the Coniacian–Santonian boundary (Lamolda et al., 1996).

The lowest occurrence of stemless crinoid *Uintacrinus socialis* is commonly used to place the base of the Upper Santonian, and this level is near the FAD of nannofossil *Arkhangelskiella cymbiformis* (Lamolda et al., 1996; D'Hondt et al., 2007).

27.1.2.5 Campanian

27.1.2.5.1 History, definition, and boundary stratotype

The Campanian Stage of Coquand (1857b) was named after the hillside exposures of Grande Champagne near Aubeter-sur-Dronne (45 km west of Périgueux, northern Aquitaine province, France), but bulk of the type “Campanian” at Aubeterre is now classified as Maastrichtian (e.g., van Hinte, 1965; Séronie-Vivien, 1972).

The lower part of the type section had no obvious base to the shallow-water limestone formation. The base of the Campanian was placed at the lowest occurrence of ammonite *Placenticeras bidorsatum* by De Grossouvre (1901), but this extremely rare species is not a practical marker (reviewed in Hancock and Gale, 1996). In contrast, stemless benthonic crinoids of the genera *Uintacrinus* and *Marsupites* have a near-global distribution in shelf chalks (Gale et al., 1995, 2007). Therefore the extinction of crinoid *Marsupites testudinarius* has been an informal boundary marker for the base of the Campanian Stage (Hancock and Gale, 1996), although the occurrence of this taxon is restricted to certain paleoenvironments. The base of the traditional Campanian is probably within the lower portion of reversed-polarity Chron C33r. Therefore the Campanian Working Group is

presently considering using the beginning of Chron C33r as the primary boundary definition, thereby enabling global recognition in pelagic, continental, and other nonshallow-marine settings. A likely locality for the GSSP is the Bottacione Gorge at Gubbio, Umbria, Italy. The reversal falls very close to the extinction of *D. asymetrica*, widely identifiable in the Tethyan Realm, and various changes in the nannofossil *Broinsonia*, all of which are being studied at present. The presence of a distinctive double positive excursion in $\delta^{13}\text{C}$, the Santonian–Campanian Boundary Event (Jarvis et al., 2006; Thibault et al., 2016), further enables detailed correlation of this interval globally.

The base-Campanian is generally correlated to the base of the *Scaphites leei* III ammonite zone of the North American Western Interior (e.g., Cobban et al., 2006). The age of the base of this ammonite zone is constrained by $^{40}\text{Ar}/^{39}\text{Ar}$ dates to be between 83 and 84 Ma (Obradovich, 1993; Siewert, 2011; Sageman et al., 2014). Until there is more detailed interpolation with uncertainty estimates, we here take the base of the Campanian at 83.65 Ma, based on extrapolation to the base of Chron 33R, which likely falls in eccentricity cycle 207.

27.1.2.5.2 Substages of Campanian

In the Western Interior of North America, the Campanian is generally subdivided into Lower, Middle, and Upper substages of approximately equal duration, informally placed by Cobban (1993) and Cobban et al. (2006) as the lowest occurrences of the endemic ammonites *Baculites obtusus* and *Didymoceras nebrascense*, respectively. In northwest Europe, the Campanian is traditionally divided into Lower and Upper substages, and the boundary is marked by the extinction of the belemnite *Goniot euthis quadrata* (Christensen, 1990, 1997a,b). As so defined, the Upper Campanian is considerably longer than the Lower Campanian and the boundary correlates approximately with the base of the *Baculites* sp. (smooth) Zone of Cobban et al. (2006). This correlation is based on the occurrence in both regions of *Scaphites hippocrepis* III in both regions (Kennedy, 2019), associated with the highest *G. quadrata* in Europe. *Inoceramus azerbaijanensis* appears in the overlying basal *Belemnitella mucronata* Zone in Europe, and in the *Baculites* sp. (smooth) Zone in the Western Interior. The tradition of splitting the Campanian into Lower and Upper divisions is deeply embedded in European literature, and change would create confusion.

Campanian correlation has been significantly improved by the discovery of a sharp, short negative excursion in $\delta^{13}\text{C}$, the Late Campanian Event (Voigt et al., 2012), which lies beneath and in the lower part of the range of *Radotruncana calcarata*. This has been discovered as far afield as Tibet (Wendler et al., 2011).

27.1.2.6 Maastrichtian

27.1.2.6.1 History, definition, and boundary stratotype

The Maastrichtian Stage was introduced by Dumont (1849) for the “Calcaire de Maastricht” with a type locality at the town of Maastricht (southern Netherlands near border with Belgium). The stratotype was fixed by the Comité d'étude du Maastrichtian as the section of the Tuffeau de Maastricht exposed in the ENCI company quarry at St. Pietersberg on the outskirts of Maastricht, but this local coarse carbonate facies would correspond only to part of the upper Maastrichtian in current usage (reviewed in Rawson et al., 1978; Odin and Lamaurelle, 2001). A revised concept of Maastrichtian Stage was based on belemnites in the white chalk facies. Accordingly, the base of the stage was assigned to the lowest occurrence of belemnite *Belemnella lanceolata*, with a reference section in the chalk quarry at Kronsmoor [50 km northwest of Hamburg, north Germany (e.g., Birkelund et al., 1984; Schönfeld et al., 1996)]. The lowest occurrence of ammonoid *Hoploscaphites constrictus* above this level provided a secondary marker. Comparison of strontium-isotope stratigraphy and indirect correlations by ammonoids indicate that this level is approximately equivalent to the base of the *Baculites eliasi* ammonoid zone of the North American Western Interior (Landman and Waage, 1993; McArthur et al., 1992).

However, belemnites, including *B. lanceolata* are largely restricted to Boreal chalks and are absent in the Tethyan faunal realm, where the ammonoid *Pachydiscus neubergicus* has a much wider geographical distribution (reviewed in Hancock, 1991). Therefore the Maastrichtian Working Group recommended the base of the Maastrichtian to be taken at the lowest occurrence of ammonoid *P. neubergicus* (Odin et al., 1996). In retrospect, this was a poor decision, because the occurrence of *P. neubergicus* is strongly diachronous across its geographic range and uncommon in most localities.

The ratified Maastrichtian GSSP boundary is in an abandoned quarry near the village of Tercis les Bains in southwest France, at 90 cm beneath a coincident lowest occurrence of *P. neubergicus* and *H. constrictus* ammonoids (Fig. 27.8; Odin, 1996, 2001; Odin and Lamaurelle, 2001). The GSSP level was selected, bizarrely as the arithmetic mean of 12 biohorizons with potential correlation potential, including ammonoids, dinoflagellate cysts, planktonic and benthic foraminifers, inoceramid bivalves, and calcareous nannofossils (Odin and Lamaurelle, 2001). The history, stratigraphy, paleontology, and intercontinental correlations are compiled in a large special (and outrageously expensive) volume (Odin and Lamaurelle, 2001).

In many ways the GSSP was poorly chosen; the ammonite marker is inappropriate, the section lacks key planktonic foraminifers above the occurrence of *R.*

calcarata, and remnant paleomagnetism is weak or absent. The abandoned quarry section is growing over, and a tree now covers the GSSP marker. However, the section at Tercis provides a detailed carbon-isotope record, which permits correlation with both Boreal chalks and the deep-water Tethyan succession at Gubbio (Voigt et al., 2012). Some distance above a well-marked late Campanian negative event, the carbon-isotope values decline by about 0.3 ppt, the Campanian–Maastrichtian Boundary Event, then rise slightly to a minor peak. The fine details of this curve can be matched precisely in the Boreal chalk successions of northern Germany, Denmark and the United Kingdom, and the Tethyan section at Gubbio, Italy, which allows the level of the Tercis GSSP to be equated with the base of the *Belemnella obtusa* Zone in the Boreal chalks.

This correlation is also aided by the use of inoceramid bivalves, because the boundary marker falls just beneath the first occurrence of *Endocosta typica* at Tercis (Walaszczyk et al., 2002). The base of the *E. typica* zone is equated with the base of the *Baculites baculus* Zone in the North American ammonite succession (Cobban et al., 2006). The age for the base of this ammonite zone is 72.1 Ma according to the spline-fit of dates from bracketing bentonites.

This agreement between the independent sets of correlations implies that the base-Maastrichtian is essentially equivalent to the base of the *B. obtusa* belemnite zone, the base of *E. typica* inoceramid zone, the base of *B. baculus* ammonite zone of North American, and approximately to the base of nannofossil zone UC17. The magnetostratigraphic placement is Chron C32n.2n.88, and the age for all of these base-Maastrichtian levels is approximately 72.2 Ma.

27.1.2.6.2 Upper Maastrichtian substage

The Maastrichtian is commonly divided into two substages in the Boreal chalks, based on belemnite occurrences in northern Europe (Germany, Poland, Denmark, the United Kingdom). The Lower Maastrichtian includes the zones of *B. obtusa*, *Belemnella sumensis*, *Belemnella cimbrica*, and *Belemnella fastigata*, the Upper Maastrichtian includes the zones of *Belemnitella junior* and *Belemnitella casimirovensis* (Christensen, 1990, 1997a,b). It is not clear how this zonation relates to the occurrences of ammonites in other successions. In the Western Interior Basin, the lowest occurrence of ammonoid *Hoploscaphites birkelundi* (formerly *H. aff. nicolleti*) is an informal marker for the base of the Upper Maastrichtian (Landman and Waage, 1993; Cobban, 1993; Cobban et al., 2006).

As indicated by this review, the main chronostratigraphic markers for the boundaries of Cretaceous stages, as defined by ratified GSSPs or as the informal working

Base of the Maastrichtian Stage of the Cretaceous System at Tercis les Bains, Landes, France

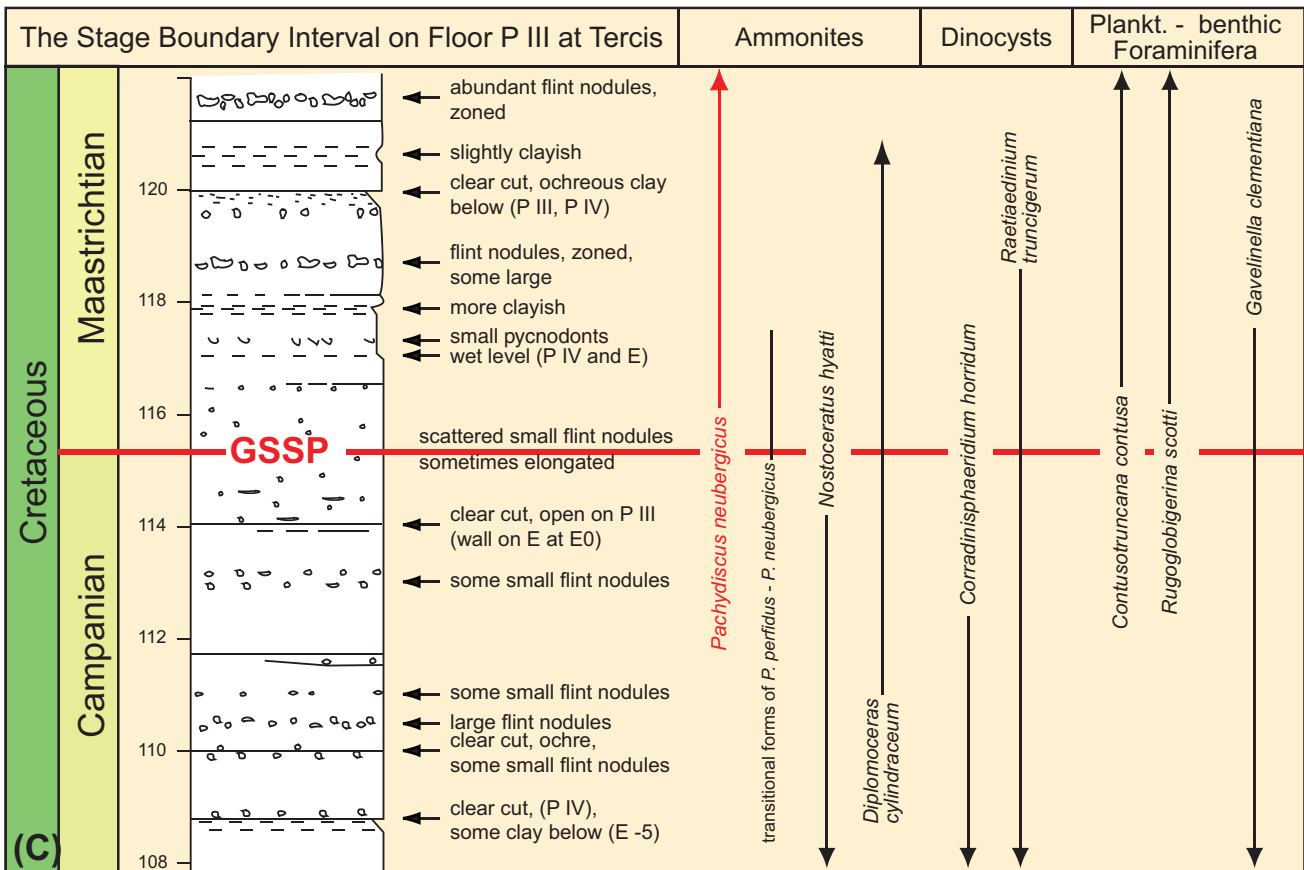
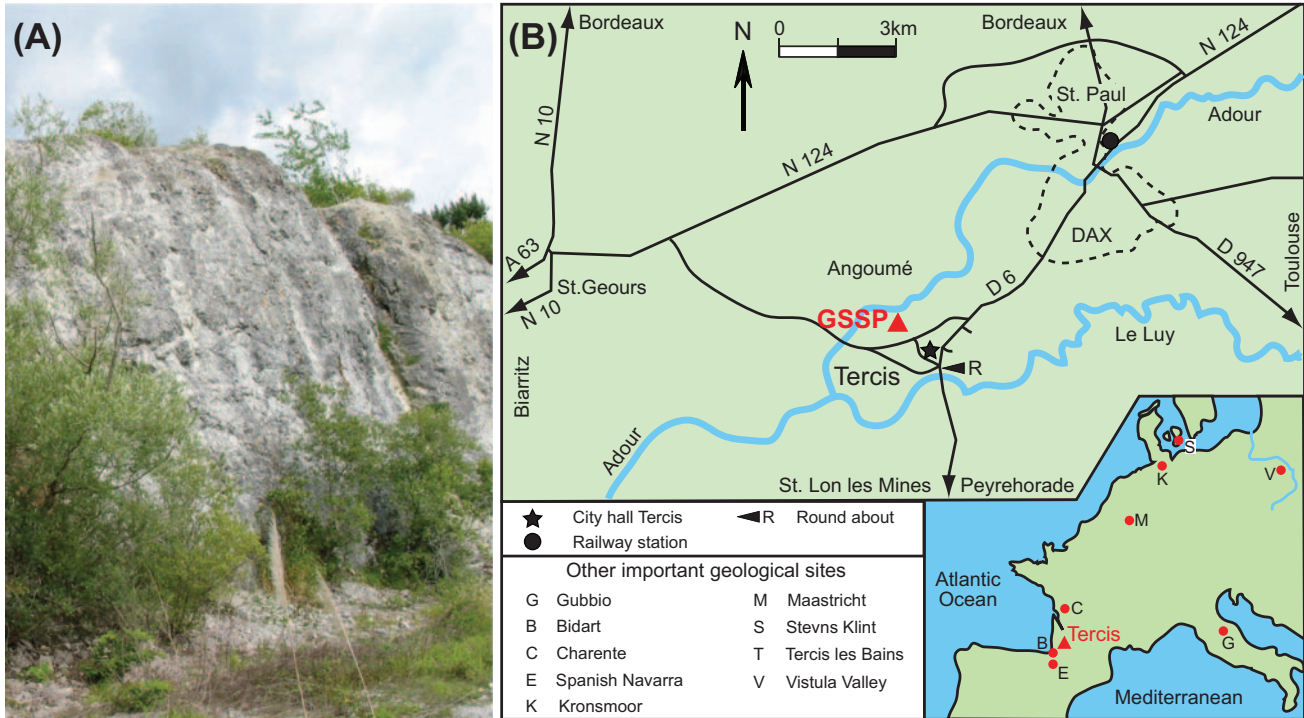


FIGURE 27.8 GSSP for base of the Maastrichtian Stage at Tercis, Landes, southwest France (A and B). The GSSP is situated 90 cm below the lowest occurrence of the ammonite *Pachydiscus neubergicus* (C). Photograph provided by Andy Gale. GSSP, Global Boundary Stratotype Section and Point.

TABLE 27.1 Main biostratigraphic or other chronostratigraphic markers for ratified Global Boundary Stratotype Section and Points (GSSPs) (R) and potential GSSPs for the Callovian through Maastrichtian time scale segment.

base of Stage	Ratified GSSP (R) or potential GSSP main marker(s)
Danian (Paleogene base)	Iridium anomaly (R), within Chron C29r
Maastrichtian	near FAD <i>P. neubergicus</i> (R), projected to about 88% in subchron C32n.2n
Campanian	base Chron C33r; base of <i>S. leei</i> III Zone; LAD <i>M. testidunarius</i>
Santonian	FAD <i>P. undulatopticatus</i> (R)
Coniacian	FAD <i>C. deformis erectus</i>
Turonian	FAD <i>W. devonense</i> (R)
Cenomanian	FAD <i>T. globotruncanoides</i> , just below <i>M. mantelli</i> Zone (R)
Albian	FAD <i>M. renilaevis</i> , base Kilian OAE (R)
Aptian	base of Chron M0r, ~FAD <i>D. oglanlensis</i> Zone
Barremian	FAD <i>T. hugii</i> , upper part of Chron M5n, 0.7 Myr above Faraoni OAE
Hauterivian	FAD <i>A. radiatus</i> Zone (R)
Valanginian	FAD <i>C. darderi</i> , base of calpionellid Zone E, lower part of Chron M14r
Berriasian (Cretaceous base)	base of <i>C. alpina</i> ; mid Chron 19n.2n.2
Tithonian	near bases of <i>H. hybonotum</i> Zone and of Chron M22An
Kimmeridgian	Base of <i>P. flodigarriensis</i> Zone, base of Chron M26r
Oxfordian	FAD of <i>B. thuouxis</i> , within lower part of Chron M36Br
Callovian	FAD of <i>Kepplerites</i> , within Chron M39n.3n

This is the interval used in the spline fits of Figs. 27.11 and 27.12. OAE, Oceanic Anoxic Event. Full name and explanation of each chronostratigraphic marker is in the appropriate text for that stage.

definitions used in GTS2020 are a combination of ammonites, inoceramids, planktonic foraminifers and calpionellids, geomagnetic polarity chrons, and other events (Table 27.1).

27.2 Cretaceous stratigraphy

As in the Jurassic, the ammonite and other macrofossil zones of European and North American basins had provided the traditional standards for subdividing Cretaceous stages. With the advent of petroleum and scientific drilling, microfossil datums from pelagic successions are commonly used for global correlations, especially when augmented by magnetostratigraphy. Cycle stratigraphy has now enabled scaling of many of these zonations, and detailed carbon-isotope curves are becoming a major method for interregional correlation.

27.2.1 Marine biostratigraphy

Ammonites dominate the historical zonation of the Lower Cretaceous of Europe, but ammonites are of restricted occurrence in the European Upper Cretaceous Chalk facies, and

belemnites, inoceramid bivalves and pelagic or benthic crinoids (e.g., *Marsupites*) provide important information. Buchiid bivalves, belemnites, and brachiopods are used for correlation within the Lower Cretaceous within the Boreal Realm. Important microfossil biostratigraphic zonations include planktonic foraminifers, calcareous nannoplankton, dinoflagellate cysts, and calpionellids.

27.2.1.1 Ammonites

Ammonites, despite various limitations, provide the primary reference scale for the majority of the marine Cretaceous sequences in all paleogeographic regions. The Lower Cretaceous standard zonation is the Tethyan ammonite succession of the western Mediterranean region with its revised and enhanced zonal schemes developed by the Kilian working group (e.g., Reboulet et al., 2006, 2009, 2011, 2018). The Upper Cretaceous succession of the Western Interior Basin of the United States, locally yields abundant ammonites on which a standard zonation (Fig. 27.9) is based, and abundant radioisotopically dated volcanic ash beds in the region form the basis for the Late Cretaceous age model (Cobban et al., 2006; Sageman et al., 2014). However, many of the Western Interior

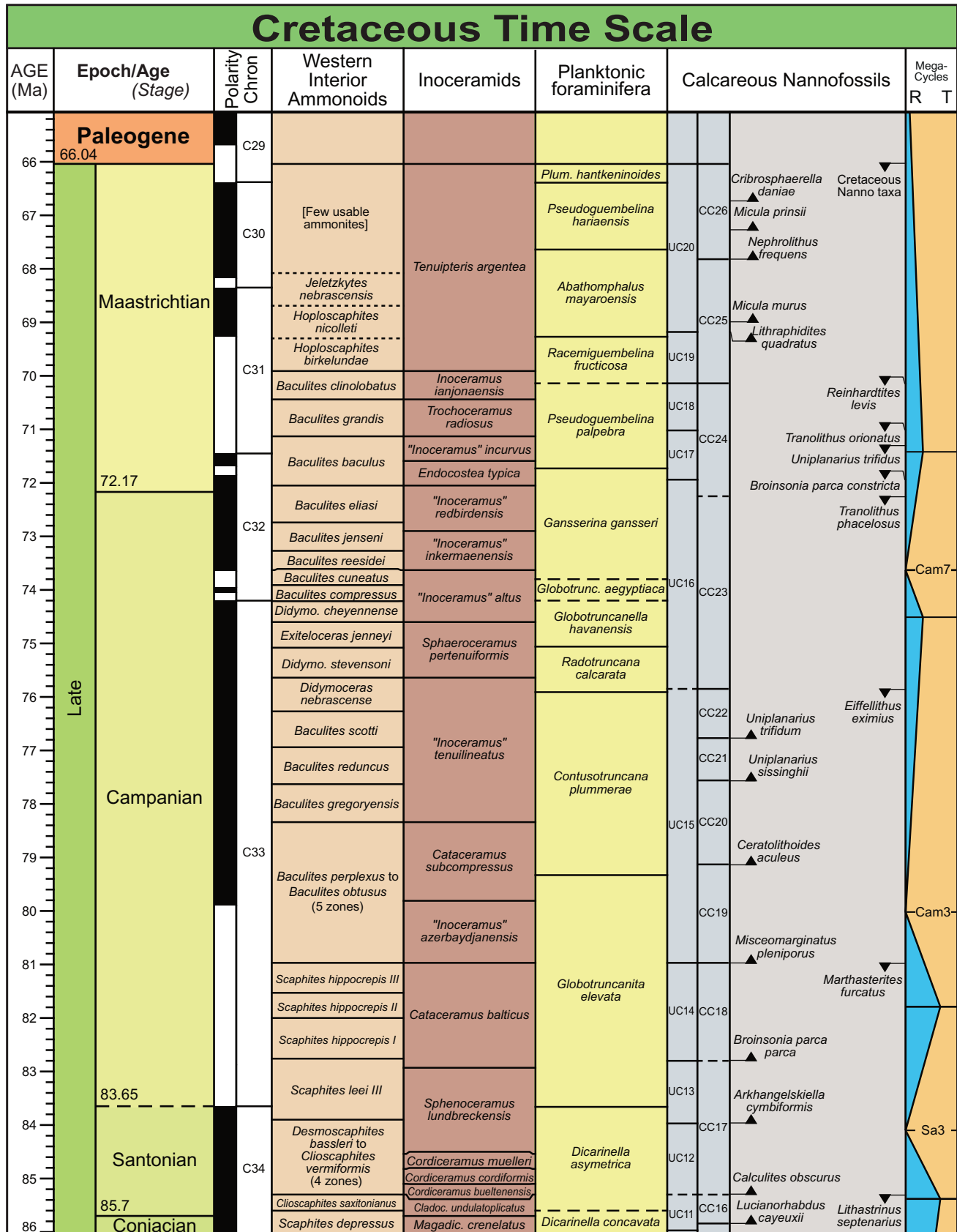


FIGURE 27.9 Cretaceous integrated time scale. Summary of numerical ages of epoch/series and age/stage boundaries of the Cretaceous with selected marine biostratigraphic zonations and principal trends in sea level. ("Age" is the term for the time equivalent of the rock-record "stage.")

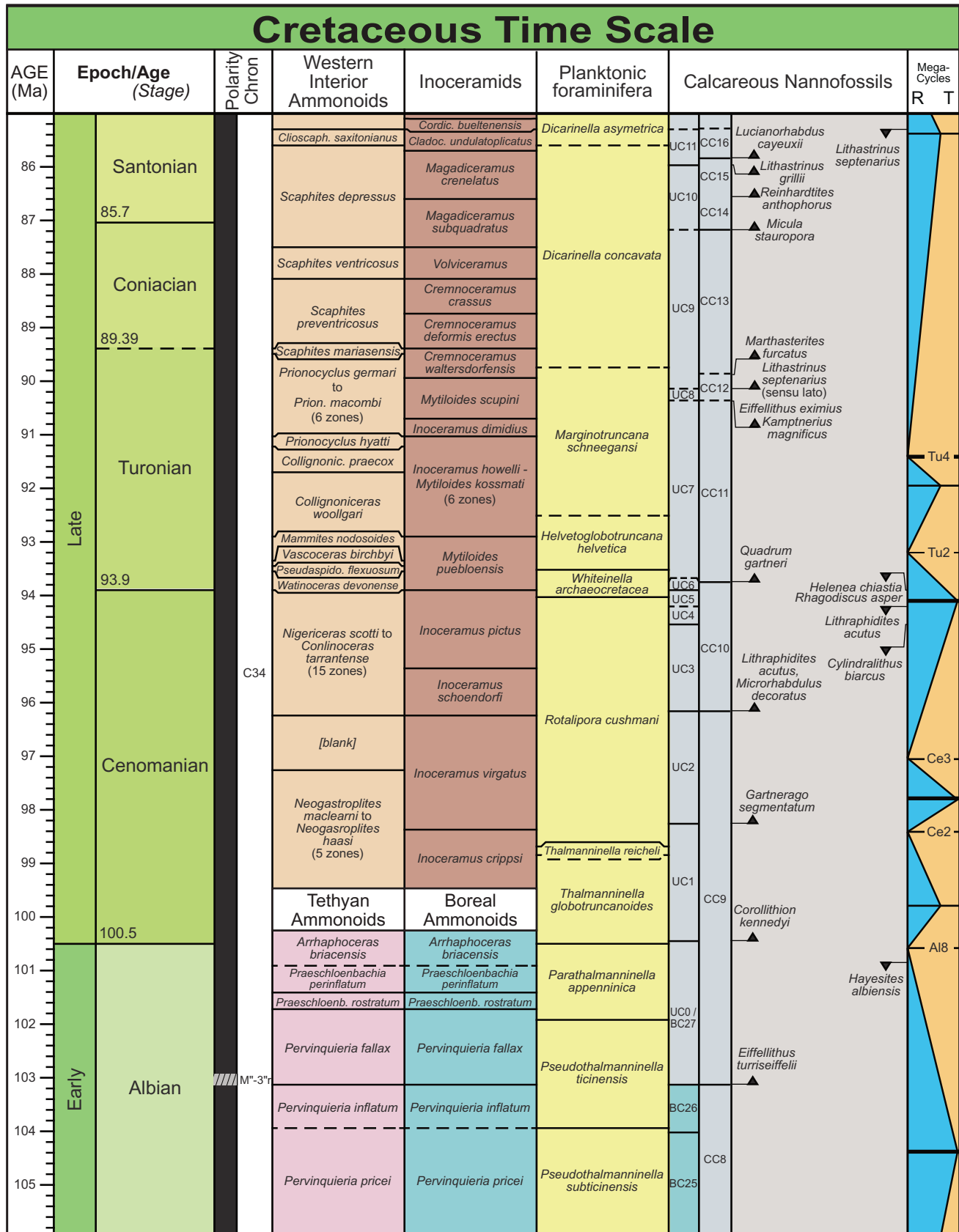
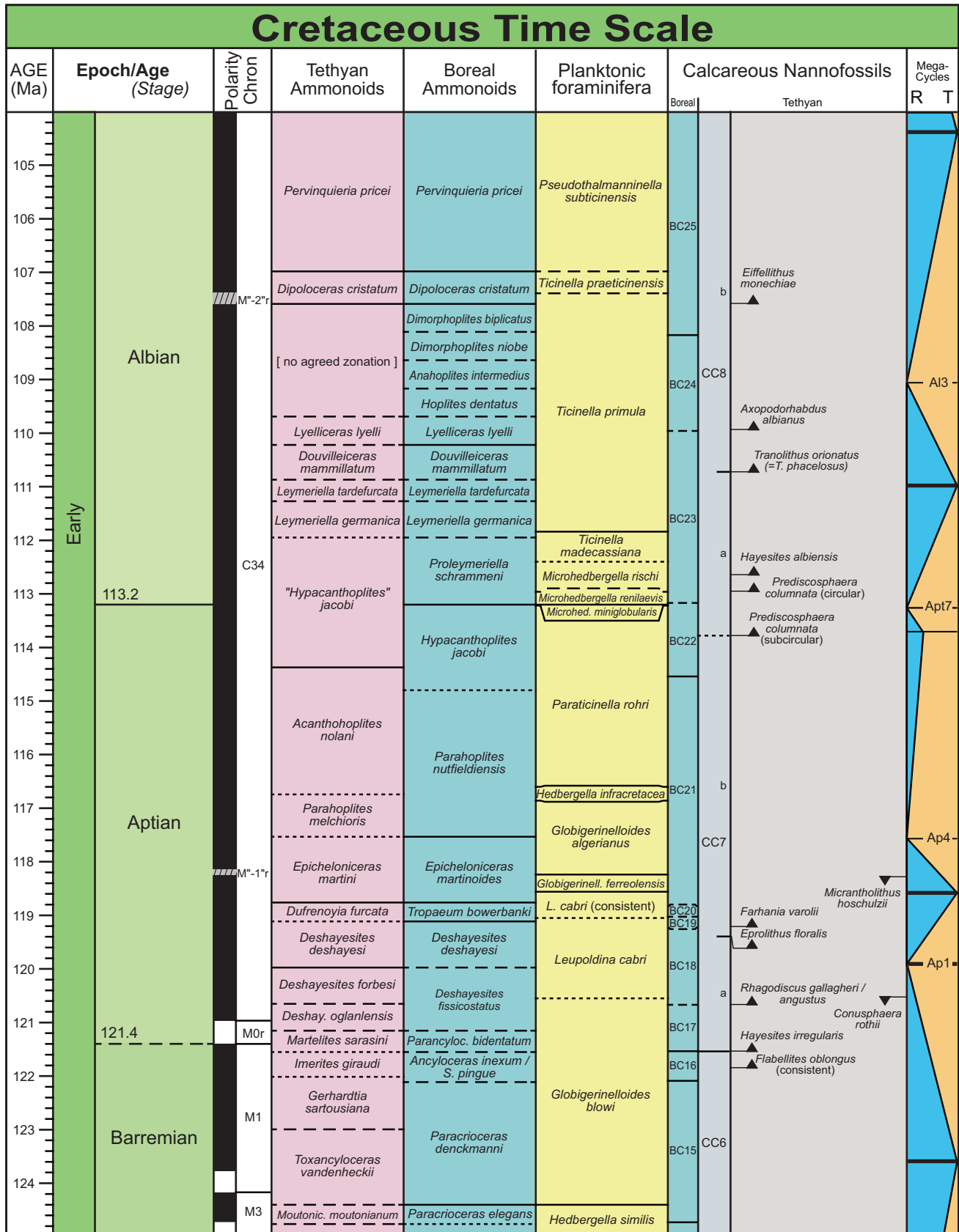


FIGURE 27.9 (Continued)

Selected marine macrofossil biostratigraphy columns for Early Cretaceous are ammonoid zones for the Tethyan realm (Sub-Mediterranean province; Reboulet et al., 2018) and Sub-Boreal realm (Mutterlose et al., 2014). Marine macrofossil zones for Late Cretaceous are ammonoids of the Western Interior



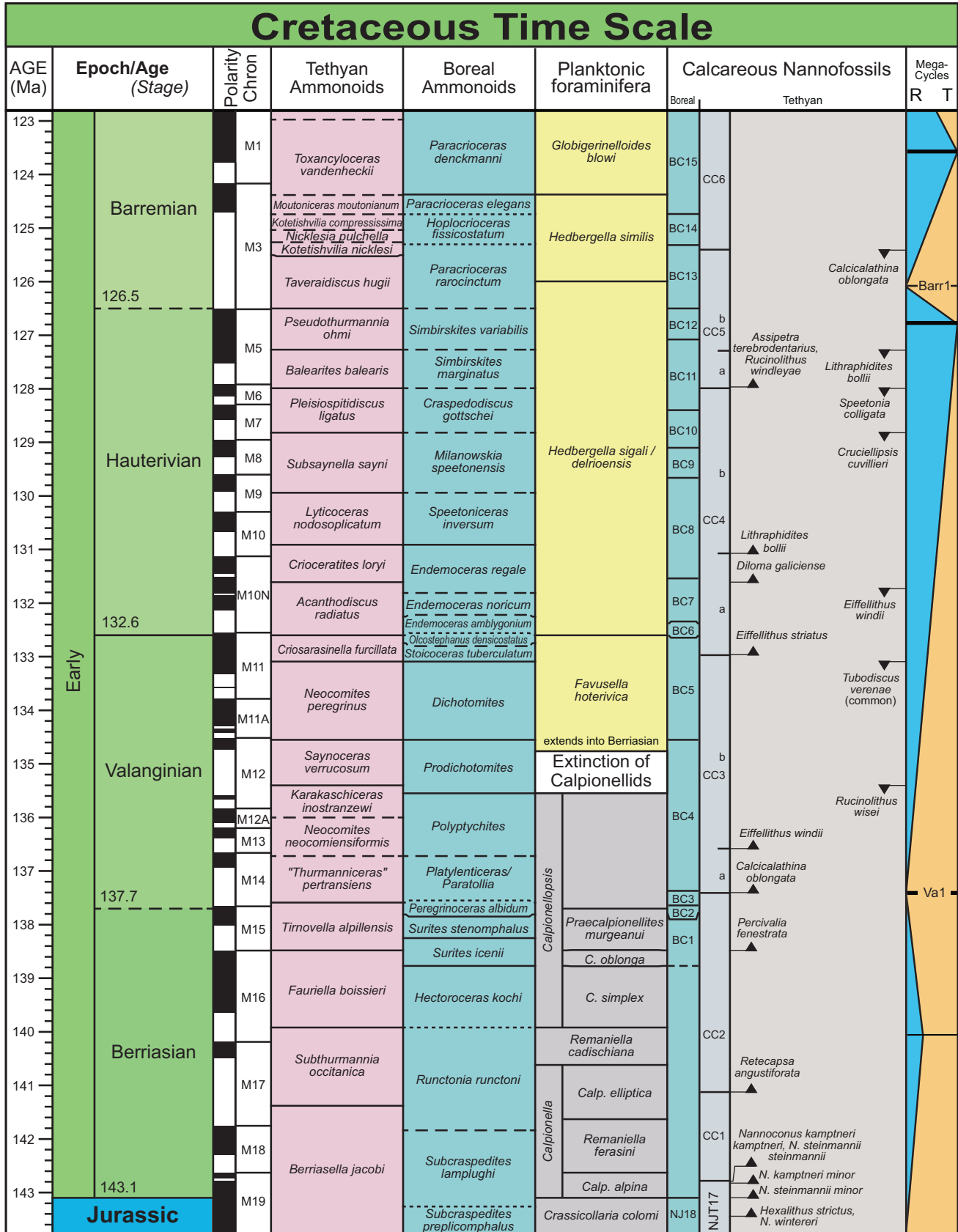


FIGURE 27.9 (Continued)

and other sources, including Huber and Petrizzo, pers. comm., 2019) and early Cretaceous calpionellid zones (Remane, 1998). Early Cretaceous calcareous nannofossil zones are Boreal (BC; Bown et al., 1998) and Tethyan (CC with selected zone/subzone markers; with calibrations compiled from Bergen, 1994; Bralower et al., 1995; and other sources, including Watkins, pers. comm., 2019).

ammonite faunas are endemic to the region, and correlation to the rest of the world has to be made indirectly.

Extreme faunal provincialism necessitated the establishment of different regional scales throughout most of the Cretaceous, and these regional scales were commonly nonstandardized among publications. To partially rectify this situation, the grouping of ammonoid datums into zones and subzones has undergone significant revisions since 1990. Only a few of the Cretaceous ammonoid zones compiled by Hancock (1991) are currently used by the various Cretaceous working groups (e.g., Rawson et al., 1996b; Reboulet et al., 2011, 2018). The relative grouping into zones also varies among regions and stages. For example, many of the high-resolution “zones” of the western interior of North America would be classified as “horizons” in the broader zonal schemes used in Europe.

In particular, the IUGS Lower Cretaceous Working Group (Kilian Group) for the Lower Cretaceous has been striving to develop a systematic zonation for the Tethyan region that can be applied over large regions (Hoedemaeker et al., 1993; Reboulet et al., 2006, 2009, 2011, 2018). In particular, the new schemes have a more logical nomenclature in which most of the revised zones begin with the first occurrence of the index species. This is in contrast to the irregular association of zonal spans with their “index” taxa in the “traditional” schemes for Cretaceous and still used for much of the Jurassic. As a result, the current Tethyan zonation for Berriasian through Albian has only a few zonal names in common with the Lower Cretaceous zonation in Hardenbol et al. (1998) or even in GTS2004. For example, the uppermost Albian “classic *Stoliczkaia dispar* Zone,” which had varying definitions among different authors, is replaced by elevating its subzones to zone status (summarized by Kennedy in Gale et al., 2011). These zones are cross-calibrated to microfossil datums and cycle stratigraphy in southeastern France (Gale et al., 2011). The “Kilian Group” is undertaking the challenging task of correlating the revised Tethyan scales to the Boreal ammonite zonations.

This revision of zone definitions, taxonomic changes in general assignment of index species, and extensive high-resolution subzonal divisions will simplify and standardize correlations, but will undoubtedly lead to confusion when trying to decipher zonal scales in older literature. Another problem is that details of reference sections for these revised and enhanced zonations have not yet been published; therefore it is uncertain how to correlate other microfossil, geochemical, and paleomagnetic stratigraphy to the zones. Estimates of zonal durations with the revised definitions also require precise placement onto the existing reference sections that had been used for strontium-isotope trends and

cycle stratigraphy. Estimates of the placement of these renamed/redefined zones relative to the former “intercalibrated” ammonite zones were used to make an approximate age model.

Ammonites suffer from a further problem, as they are only rarely preserved, or completely absent in the widespread white chalk facies developed from the Turonian to Maastrichtian stages across northern Europe and eastwards into central Asia. Their preservation in these facies usually depends upon early diagenetic hardening preceding aragonite dissolution in hardgrounds and nodular chinks. Thus standard international ammonite stratigraphy can only be applied very coarsely to the white chalk (Turonian–Maastrichtian) of the Anglo–Paris Basin, for example.

A detailed ammonite zonation for the Cenomanian through lower Maastrichtian of the North American Western Interior has been standardized by Cobban (1993) and Cobban et al. (2006). However, many of the North American ammonite taxa are endemic to the region, which creates problems for wider correlation, and for interpolation of radioisotopic dates into other regions. Occasional records of Western Interior and Gulf coast ammonites in European and African successions do provide useful evidence. For example, the occurrences of the Gulf coast Cenomanian genus *Budaiceras* in Normandy, France (Kennedy et al., 1990) in an assemblage of *Mantelliceras dixonii* Zone age is a valuable correlation tie-point, as is the occurrence of the Western Interior Lower Cenomanian species *Metengonoceras teigense* in Normandy (Amédéo et al., 2002). Records of the North American Middle Cenomanian species *Acanthoceras amphibolum* in Tunisia (Robaszynski et al., 1990) and Nigeria (Zaborski, 1985) also provide important links. Likewise, the remarkable occurrences of North American Turonian ammonites at Uchaux in southern France allow important correlations to be made (Robaszynski et al., 2014). For the Turonian to Maastrichtian the co-occurrences of inoceramid taxa in North America and Europe (Walaszczyk and Cobban, 2000, 2001, 2007, 2016) has enabled correlation of most European ammonite zones (and other marine macrofossils) to the North American ammonite zonation.

27.2.1.2 *Inoceramid bivalves*

Benthonic pteriomorph bivalves of the family Inoceramidae, which first appeared in the Jurassic and went extinct in the mid-Maastrichtian, are a locally rock-forming group in the Upper Cretaceous, and their rapid evolution and widespread distribution provide a detailed zonal scheme for the Albian to Maastrichtian stages. Their shells comprise an outer prismatic calcite layer, ubiquitously preserved, and an inner nacreous one composed of aragonite, which is usually not

normally preserved in sandstones and limestones. They thus partially compensate for the absence of ammonites in sediments such as chalk, in which dissolution on or in the seafloor has removed taxa which possess aragonitic shells (see above). Inoceramids occupied a considerable diversity of habitats, from deep-water dysaerobic muds, chalks, to shallow marine sandstones, but were largely absent from carbonate platforms. The exceptionally widespread occurrence of species, often effectively global, and relatively low endemism (except in New Zealand) makes them excellent fossils for interregional correlation. Inoceramid stratigraphy had advanced considerably over the last decade, largely thanks to taxonomic revision and increased collecting. The Albian genus *Actinoceramus* provides high-resolution global correlation across the Middle–Upper Albian transition (Crampton and Gale, 2005, 2009). Important additional references are Walaszczyk and Cobban (2000, 2001, 2007, 2016), and Walaszczyk et al. (2001, 2002, 2010, 2016). A standard zonation is presented here based on this work.

27.2.1.2.1 Planktonic microcrinoids

Cretaceous microcrinoids belonging to the Roveacrinida were tiny, pelagic organisms that were common from the Albian to Maastrichtian in open marine sediments, locally occurring in rock-forming abundance. Although species have been used locally to characterize intervals, it has recently become apparent that they are far more diverse and widely distributed than previously thought (Gale, 2016, 2017, 2019a,b). Their rapid evolution and widespread distribution offer considerable potential for interregional correlation, and a series of zones have been proposed for the Albian to Campanian interval (Gale, 2017, 2019a; see also Ch. 3K: Cretaceous microcrinoids (this book)).

27.2.1.2.2 Other marine macrofauna

Workers on chalk facies successions have also employed zonations based upon diverse calcitic fossils, including benthonic crinoids, echinoids, and brachiopods. Most of these schemes have only local (basin-scale) application, but Campanian and Maastrichtian microbrachiopod zones can be applied for high-resolution correlation across northern Europe (Surlyk, 1984). The stemless crinoids of the genera *Uintacrinus* and *Marsupites* have short ranges and global distribution and are very useful fossils in interregional correlation (Gale et al., 2007).

The correlation of shallow-water carbonate platforms is achieved using larger benthonic foraminifers, calcareous algae, and rudist bivalves. The latter group is highly diverse and of considerable value in correlation (Masse and Philip, 1998; Steuber et al., 2016). These groups were strongly affected by OAEs, such that in the latest Cenomanian.

Belemnites have been used quite widely for stratigraphical correlation in the Cretaceous. The belemnite assemblages of the Kimmeridgian to Barremian interval show a distinctive provincialism. The Tethys was characterized by representatives of the Duvaliidae and Belemnopseidae, the Boreal Realm was dominated by *Cylindroteuthidae* (e.g., Combemorel and Christensen, 1998; Mutterlose et al., 1996; Mutterlose and Böckel, 1998; Dzyuba et al., 2013). This paleobiogeographic situation changed entirely in the Aptian, when the boreal *Cylindroteuthidae* and the Tethyan Duvaliidae went extinct. They were globally replaced by *Neohibolites*, which experienced a major radiation.

For the Tethys no precise zonation schemes are available, the stratigraphic resolution of specific taxa is on the scale of a substage. Detailed belemnite zonation schemes exist for the Boreal–Atlantic and Boreal–Arctic Provinces of the Boreal Realm. For the Berriasian–Hauterivian succession of the Boreal–Atlantic Province (northwest Europe) six belemnite zones, based on different species of the genera *Acroteuthis* and *Hibolithes*, have been recognized. The Barremian can be subdivided into five belemnite zones, defined by species of a biometrically well-defined evolutionary lineage. The genera *Oxyteuthis* and *Aulacoteuthis* allow thereby a detailed biozonation of the Barremian, which otherwise is difficult to subdivide. The Berriasian–Hauterivian assemblages of the Boreal–Arctic province are characterized by taxa attributed to *Cylindroteuthis*, *Arctoteuthis* and *Simobelus*. The Aptian–Albian of the Boreal Realm can successfully be subdivided into nine belemnite zones using species of *Neohibolites*.

Belemnites of the family Belemnitellidae occur from the Cenomanian to Maastrichtian stages and are used extensively in Boreal Upper Cretaceous chalk successions of northern Europe, and some species also occur less frequently in North America. The family displayed considerable provinciality, and Central European and Central Russian subprovinces are recognized, the latter extending far eastwards into central Asia (Christensen, 1990, 1996, 1997a,b). A few species show short-term extensions into northern Tethys. Belemnites are particularly important in the biostratigraphy of the Boreal chalks of Campanian and Maastrichtian range, with the genera *Goniotteuthis*, *Belemnitella* and *Belemnella* displaying evolutionary changes which permit development of a refined zonation (Combemorel and Christensen, 1998).

27.2.1.2.3 Planktonic foraminifera

Planktonic foraminifera originated in late Early Jurassic (e.g., Hart, 1980; Caron, 1983; Gradstein et al., 2017) and only underwent radiation and geographic spreading from mid-Cretaceous onward. In general, planktonic foraminifera from Berriasian to Barremian have a scattered geographic and stratigraphic record. A progressive increase

in abundance and diversification of genera and species is observed from the mid-Barremian (Aguado et al., 2014) to the Aptian (Premoli Silva and Sliter, 1999). The major turnover observed across the Aptian–Albian boundary interval represents the most dramatic event in the Cretaceous evolutionary history of planktonic foraminifera after the mass extinction at the Cretaceous/Paleogene (K/Pg) Boundary (e.g., Leckie et al., 2002; Huber and Leckie, 2011; Petrizzo et al., 2012, 2013; Kennedy et al., 2014). During the early to middle Albian planktonic foraminifera diversified rapidly with the continuous increase in morphological complexity and the appearance of newly evolving lineages all characterized by novel morphological and wall texture features.

The Early Cretaceous biozonal scheme currently adopted is based on the work by Moullade (1966) implemented and/or modified according to subsequent biostratigraphical studies or syntheses by Longoria (1977), Sigal (1977), Salaj (1984), Caron (1985), Gorbachik (1986), Banner et al. (1993), Coccioni and Premoli Silva (1994), Robaszynski and Caron (1995), BouDagher-Fadel et al. (1997), Moullade et al. (2005), and Premoli Silva et al. (2018).

The subsequent pattern of evolutionary changes in the planktonic foraminifera from the Cenomanian to the Turonian corresponds to increased speciation and enlargement in test size of trochospiral keeled and unkeeled taxa and mirror the overall trend of rising sea level and global warming and increase of the density gradient within the surface water. After the maximum Late Cretaceous global Warmth registered in the early Turonian, and a relatively stasis from the late Turonian to the early–middle Coniacian, planktonic foraminifera underwent a major compositional changes in the late Coniacian–Santonian marked by high rates of species diversification and the appearance of newly evolved keeled, biserial, and multiserial taxa (e.g., Wonders, 1980; Caron and Homewood, 1983; Hart, 1999; Premoli Silva and Sliter, 1999). The radiation in the late Coniacian–Santonian time interval is followed by extinctions of some keeled taxa in the latest Santonian–earliest Campanian. In general, the Coniacian–Santonian time interval represents the transition from the mid-Cretaceous extreme greenhouse to more temperate climatic conditions in the Campanian–Maastrichtian that determined the onset of climatic bioprovinces. As a consequence, distinct biozonation schemes for the Tethyan, Boreal, Austral, and Transitional Provinces have been developed (e.g., Caron, 1985; Nederbragt, 1990; Huber, 1992; Premoli Silva and Sliter, 1999; Robaszynski and Caron, 1995; Li et al., 1999; Petrizzo, 2003; Campbell et al., 2004).

The Late Cretaceous biozonal scheme currently adopted is based on Caron (1966), Pessagno (1967), Robaszynski et al. (1984, 1990, 2000), Robaszynski and Caron (1979), Masters (1977), Robaszynski and Caron (1995), Premoli

Silva and Sliter (1995) and implemented and/or modified according to studies by Tur et al. (2001), Petrizzo (2000, 2001, 2003, 2019), Bellier and Moullade (2002), Lamolda et al. (2007), Petrizzo and Huber (2006), González-Donoso et al. (2007), Huber et al. (2008), Gale et al. (2011), Petrizzo et al. (2011, 2015, 2017), Pérez-Rodríguez et al. (2012), Elamri and Zaghbib-Turki (2014), Coccioni and Premoli Silva (2015), Haynes et al. (2015), Huber et al. (2017).

The taxonomy of Early and Late Cretaceous planktonic foraminifera is currently under revision using a more systematic and evolutionary framework by the Mesozoic Planktonic Foraminiferal Working Group that has produced a taxonomic database (pforams@mikrotax) available online at <http://www.mikrotax.org> (see Huber et al., 2016 for further details).

27.2.1.2.4 Benthonic foraminifera and calpionellids

A detailed suite of correlations of smaller and larger benthic foraminifera datums to ammonoid zones is partially established (e.g., Magniez-Jannin, 1995; Arnaud-Vanneau and Bilotte, 1998), although these zonations are mainly applicable to European basins.

Calpionellids are enigmatic pelagic microfossils with distinctive vase-shaped tests in thin-section. Calpionellids appeared in the Tithonian and vanished in the latest Valanginian or earliest Hauterivian (Remane, 1985), and their abundance in carbonate-rich shelf to basinal settings within the Tethyan realm enables biostratigraphic correlation prior to the increase in the diversity of planktonic foraminifera. Six standard zones (Allemann et al., 1971) with finer subdivisions (e.g., Remane et al., 1986) provide the basic framework for interregional correlation (summarized by Remane, 1998). There are variations upon this basic framework (e.g., Pruner et al., 2010), but a nomenclature using lettered-zones is a common system.

27.2.1.2.5 Calcareous nannofossils

The Cretaceous Period was named for the immense chalk formations that blanket much of northwestern Europe, and the main components of this chalk are calcareous nannofossils. Following their rapid surge in abundance at the end of the Jurassic (e.g., Caselleto et al., 2010), calcareous nannofossils remained ubiquitous throughout the Cretaceous and Cenozoic in all oceanic settings and sediments above the carbonate dissolution depth.

Calibration of major calcareous nannofossil datums to ammonoid zones or magnetic polarity zones is established for several intervals in the Tethyan and Boreal Realms (e.g., Lower Cretaceous of Tethyan realm by Bergen, 1994; Bralower et al., 1995; Erba et al., 1999; Channell et al., 2000, 2010); Lower Cretaceous of Subboreal–Boreal realm by Bown et al., 1998; Upper Cretaceous by Burnett et al., 1998;

von Salis, 1998; Huber et al., 2008; Corbett et al., 2014). The calibrations for the zonations are a synthesis of selected zonal scales and markers.

27.2.1.2.6 Organic and siliceous microfossils

Organic-walled cysts of dinoflagellates have been correlated directly to ammonoid zones in the Tethyan realm for Berriasian through Turonian, and in the Boreal realm for Berriasian through Aptian (compiled by Monteil and Foucher, 1998). In some intervals, these widespread dinoflagellate cysts have aided to resolve uncertainties in interregional correlations [e.g., earliest Cretaceous between Sub-Boreal and Boreal realms by Harding et al., 2011; Barremian–Aptian between Tethyan and Austral realms by Oosting et al., 2006].

Siliceous radiolarians (pelagic sediments), charophytes (brackish-water algae tests), and calcareous algae have a relatively lower resolution set of datums and zones compared to other Cretaceous microfossil groups (e.g., respective syntheses by De Wever, 1998; Riveline, 1998; Masse, 1998). Siliceous diatoms evolved in the Jurassic but did not undergo a major evolutionary radiation until the mid-Cretaceous, especially after the Cenomanian–Turonian boundary (e.g., Round et al., 1990; Sinninghe Damsté et al., 2004).

27.2.2 Terrestrial biostratigraphy

It is beyond the scope of this chapter to make a thorough review of terrestrial biostratigraphy, and only a few highlights will be mentioned. Authoritative books on this topic include Lucas et al. (1998), Woodburne (2004), and Kemp (2005).

Dinosaurs, the most renowned group of Cretaceous vertebrates, provide only a broad biostratigraphy (Lucas, 1997). Early Cretaceous sauropods were smaller, but ornithopods (such as *Iguanodon*) were larger than their Jurassic cousins. Stegosaurids, iguanodontids, hypsilophodontid ornithopods and sauropods (except in South America) were nearly extinct by the end of the Early Cretaceous. The rapid diversification of angiosperms (flowering plants) displaced gymnosperms in the mid-Cretaceous and was probably a major factor in the evolution of the suite of hadrosaurid ornithopods, ceratopsians and ankylosaurid browsers. This suite and their tyrannosaurid and coelurosaurian theropod predators were dramatically terminated at the end of the Cretaceous.

The Yixian Formation in China is famous for the well-preserved Jehol Biota (plants, birds, terrestrial life). Radioisotope dating suggests a Barremian to early Aptian age for the main Yixian Formation fossil localities. The Jehol Biota and other localities indicate that placental and marsupial mammals appeared in the later part of the Early Cretaceous. The North American mammal age

“Judithian” began in early Campanian (e.g., Jinnah et al., 2009), and the earliest NALMA of “Aquilan” is possible of Santonian age.

27.2.3 Physical stratigraphy

27.2.3.1 Magnetostratigraphy

27.2.3.1.1 Cretaceous portion of M-sequence

The M-sequence of marine magnetic anomalies formed from the Late Jurassic to the earliest Aptian. Several biomagnetostratigraphic studies have correlated Early Cretaceous calpionellid, calcareous microfossil, and dinoflagellate datums to the M-sequence polarity chrons (e.g., Channell and Grandesso, 1987; Channell et al., 1987, 1993, 1995b, 2000, 2010; Ogg, 1987, 1988; Speranza et al., 2005; Pruner et al., 2010). Correlation of Tethyan ammonite zones to the M-sequence have been achieved for the Berriasian spanning Chrons M18–M15 (Galbrun, 1984), the Berriasian–Valanginian boundary interval spanning M15–M13 (Ogg et al., 1988; Aguado et al., 2000), and less-precise calibrations for portions of the Hauterivian–Barremian interval of Chron M10N to M1 (Cecca et al., 1994; Channell et al., 1995a; Sprovieri et al., 2006). Cycle-calibrated durations of polarity zones in some of these sections indicate a fairly constant spreading rate for the Hawaiian magnetic lineations during the Valanginian through Barremian (e.g., Sprovieri et al., 2006). Polarity zone M0r is a primary marker associated with the proposed GSSP at the base of the Aptian. Andesite volcanic beds in the lower Yixian Formation of China, which are interpreted as eruptions during a reversed-polarity episode, have an Ar–Ar date of 122.0 ± 0.5 Ma (He et al., 2008), which may indicate a correlation to either Chron M0r or M1r in the GTS2020 age model. When coupled with a spreading rate model for the Pacific magnetic lineations within each individual stage (see Ogg, 2020, Ch. 5: Geomagnetic polarity time scale, this book), these correlations partly constrain the relative duration of each ammonite zone within the Berriasian, Hauterivian and Barremian stages.

Correlation of Boreal ammonite zones to the M-sequence has been directly achieved only for the equivalent of uppermost Tithonian and Berriasian in Siberia (Houša et al., 2007) and indirectly for the equivalent of the Berriasian Stage in the Purbeck beds of southern England (Ogg et al., 1991, 1994).

27.2.3.1.2 Reported brief subchrons within Aptian and Albian

An extended 40-Myr normal-polarity Chron C34n or “Cretaceous Normal Polarity Superchron” spans the early Aptian through middle Santonian. Brief reversed-polarity chrons have been reported from three intervals—middle Aptian, middle Albian, and mid-late Albian—especially within drilling cores of deep-sea sediments. However,

none of these proposed subchrons have been unambiguously interpreted from marine magnetic anomaly surveys nor have M''-2r'' or M''-3r'' been verified in outcrop sections. The following summary is revised from GTS2012; and the reported possible placement relative to microfossil zones is illustrated in Fig. 27.9. Ryan et al. (1978) proposed a negative numbering for these three “pre-M0r” reversed-polarity events or clusters of events:

1. M''-1r'' in middle Aptian with a biostratigraphic age near the base of the *Globigerinelliodes algerianus* planktonic foraminifer zone (Pechersky and Khrumov, 1973; Jarrard, 1974; VandenBerg et al., 1978; Keating and Helsley, 1978a,b,c; Hailwood, 1979; VandenBerg and Wonders, 1980; Lowrie et al., 1980; Tarduno et al., 1989; Ogg et al., 1992). This subchron has also been called the “ISEA” event from an Italian outcrop sample code (Tarduno et al., 1989) and has an estimated duration of less than 100,000 years (Tarduno, 1990). Based on cycle stratigraphy, the base of this foraminifer zone is at approximately 122 Ma in the GTS2012.
2. M''-2r'' set of Middle Albian events near the boundary of the *Biticinella breggiensis* and *Ticinella primula* planktonic foraminifer zones (Keating and Helsley, 1978a; Jarrard, 1974; VandenBerg and Wonders, 1980; Tarduno et al., 1992; Shipboard Scientific Party, 1998; Ogg and Bardot, 2001).
3. M''-3r'' set in Late Albian (Green and Brecher, 1974; Jarrard, 1974; Hailwood, 1979), which may occur at the end of the *Praediscosphaera cretacea* or within the *Eiffellithus turriseiffeli* nannoplankton zones (Tarduno et al., 1992).

Another reversed-polarity event, possibly near the Aptian–Albian boundary, has been reported within basal flows with a radioisotopic date of 113.3 ± 1.6 Ma (Gilder et al., 2003) but has not yet been verified by other studies.

27.2.3.1.3 Cretaceous portion of C-sequence

Polarity Chrons C33r through lower C29r have been correlated to microfossil and nannofossil datums from basal Cenomanian to the base of the Cenozoic (e.g., Alvarez et al., 1977; Lowrie and Alvarez, 1977; Huber and Leckie, 2011). This polarity time scale has been partly calibrated in the North American Western Interior seaway to regional ammonoid zones and an array of $^{40}\text{Ar}/^{39}\text{Ar}$ dates from bentonites (e.g., Obradovich, 1993; Hicks and Obradovich, 1995; Hicks et al., 1995, 1999; Lerbekmo and Braman, 2002), and Chrons C32–C29 have been scaled from cycle stratigraphy in ocean-drilling cores (Herbert et al., 1995; Husson et al., 2011; Thibault et al., 2012) (see tables in Chapter 5: Geomagnetic polarity time scale, and Speijer et al., 2020, Ch. 28: The Paleogene Period, this book). The base of Chron C33r was reported as being within

the regional “upper Santonian” of England (Montgomery et al., 1998), but this polarity reversal is now being considered to mark the base of the Campanian. The ages on the Campanian–Maastrichtian portion of the C-sequence constrain the synthetic age-distance model for the magnetic anomalies of the South Atlantic (revised from Cande and Kent, 1992, 1995; see Ogg, 2020, Ch. 5: Geomagnetic polarity time scale, this book).

27.2.3.2 Geochemical stratigraphy

27.2.3.2.1 Carbon stable isotopes and carbon-enrichment episodes

Several significant excursions in the carbon cycle, called OAEs, punctuate the Cretaceous stratigraphic record, of which the early Aptian OAE1a and latest Cenomanian OAE2 events are the most significant global events (Jenkyns, 2010). Many of the major excursions (> 1.5 per mil) in $\delta^{13}\text{C}$ are associated with widespread organic-rich sediments and changes in facies indicating drowning of carbonate platforms, and many appear to be preceded by or coincide with the eruption of major flood basalts (large igneous provinces: LIPs) that provided a source of the excess carbon (e.g., reviews and syntheses by Weissert et al., 1998; Jenkyns, 1999, 2010, 2017; Larson and Erba, 1999; Erba, 2004; Wortmann et al., 2004). In some cases, relatively elevated concentrations of mercury in black shales are considered a fingerprint of coincident volcanic activity (e.g., Scaife et al., 2017). The middle Cretaceous concentrations of black shales, which are the source rocks for over a quarter of current hydrocarbon deposits, were originally considered as indications of widespread oceanic anoxia (e.g., Schlanger and Jenkyns, 1976; Jenkyns, 2017). Enhanced oceanic productivity and carbon flux to the seafloor, perhaps in response to ultra-greenhouse conditions, as well as improved preservation of organic matter, are considered as first-order controls (e.g., Hochuli et al., 1999; Leckie et al., 2002; Jenkyns, 2010). The nomenclature for the main events is partly derived from distinctive European organic-rich horizons and some have an OAE numbering (Fig. 27.1).

1. *Weissert Event*. The Late Valanginian positive $\delta^{13}\text{C}$ excursion of ~ 2 per mil has an onset in the mid-Valanginian (base of *S. verrucosum* ammonite zone), peaks in the following *Neocomites peregrinus* ammonite zone, and returns to background levels at the beginning of the Hauterivian (Lini et al., 1992; Channell et al., 1993; Weissert et al., 1998; Martinez et al., 2015). The excursion approximately coincides with the early phases of eruption of the Paraná–Etendeka LIP of South America and Namibia (Erba et al., 2004; Martinez et al., 2015). The onset of this excursion is heralded by four thin organic carbon-rich layers (“Barrande” layers

- B1–B4) in the Vocontian basin of southeastern France (Reboulet, 2001; Reboulet et al., 2003).
2. **Faraoni Event.** A latest Hauterivian organic-enrichment episode during the *Pseudothurmannia catulloi* ammonite subzone (middle of *Pseudothurmannia ohmi* Zone) is documented by a pair of organic-rich sediments in Mediterranean and Atlantic pelagic sections (Bodin et al., 2006). It coincides with only a relatively minor positive $\delta^{13}\text{C}$ excursion (e.g., Baudin et al., 1997, 1999; Coccioni, 2003; Föllmi et al., 2006).
 3. **Selli Event (OAE1a)** with a complex $\delta^{13}\text{C}$ signature that begins in the Lower Aptian *Deshayesites forbesi* ammonite zone has been extensively studied. The organic-rich “Selli” event (called Goguel level in SE France) in the lower portion of the *Leopoldina cabri* foraminiferal zone is typically preceded by a sharp negative followed by a major positive excursion in $\delta^{13}\text{C}$ (e.g., Menegatti et al., 1998; Weissert and Lini, 1991; Weissert et al., 1998; Mutterlose and Böckel, 1998; Moullade et al., 1998b; Hochuli et al., 1999; Larson and Erba, 1999; Leckie et al., 2002; Renard et al., 2005) and a global nannoconid crisis, represented by a major decrease of these rock-forming calcareous nannofossils, precedes and continues through the main level of black shale (e.g., Erba, 1994, 2004). The beginning of this OAE1a Selli event appears to be synchronous with the main eruptive phase of the massive Ontong Java Plateau flood basalts in the eastern equatorial Pacific. The major positive-isotope excursion continues into the early Late Aptian. A relatively minor organic-rich “Noir” bed at the base of the Upper Aptian *E. martinoides* ammonite zone in the reference sections in southeastern France occurs at the level of the top of the main positive-isotope peak, and another minor “Fallot” organic-rich level occurs at a minimum in $\delta^{13}\text{C}$ near the top of that ammonite zone (Föllmi et al., 2006).
 4. **OAE1b cluster.** A complex multiphase set of mostly negative $\delta^{13}\text{C}$ excursions spanning the Aptian–Albian boundary interval contains widespread organic-rich layers in the reference sections of southeastern France—the Jacob, Kilian, Paquier (called Urbino in Italy), Leenhardt, and l’Arbouysse Events (Bréheret, 1988; Weissert and Bréheret, 1991; Herrle et al., 2004; Gale et al., 2011). The confusing designation of OAE1b has been applied either to all or to only part of this interval, especially the Paquier level. Cyclostratigraphic studies have quantified the placement of the Jacob, Kilian, and Paquier/Urbino events as approximately 36, 31, and 26.5 long-eccentricity 405-kyr cycles prior to the base-Cenomanian, respectively (e.g., Fiet et al., 2001; Grippo et al., 2004; Huang et al., 2010; Gale et al., 2011).
 5. **Jassines Event (Gale et al., 2011),** Middle Albian, possibly correlative with OAE1c of authors, which may or may not correspond with the organic-rich “Amadeus” layer (after Mozart) or “Toolebuc” level (e.g., Leckie et al., 2002; Coccioni, 2003).
 6. **Albian–Cenomanian Boundary Event (Jarvis et al., 2006; Gale et al., 2011),** a series of four positive $\delta^{13}\text{C}$ excursions called the Albian/Cenomanian Boundary Event (the lower part coinciding locally with a set of organic-rich “Breistroffer” or “Pialli” layers). The record of this event extends from the *perinflatum* Subzone of the Albian to the *M. mantelli* Zone of the Cenomanian: it has been referred to as OAE1d (Gambacorta et al., 2015).
 7. **Middle Cenomanian Event.** A minor but distinctive, brief double positive peak is widely recognized in the *C. inerme* and basal *A. rhotomagense* zones in Europe and North America (Jenkyns et al., 1994; Paul et al., 1999; Coccioni and Galeotti, 2003; Gale et al., 2007; Zheng et al., 2016; Eldrett et al., 2015) and is also found in Tibet (Li et al., 2006). This interval is locally represented by a thin, laminated dark marl in Tethyan sections (Gale, 1995).
 8. **OAE2 (Bonarelli Event, Thomel Event).** Cenomanian–Turonian boundary excursion spans the *Metoicoceras geslinianum* to *W. devonense* ammonite zones, with the peak in uppermost Cenomanian (e.g., Schlanger et al., 1987; Jenkyns et al., 1994; Kerr, 1998; Jenkyns, 1999, 2010; Jarvis et al., 2011; Gale et al., 2019a). The associated organic-rich levels are named Bonarelli in central Italy, Thomel in southern France, and Bahloul in Tunisia. The excursion has a distinctive form, comprising an initial rapid rise in $\delta^{13}\text{C}$ values, locally with minor positive excursions (the precursor events), then a brief fall, which coincides with the southerly migration of a Boreal fauna (the Plenus Cold Event; Gale and Christensen, 1995; Zheng et al., 2013; O’Connor et al., in press), and subsequent rise to a plateau in the upper *geslinianum* and *juddii* zones, and fall into the lowermost Turonian. Above the Cenomanian–Turonian boundary, detailed study of the English chalk provided a very high-resolution carbon-isotope succession up to the level of the lower Campanian, including numerous minor excursions, many of which were named (Gale et al., 2008; Jarvis et al., 2006). The discovery that the same excursions are present in the Western Interior Basin (Joo and Sageman, 2014) and in Japan (Takashima et al., 2019) significantly increases their correlative value. The carbon-isotope stratigraphy of the Campanian and Maastrichtian was described in detail by Voigt et al. (2012) from sections in central Italy, northern Germany, southwest France, and eastern England.
 9. **Holywell Event (Jarvis et al., 2006).** A short, but distinctive positive excursion in the low Turonian *Fagesia catinus* Zone, which goes against the trend of overall falling values after OAE2. This is recorded widely, from the United Kingdom (Jarvis et al.,

- 2006), western France (Kennedy and Gale, 2015), southern France (Gale et al., 2019a), the Western Interior of the United States (Joo and Sageman, 2014), and Japan (Takashima et al., 2019).
10. *Round Down Event* (Jarvis et al., 2006). A minor positive carbon-isotope excursion (+0.4 ppt) in the mid-Turonian, marking the base of a significant overall fall in $\delta^{13}\text{C}$ values, falls approximately at the base of the *Romaniceras ornatissimum* ammonite zone.
 11. *Pewsey Event* (Gale et al., 2008; Jarvis et al., 2006). A minor positive $\delta^{13}\text{C}$ excursion low in the Upper Turonian (*S. neptuni* Zone) set against an overall falling trend. It is identified in Germany (Wiese and Kaplan, 2001), the Western Interior Basin (Joo and Sageman, 2014), and Japan (Takashima et al., 2019).
 12. *Hitch Wood Event* (Gale et al., 2008; Jarvis et al., 2006). A major positive carbon-isotope excursion in the Upper Turonian, with the peak in the upper *S. neptuni* Zone. The event is also present in northern Germany (Wiese, 1999), Spain and Italy (Stoll and Schrag, 2000), Japan (Takashima et al., 2019), and the Western Interior Basin (Joo and Sageman, 2014), and Japan.
 13. *Navigation Event*. A broad negative $\delta^{13}\text{C}$ excursion whose minimum falls in the uppermost Turonian *Forresteria petrocoriense* Zone (Jarvis et al., 2006) at the level of the Navigation Marls in the United Kingdom succession. Recorded possibly in the Western Interior Basin (Joo and Sageman, 2014) and Japan (Takashima et al., 2019).
 14. *White Fall Event* (Jarvis et al., 2006). There is an overall rise in values through the Lower and Middle Coniacian, which culminate in a peak within the lower part of the range of the inoceramid *Volviceramus involutus*. Recorded in the Western Interior Basin (Joo and Sageman, 2014).
 15. *Horseshoe Bay Event* (Jarvis et al., 2006). A minor but distinctive positive event that occurs beneath the FO of *Uintacrinus*. It is also identified in northern Germany and at Gubbio (Thibault et al., 2016).
 16. *Buckle Event* (Jarvis et al., 2006). A minor but distinctive negative $\delta^{13}\text{C}$ excursion that occurs at the base of the *U. socialis* Zone in England and Germany and can also be identified at Gubbio, Italy (Thibault et al., 2016).
 17. *Santonian–Campanian Boundary Event* (Jarvis et al., 2006; Thibault et al., 2016). A double positive $\delta^{13}\text{C}$ excursion of nearly 1‰ that occurs within and just above the *Marsupites* zones. Also identified in the WI Basin (Joo and Sageman, 2014), in northern Germany and at Gubbio (Thibault et al., 2016) and in Japan (Takashima et al., 2019).
 18. *Late Campanian Event* (Voigt et al., 2012). A distinctive negative excursion, partly coterminous with the *R. calcarata* Zone, has been found extensively in Europe, from Germany and Denmark, the Trunch borehole, the United Kingdom, Tercis, France, Gubbio, Italy, and Tibet (Li et al., 2006).
 19. *Campanian–Maastrichtian Boundary Event* (Voigt et al., 2010, 2012). A prominent negative carbon-isotope shift lasting approximately 2.5 Myr, with a detailed structure, which has been recorded extensively across northwest Europe (Germany, Denmark, the United Kingdom), at Gubbio, Italy, and is recorded from both the Pacific and Atlantic Oceans.
 20. *Mid-Maastrichtian Event*. Lower Maastrichtian values climb to a double $\delta^{13}\text{C}$ peak, close to the base of magnetochron C31n, between the LO of *Rheinhardites laevis* and the FO of *Lithrapidites quadratus* (Voigt et al., 2012).
 21. *K–Pg Event*. The K–Pg boundary is associated with a short-lived negative $\delta^{13}\text{C}$ excursion (Voigt et al., 2012).
- OAE3, initially described by Scholle and Arthur (1980), has been described from the Atlantic region (Wagerich, 2012) and identified in the Upper Coniacian of the Western Interior Basin by Joo and Sageman (2014), but it is not a discrete event. In addition to the excursions listed above, Jarvis et al. (2006) named numerous minor carbon-isotope excursions within the Cenomanian to Campanian interval, the lateral extent of which is not known. Increasing numbers of studies on carbon-isotope stratigraphy will extend and refine the record in the near future.
- #### 27.2.3.2.2 Oxygen stable isotopes and other climate proxies
- In the Cenozoic, $\delta^{18}\text{O}$ provides an accurate record of oceanic temperature, but problems of diagenetic alteration of foraminiferan tests (Pearson et al., 2001; Wilson et al., 2002; see review by Pearson, 2012) mean that values have commonly been reset to cooler values, especially in older sediments. Work on exceptionally preserved “glassy” material demonstrates the great value of these (Huber et al., 1995, 2002). Although the actual temperature values derived from oxygen isotopes may be contentious, the trends are not, and when compared with data derived from the organic molecule TEX₈₆, provide an accurate record of Cretaceous climate trends (O’Brien et al., 2017). Additional evidence from cool-water indicators, such as pseudomorphs after ikaite, called glendonites, provide additional evidence of colder periods.
- Early work on bulk oxygen isotopes from the English chalk (Jenkyns et al., 1994) and phosphate from Israeli shark teeth (Kolodny and Raab, 1988) demonstrated a clear temperature pattern through the Late Cretaceous, with warming up to the Cenomanian–Turonian boundary, followed by gradual progressive cooling, which accelerated in the Maastrichtian. This pattern is now corroborated by data from TEX₈₆, and a much more extensive

$\delta^{18}\text{O}$ dataset extending back to the Aptian (O'Brien et al., 2017). The Early Cretaceous story is more problematic; $\delta^{18}\text{O}$ shows a progressive warming through the Albian and Cenomanian from low temperatures in the Late Aptian, whereas TEX_{86} demonstrates more variability, including a warm peak in the Early Aptian.

The occurrences of ikaite pseudomorphs in the Cretaceous have been taken as evidence of cool periods, because the mineral only forms at very low temperatures (Price, 1999). These occurrences are concentrated in the Valanginian, Aptian, Albian and Maastrichtian, and have been taken as supporting evidence for high-latitude glaciation during these intervals. This is supported by evidence for larger magnitude sea-level changes during these times (Ray et al., 2019).

27.2.3.2.3 Strontium and osmium isotope ratios

The marine $^{87}\text{Sr}/^{86}\text{Sr}$ record displays a progressive rise from the Berriasian to a maximum of 0.707493 in the Barremian *P. elegans* ammonite zone (see McArthur et al., 2020, Ch 7: Strontium isotope stratigraphy, this book). If one assumes that this was a quasilinear trend through the Valanginian and Hauterivian, then the relative duration of each ammonite zone and its subzones can be estimated from the reference sections in southeastern France (McArthur et al., 2007).

The Strontium-isotope ratio decreases to a pronounced minimum of 0.707220 just before the Aptian/Albian boundary, rises sharply during the early Albian, flattens to a broad maximum through the mid-to-late Albian, then declines to a late Turonian minimum of approximately 0.707275. From this Turonian minimum, it rises to 0.707830 at the end of the Cretaceous (Jones and Jenkyns, 2001).

These $^{87}\text{Sr}/^{86}\text{Sr}$ trends enable global correlation and relative dating (e.g., McArthur et al., 1993), except on the cusps of reversals [Aptian/Albian boundary, Late Turonian, middle Barremian (*sensu lato*) or where the curve is relatively flat (e.g., mid-to-late Albian)]. For example, the age of the Campanian–Maastrichtian was calibrated in GTS2004, using $^{87}\text{Sr}/^{86}\text{Sr}$ curve correlations between Kronsmoor, Germany, and the US Western Interior (chapter on Cretaceous in GTS2004).

27.2.3.3 Cyclostratigraphy

The ideal Cretaceous time scale encompasses a full record of the sedimentary expressions of every long (405 kyr) eccentricity cycle, the only available stable tuning target from the astronomical solution beyond 52 Ma (Laskar et al., 2011; Zeebe, 2017), with additional tie-points provided by the identification of very long (~ 1.2 or ~ 2.4 Myr) eccentricity minima in the geologic record. Currently, the construction of a fully 405 kyr tuned time scale for the Cretaceous is limited by (1) the availability of cyclic successions and the resolution of

cyclostratigraphic studies; (2) the difficulty in determining phase relationships between orbital forcing and sedimentary response; and (3) the availability of radioisotopic dates and difficulties in correlating cyclic successions to available numeric age control. Despite these challenges, there is increasing consistency between cyclostratigraphically obtained durations and available radioisotopic date control, as well as between cyclostratigraphic studies. This section presents the state-of-the-art of the Cretaceous astronomically tuned time scale with a selection of cyclostratigraphic studies used for the scaling of the GTS2020 bio-magnetostratigraphy. It is also important to note that lithological time-series are preferable to those based on $\delta^{13}\text{C}$, because lithology directly reflects climatic events, with no phase difference or lag time.

Cyclostratigraphy is only really of value in time scale construction when it is fully integrated with other well established stratigraphical data including magnetostratigraphy, biostratigraphy, and chemostratigraphy (Hilgen et al., 2014), and constrained by high-resolution radioisotopic dates.

27.2.3.3.1 Berriasian–Barremian Stages

Many important studies of cyclostratigraphy of this interval are based on the conspicuously rhythmic limestone–marl successions developed in the Vocontian Basin, SE France, and eastern Spain (e.g., Cotillon, 1987; Cotillon et al., 1980; Sprenger and ten Kate, 1993; Fiet et al., 2006; Martinez et al., 2012, 2013, 2015). However, problems exist with the Berriasian Stage in SE France, because of penecontemporaneous slumping (Pasquier and Strasser, 1997). In addition, the paper by Sprenger and ten Kate (1993) only studied approximately the uppermost third of what would now be considered to be Berriasian. The detailed studies of Martinez et al. (2012, 2013, 2015) identified a complete sequence of 405-kyr eccentricity cycles for the Valanginian and Hauterivian stages, which were fully integrated with ammonite, nannofossil, and carbon-isotope stratigraphy. The proposed durations from these studies for the Valanginian-Hauterivian stages and of Tethyan ammonite zones within those stages is used in GTS2020 (Fig. 27.9). Intercalibration to sections in Argentina with radioisotopic dates provide evidence that the Hauterivian–Barremian boundary fell at 126.07 ± 0.25 Ma. There is currently no reliable study on the cyclostratigraphical duration of the Berriasian Stage, but several studies provide a likely duration of 4–5 Myr (e.g., Kietzmann et al., 2015). Similarly, the entire Barremian Stage currently remains unstudied in detail, but there is evidence from cycle counting that the stage lasted approximately 5.1 Myr (Fiet et al., 2006). Cyclostratigraphy studies on Spanish reference sections have enabled a preliminary scaling of Tethyan ammonite zones of the Barremian (Martinez et al., 2020), and a modified version is used in GTS2020 (Fig. 27.9).

The cyclostratigraphic dataset from the Greenland–Norwegian sea used by Huang (2018) to calibrate the

Tithonian to Barremian interval remains unpublished, and the log does not show any primary bio- or chemostratigraphical data. Therefore we do not consider it in the present study.

27.2.3.3.2 Aptian–Aptian Stages

Much of the tuning of Aptian–Albian time has been based on the Piobboco core, drilled into pelagic and hemipelagic strata in the Umbria–Marche Apennines, central Italy (Herbert et al., 1995; Grippo et al., 2004). Grippo et al. (2004) used image-processed photos to generate spectra, and identified 26 405-kyr cycles through the Albian, with older levels providing only poor spectra (their Fig. 15). Gale et al. (2011) correlated the 405-kyr cycles into the succession of the Vocontian Basin with the aid of planktonic foraminiferans and used this to calibrate the duration of ammonite zones for the Albian and is used in GTS2020 (Fig. 27.9). The presence of 32 405-kyr eccentricity cycles in the Albian of the Piobboco core matches well radioisotopic estimates for the duration of the stage.

Huang et al. (2010) studied the lower part of the Piobbico core, and from the 405-kyr cycles which they identified estimated the base of the Aptian Stage (base of Chron M0r) to fall at 125.45 Ma. This date was subsequently modified by the changed estimate for the age of the base-Cenomanian and used in GTS2012 (Ogg et al., 2012) to place the base of the Aptian at 126.3 Ma. However, three independent lines of evidence cast doubt on this conclusion. The first is the placement of the Hauterivian–Barremian boundary, based on radioisotopic dates, at 126.02 Ma (Martinez et al., 2015). The second is new radioisotopic dates from the Svalbard, which place the Barremian–Aptian boundary at 121–122 Ma (Midtkandal et al., 2016). The actual date by Midtkandal et al. (2016) of 123.10 ± 0.3 Ma has now been revised by Zhang et al. (2019) to be of mid-Barremian age in the upper half of M1r, casting severe doubt on a 126 Ma age of Chron M0r. In addition, new spreading rate estimates change the date of the base Aptian (base of Chron M0r) to 121.5 Ma (Malinverno et al., 2012). There is evidently a problem with the cyclostratigraphical interpretation of the lower part of the Piobboco core. Ghirardi et al. (2014) applied cyclostratigraphy analysis to the middle Aptian interval of sections in the Vocontian Basin of SE France which have ammonite zones and carbon-isotope stratigraphy (Herrle et al., 2004; with revised ammonite zones by Lubber et al., 2017, 2019), and this scaling is used for the middle Aptian in GTS2020 (Fig. 27.9).

The duration of Oceanic Event OAE1a was estimated using cyclostratigraphy at 1.0–1.3 Myr (Li et al., 2008) with a rapid, short-lived initial negative excursion lasting between 27 and 44 kyr. The duration was further constrained by Malinverno et al. (2010) to 1.1 ± 0.11 Myr.

27.2.3.3.3 Cenomanian–Turonian Stages

Reliable radioisotopic dates for the base of the Cenomanian (99.8 ± 0.4 Ma; Obradovich et al., 2002, Japan), assigned on more evidence to 100.5 ± 0.14 Ma, and the base of the Turonian (93.9 Ma; Meyers et al., 2012) imply that the duration of the stage was near 6 Myr. Cyclostratigraphic estimates of the duration of the Cenomanian based on the pelagic succession in the Italian Apennines vary from 6.0 ± 0.5 (Herbert et al., 1995) to 5.4 Myr (Sprovieri et al., 2013). The estimate of Gale (1995) of 4.45 Myr was based on sections that are now known to contain multiple hiatuses. Gale et al. (1999) estimated the Middle and Late Cenomanian to span 3 Myr.

Several cyclostratigraphic studies (Batenburg et al., 2016; Gale et al., 1999; Eldrett et al., 2015) estimate the duration between the onset of the carbon-isotope excursions accompanying the mid-Cenomanian event (MCE) and OAE2 at 1.9–2.0 Myr. Duration estimates for the OAE2 itself are more problematic, as many sedimentary environments with rhythmic deposition experienced a strong change in oxygenation, resulting in potential hiatuses in the lithologic record. Nevertheless, recent duration estimates between the start of the carbon-isotope excursion and the Cenomanian–Turonian boundary range from 430 to 560 kyr with most estimates around 500 kyr (Batenburg et al., 2016; Eldrett et al., 2015; Ma et al., 2014; Meyers et al., 2012; Sageman et al., 2006; Takashima et al., 2019; Voigt et al., 2008). The combined estimated duration between the MCE and the Cenomanian–Turonian boundary of ~ 2.4 Myr agrees well with radioisotopic date constraints on the first positive peak of the MCE of 96.21 ± 0.36 Ma (Batenburg et al., 2016), and the Cenomanian–Turonian boundary of 93.90 ± 0.15 Ma (Meyers et al., 2012). The Cenomanian–Turonian boundary falls near the maximum of 405-kyr cycle 232 (Batenburg et al., 2016) of the La2011 astronomical solution (Laskar et al., 2011). Gale (2019b) tentatively identified 405-kyr cycles in the Anglo–Paris Basin, using repetitive marly levels in the chalk succession, guided by radioisotopic dates correlated in from the Western Interior of the United States with ammonites. The upper limit of the Turonian Stage was discussed by Ma et al. (2019) on the basis of cyclostratigraphic analysis of the Iona (89.52 ± 0.17 Ma) and Libsack (89.75 ± 0.38 Ma) cores. Sprovieri et al. (2013) obtained a similar duration of the Turonian stage in the Gubbio section based on time-series analysis of $\delta^{13}\text{C}$ data.

27.2.3.3.4 Coniacian–Santonian Stages

Borehole-resistivity and lithostratigraphy of the Niobrara Formation of the Western Interior Basin tied to North American ammonite zones in coeval outcrops have been tuned to short- and long-eccentricity cycles (Locklair and Sageman, 2008; Sageman et al., 2014). The Coniacian

stage spans 3.4 ± 0.13 Myr, and the Santonian spans 2.39 ± 0.15 Myr. In the southern English chalk, Thibault et al. (2016) tuned a long time-series of carbon-isotope data through the upper Coniacian to lower Campanian and identified five 405 kyr in the Santonian, giving it a duration of approximately 2.25 Myr. Thibault et al. (2016) also matched the record to the La2011 solution in an attempt to anchor the floating time scale.

27.2.3.3.5 Campanian and Maastrichtian Stages

The Campanian is relatively poorly constrained by cyclostratigraphic studies, due to the long length of the stage, the paucity of rhythmic records, and difficulties in correlation due to provincialism of faunas and an absence of major climatic events. The long cyclostratigraphic record of the Western Interior (Sageman et al., 2014) extends four 405-kyr cycles upward into the Campanian, and the Umbria–Marche Basin record 12 (Sprovieri et al., 2013). From the Maastrichtian downward, the 405 kyr interpretation of Site 762C extends 6 405-kyr cycles into the Campanian (Husson et al., 2011) and a composite of German successions spans the topmost 14 405-kyr cycles (Voigt and Schonfeld, 2010), leaving a gap in the middle Campanian. Rhythmic limestone–marl alternations from the Mississippi embayment (O'Connor et al., 2020) span the middle Campanian, but the succession is condensed near the upper and lower stage boundaries. Nevertheless, their estimated duration of the Campanian of 12 Myr (O'Connor et al., 2020) is in good agreement with existing estimates. For the Maastrichtian, independent cyclostratigraphic studies (Batenburg et al., 2012, 2014, 2018; Husson et al., 2011; Thibault et al., 2012; Wu et al., 2014) are in good agreement, supporting a duration of the Maastrichtian stage of 6.1 Myr. The top of the Maastrichtian is anchored to the intercalibrated K/Pg boundary, placed at 66.04 (Renne et al., 2013). Kuiper et al. (2008) identified the K/Pg as representing a 405-kyr minimum, which can be correlated to the base of 405-kyr eccentricity cycle 163 in the La2011 solution (Laskar et al., 2011).

27.2.3.4 Sequence stratigraphy

Cretaceous marginal-marine to deep-shelf successions in Europe and North America record an abundance of basinal and regional transgressions and regressions. At the largest scale, the Cretaceous strata encompass a single transgressive–regressive cycle (the “North Atlantic” cycle of Jacquin and de Graciansky, 1998). The lower boundary is a widespread unconformity during Late Berriasian, the transgression peaked in the Early Turonian, and average sea levels continued to decrease into the Paleocene.

The common features from an extensive suite of compilations edited by de Graciansky et al. (1998) were assembled in a comprehensive synthesis and systematically numbered from the base of each stage (Hardenbol et al., 1998). Coeval emergent horizons recorded by Aptian–Albian seamount carbonate platforms in the central Pacific Ocean imply that some of these depositional sequences reflect global eustatic sea-level oscillations (Röhl and Ogg, 1996). Detailed analysis of facies successions and biostratigraphic constraints across the Arabian Plate yielded a detailed sequence stratigraphy for the Cretaceous (e.g., Sharland et al., 2001, 2004; Simmons et al., 2007; van Buchem et al., 2011), in which many of the main features appear to coincide with the European–American-derived sequence scale. These compilations and additional reference sections were synthesized and recalibrated by Haq (2014) into a revised eustatic and coastal onlap curve for the Cretaceous (used in Fig. 27.1). The magnitude and cause of these sea-level changes during the presumed “supergreenhouse” of the mid-Cretaceous remain controversial (e.g., Miller et al., 2003, 2004), and many features require additional verification and documentation in multiple reference sections. See also review in Simmons et al. (2020, Ch. 13: Phanerozoic eustasy, this book).

Details of the Cretaceous sequence stratigraphy are continually undergoing refinement, but the major global oscillations have probably been identified. The main large-scale deepening and shallowing trends from the sequence stratigraphy charts (Hardenbol et al., 1998; Haq, 2014) are summarized in Fig. 27.9.

27.2.3.5 Other major stratigraphic events

27.2.3.5.1 Large igneous provinces

At least five major LIPs formed during the Cretaceous. Most of these appear to be associated with major distortions in the global carbon budget as indicated by excursions in carbon isotopes, widespread organic-rich shales or “OAE” episodes, increased oceanic carbonate dissolution, and other changes in climate and oceanic chemistry (e.g., Larson and Erba, 1999; Jones and Jenkyns, 2001; Bice et al., 2002). Age constraints and possible feedbacks from these episodes are reviewed by Wignall (2001) and Courtillot and Renne (2003); and selected ages are summarized in Tables 27.2 and 27.3.

1. *Paraná–Etendeka*, ~ 136 – 133 Ma. The early stages of rifting of the South Atlantic were accompanied by extrusion of a LIP onto South America (Paraná flood basalts) and smaller fields in Namibia (Etendeka Traps). The full suite of volcanic activity may have had multiple pulses that spanned over 10 Myr, but the main pulse of tholeiitic volcanism appears to be between 135

and 133 Ma (e.g., Stewart et al., 1996; Gibson, 2006; Gibson et al., 2006, dates are after adjustment to a $^{40}\text{Ar}/^{39}\text{Ar}$ FCS (Fish Canyon sanidine) monitor age of 28.20 Ma). The central Paraná volcanic suite spans a minimum of a triplet of polarity zones (normal-reversed-normal) (Mena et al., 2006). The onset of the northern and western Paraná volcanics from U–Pb dating of baddeleyite/zircon is 134.3 ± 0.8 Ma (Janasi et al., 2011). The onset and main eruptive phase of the Paraná–Etendeka flood basalts coincides with the late Valanginian “Weissert” C-13 positive excursion (e.g., Weissert et al., 1998; Erba et al., 2004), which has a GTS2020 age assignment of ~ 135 to 133 Ma (Fig. 27.1).

2. *Ontong Java Plateau–Manihiki Plateau*, ~ 125 – 123 Ma. During the middle of the early Aptian, the largest series of volcanic eruptions of the past quarter-billion years built the Ontong Java Plateau and Manihiki Plateau in the western equatorial Pacific. A series of deep-sea drilling legs documented that the multikilometer-thick series of volcanic flows forming the Ontong Java Plateau occurred during a short time span at ~ 125 – 122 Ma (e.g., Mahoney et al., 1993; Chambers et al., 2004). A controversial theory is that its initiation may have been caused by a bolide impact (Ingle and Coffin, 2004). The upper portions of the basalt flows are interbedded with pelagic sediments of the lower portion of the *L. cabri* foraminifer zone (Mahoney et al., 2001; Sikora and Bergen, 2004). A cascade of environmental effects from the eruption of the Ontong Java Plateau is the suspected culprit for the organic-rich deposits associated with the Early Aptian “OAE1a” or “Selli” episode which was followed by a large positive carbon-isotope excursion (e.g., Larson, 1991; Tarduno et al., 1991; Larson and Erba, 1999). However, the c. 120 Ma age for the main OAE1a in the revised GTS2020 age model is difficult to reconcile with the published dates for those Ontong Java Plateau basalts; therefore those radioisotopic dates should be reexamined.
3. *Kerguelen Plateau–Rajmahal Traps*, ~ 118 Ma. The Kerguelen Plateau in the southern Indian Ocean is the second largest oceanic plateau after the Ontong Java Plateau. The peak of construction of the southern and largest portion may have been simultaneous with the eruption of the formerly adjacent Rajmahal Traps of eastern India at ~ 118 Ma (reviewed in Wignall, 2001; Courtillot and Renne, 2003). This episode probably contributed to the broad carbon-isotope excursion that characterizes the late Aptian. A second eruptive episode at ~ 83 Ma enlarged the Kerguelen Plateau and constructed the Broken Ridge (Courtillot and Renne, 2003).
4. *Caribbean–Colombian Province*, ~ 90 Ma. The Caribbean–Colombian volcanic province is a large

Pacific Ocean plateau that was later emplaced between the North and South American plates. Its eruption may have contributed to the end-Cenomanian OAE2 carbon-isotope excursion (e.g., Kerr, 1998); however, its apparent average age of 89.5 ± 0.3 Ma coincides with the Turonian–Coniacian boundary (Courtillot and Renne, 2003).

5. *Deccan Traps*, ~ 66 – 65 Ma. The Deccan Traps cover most of central India. Their eruption peak at ~ 66 Ma coincides with the catastrophic termination of the Cretaceous (Courtillot and Renne, 2003).

In addition to these LIPs, pulses of large-scale volcanism constructed the Shatsky Rise in the central Pacific during the earliest Cretaceous (Mahoney et al., 2005), the Madagascar traps at ~ 87 Ma (Bryan and Ernst, 2008), and the Sierra Leone Rise in the central Atlantic at about 73 Ma (Ernst and Buchan, 2001; Large Igneous Provinces Commission, 2011).

27.2.3.5.2 Major bolide impacts

Five impact craters with diameters greater than 40 km are currently documented from the Cretaceous (details from Jourdan et al., 2009; Earth Impact Database, 2018; unless otherwise noted).

1. *Morokweng* crater (~ 70 km diameter; or perhaps originally over 100 km) in the Kalahari desert of South Africa has a “recommended” age from U–Pb and $^{40}\text{Ar}/^{39}\text{Ar}$ analyses of 145.2 ± 0.8 Ma (Koeberl et al., 1997; Reimond et al., 1999; Jourdan et al., 2009). This coincides with the Jurassic–Cretaceous boundary interval, although there is no unambiguous evidence of a wave of extinctions of this age.
2. *Mjølnir* crater (~ 40 km) offshore northern Norway has an estimated age of c. 142.0 ± 2.6 Ma (Earth Impact Database, 2018), and biostratigraphy of regional coring that indicates the impact was near the Volgian–Ryazanian boundary interval (Smelror et al., 2001; Tsikalas, 2005).
3. *Tookoonoka* crater (~ 50 km) in west Queensland, Australia, has a poorly constrained age estimated as 128 ± 5 Ma.
4. *Kara* crater (~ 65 km) in the northern Urals of Russia is dated as 70.3 ± 2.2 Ma.
5. The immense *Chicxulub* crater (~ 170 km) in Yucatan, Mexico, that dramatically terminated the Mesozoic Era at 66.0 Ma.

27.3 Cretaceous time scale

In this section first the GTS2012 is summarized, after which the data and methods are presented that construct the current geologic time scale. For the first time a rather detailed Early Cretaceous dataset is available to spline the

M-sequence, also taking cyclostratigraphic stage durations into account in the geomathematical analysis. The Albian through Maastrichtian scale relies on direct dating of stage and period boundaries and cyclostratigraphic duration of stages.

27.3.1 Previous scales

The numerical time scale for the Cretaceous consists of three main “primary scales”—(1) Tethyan ammonite zones of Berriasian through Barremian are calibrated to the marine magnetic anomaly M-sequence age model scaled with a spline-fit, (2) microfossil and ammonite zones in Aptian–Albian are calibrated to cycle stratigraphy that is constrained by radioisotopic dates, and (3) North American ammonite zones of Cenomanian through early Maastrichtian that have an abundance of interbedded bentonites with radioisotopic dates are scaled with cycle stratigraphy and a spline-fit. Most other Cretaceous events are assigned ages according to their calibration to these primary biostratigraphy scales or via direct calibrations to the M-sequence or C-sequence chrons.

Cretaceous time scales have been composed, using this philosophy and methods by Gradstein et al. (2004, 2012) and by Ogg et al. (2008, 2012, 2016). The GTS2012 scaling is summarized below, after which the current numerical Cretaceous model will be outlined.

27.3.1.1 Constraints from radioisotopic dates used in GTS2012

Compared with any other Phanerozoic interval, the Late Cretaceous has the highest concentration of radioisotopic dates derived from bentonites interbedded with fossiliferous limestone. In contrast, the Early Cretaceous has only a few well-constrained radioisotopic dates; and a selected subset of the main constraints is briefly reviewed here.

The Tithonian–Berriasian boundary (base of Cretaceous) is constrained by a $^{40}\text{Ar}/^{39}\text{Ar}$ date of 145.5 ± 0.8 Ma on reversed-polarity sills intruding earliest Berriasian sediments on the Shatsky Rise of the Pacific (Mahoney et al., 2005). A Berriasian–Valanginian age older than ~ 138 Ma is supported by U–Pb dates from calcareous nannofossil–zoned sediments in the Great Valley of California (Shimokawa, 2010).

Deposits in the Neuquén Basin of Argentina that are correlated to the basal ammonite zone of the Upper Hauterivian substage yielded a U–Pb SHRIMP age of 132.7 ± 1.3 Ma (Aguirre-Urreta et al., 2008). Basalts from Resolution Guyot in the Pacific with reversed-polarity magnetization interpreted as Chron M5r or M3r of Barremian yielded a $^{40}\text{Ar}/^{39}\text{Ar}$ age from whole rock incremental heating of 128.4 ± 2.1 Ma (Pringle and Duncan, 1995a), but this method and its biostratigraphy constraints are not considered to be conclusive.

Several age dates indicate that the Aptian began at approximately 126 Ma. The basaltic basement on the Ontong Java Plateau, which is interbedded and overlain by limestone assigned to the *L. cabri* foraminifer zone (Mahoney et al., 2001; Sikora and Bergen, 2004), yielded an average $^{40}\text{Ar}/^{39}\text{Ar}$ age of 124.3 ± 1.8 Ma (Chambers et al., 2004). As noted above, the eruption of this massive igneous province is considered to be a causal factor in the OAE1a or “Selli” episode of carbon-rich oceanic sediment accumulation and carbon-isotope excursion that begins at about 0.5 Myr after the end of Chron M0r (hence about 0.9 Myr after the beginning of the Aptian) and spans about 1.1 Myr (Larson and Erba, 1999; Malinverno et al., 2010). Dating of reversed-polarity basalts at MIT Guyot in the Pacific yielded an age of 125.4 ± 0.2 Ma (Pringle and Duncan, 1995b; as recomputed to FCS of 28.201 Ma). The overlying basalt is a transition into a well-developed soil that is overlain by transgressive marine sediments containing early Aptian nannofossils and then capped by a thick shallow-water carbonate platform. Initially, the reversed-polarity zone had been interpreted to be the uppermost portion of polarity Chron M1r of middle Barremian, but the nannofossil criteria and the character of the carbon-isotope values from the overlying sediments are consistent with interpreting this zone as basal Aptian and therefore uppermost Chron M0r (Pringle et al., 2003). Chron M0r spans 0.4 Myr (e.g., Herbert et al., 1995), therefore its base, which is a proposed marker for the base of the Aptian Stage, was projected in GTS2012 as approximately 126.0 Ma. This is consistent with a U–Pb date of 124.07 ± 0.17 from calcareous nannofossil–zoned sediments of Early Aptian in the Great Valley of California (Shimokawa, 2010) and with an Ar–Ar date of 124.3 ± 1.8 Ma from basalts of Ontong Java Plateau (Chambers et al., 2004) that are considered to be coeval with the onset of Early Aptian OAE1a anoxic horizon (Table 27.1 in GTS2012).

In contrast, a volcanic episode of reversed polarity within continental deposits of the Yixian Formation of China yielded a 122.0 ± 0.5 Ma date from $^{40}\text{Ar}/^{39}\text{Ar}$ step-heating method (He et al., 2008). He et al. (2008) had interpreted this reversed-polarity event to be during Chron M0r, thereby implying that the base of the Aptian was younger than 123 Ma! In the publication that had used the date cited above, an alternative interpretation, assuming that the polarity was a primary magnetization, was that this eruption might have captured the brief M[–]1r[–] or ISEA event of mid-Early Aptian (c. 122 Ma). But the revised dating for the base of the Aptian as c. 121.4 Ma in the GTS2020 age model would imply that the original interpretation by He et al. (2008) is viable.

A volcanic ash within the basal Albian strata in northwest Germany yielded a U–Pb age of 113.1 ± 0.3 Ma (Selby et al., 2009). The top of the basal Cenomanian

ammonite subzone has a $^{40}\text{Ar}/^{39}\text{Ar}$ date of 99.8 ± 0.4 Ma (Obradovich et al., 2002).

From the lowest Cenomanian through lower Maastrichtian, there are nearly 45 radioisotopic-dated horizons from the Western Interior Basin of North America (detailed in Appendix 2 of GTS2012). A Late Cretaceous time scale for North American ammonoid zones was initially calibrated by Obradovich (1993) from his extensive suite of $^{40}\text{Ar}/^{39}\text{Ar}$ dates on bentonites using a multigrain analysis of sanidine grains at the USGS lab. He added additional dates from sections calibrated to Campanian–Maastrichtian magnetostratigraphic (Hicks et al., 1995, 1999), then summarized and enhanced the sets using a refined ammonite zonation for the Western Interior basin (Cobban et al., 2006). The collections of sanidine grains from Obradovich's separates have been undergoing single-crystal analyses to narrow the uncertainties at the University of Wisconsin at Madison, and this group has analyzed additional horizons and applied U–Pb dating to zircons from the same levels (e.g., Siewert, 2011; Meyers et al., 2012). Supporting U–Pb and Ar–Ar results have been contributed by Quidelleur et al. (2011) from Japanese sections, including verification that the base of the Cenomanian is at approximately 100.0 Ma.

The youngest ammonite-zoned age from the Western Interior suite is ~ 69.9 Ma in the earliest Maastrichtian. The Maastrichtian–Danian boundary (base of Cenozoic) is well-dated as ~ 66.0 Ma.

27.3.1.2 Direct spline-fitting of radioisotopic date suite as used in GTS2012

An initial spline-fit incorporated the majority of the Cretaceous and Jurassic suite of radioisotopic dates (Appendix 2 of GTS2012) and their biochronostratigraphic assignments with uncertainties to a merged scale of North American Western Interior ammonite zones (Late Cretaceous) and Tethyan ammonite zones (basal Cenomanian through Jurassic). Some Cretaceous radioisotope dates were omitted that were difficult to correlate to the primary ammonite zonal scale (e.g., the Kneehills Tuff within *Triceratops* dinosaur beds). The spline-fit processed by Øyvind Hammer used the methods described in Chapter 14 on Geomathematics in the GTS2012 volume). The first spline run with a smoothing factor of 1.5 indicated that 11 dates did not pass the chi-squared distribution test (mainly in Jurassic); therefore a second spline run relaxed the smoothing factor to 0.975. The computed stage boundaries are listed under “Spline #1” in Table 27.2 of GTS2012.

However, the relaxed-fit for this spline did not fully utilize the detailed high-precision radioisotope dates with excellent ammonite zone placements for the Late Cretaceous. As a result, many of those dates were no longer being assigned by that spline-fit into the computed age ranges for those zones. Therefore a second hybrid spline was constructed—

the Late Cretaceous had a more strict spline-fit model, and the Early Cretaceous through Jurassic had the less restrictive smoothing factor. The resulting estimates for Cretaceous stage boundaries were listed under Spline #2 in Table 27.2 of GTS2012. The main change was for the poorly constrained base of Hauterivian, which changed by 0.4 Myr between these two spline-fit versions.

This Spline #2 also yielded a set of smoothly varying durations for Upper Cretaceous ammonite zones. However, in many intervals of the Upper Cretaceous, this smoothly varying scaling can be enhanced by using the durations for individual ammonite zones based on cycle stratigraphy. For example, the cycle-scaled duration of the *Pseudaspidoceras flexuosum* ammonite zone is 0.45 Myr (Meyers et al., 2012), but the spline-fit projected it as 0.84 Myr, twice the actual duration. In intervals of the Lower Cretaceous, improved scalings of ammonite zones can incorporate calibrations to the Pacific M-sequence, relative scalings from linear strontium-isotope trends (e.g., McArthur et al., 2007) or correlations to cycle-scaled microfossil zones (e.g., Grippo et al., 2004; Huang et al., 2010; Gale et al., 2011).

Therefore the spline-fit was enhanced by incorporating these other sets of stratigraphic studies or integrated stratigraphy (e.g., the Bayesian statistical method by Meyers et al., 2012, that optimizes the merger of radioisotopic dates with the cycle stratigraphy in the Turonian–Cenomanian boundary interval). In most cases the modification of the ages for those stage boundaries in the Upper Cretaceous based on the enhanced calibrations of the ammonite zones was less than 0.3 Myr between the spline-fit versions. An issue, not addressed by the geomathematics analysis in GTS2012, is that subjective adjusting of the geomath numerical solution also weakens the estimation of uncertainties. The latter is largely avoided in GTS2020.

27.3.1.3 Cretaceous age model used in GTS2012

The primary standards for Cretaceous calibrations are ammonite zones of the Tethyan realm (Berriasian through Albian) and North America Western Interior (Cenomanian through mid-Maastrichtian) (Table 27.3 of GTS2012). The age model for the Berriasian through Barremian ammonite zones was mainly derived from biostratigraphic correlations to the M-sequence of marine magnetic anomalies, plus intervals with cycle stratigraphy and/or linearization of strontium-isotope trends (Table 27.2 of GTS2012). The Aptian–Albian ammonite zones were scaled according to their correlation to microfossil and nannofossil datums, which, in turn, are scaled by cycle stratigraphy. A spline-fit (Spline #2, as explained above) of numerous radioisotopic dates from volcanic ash horizons interbedded with Western

Interior ammonites with adjustments for cycle stratigraphy of some intervals provided a high-resolution age model for the Cenomanian through early Maastrichtian. The late Maastrichtian correlations rely on microfossil datums calibrated to a spline- and cycle-fit of C-Sequence marine magnetic anomalies.

Only three Cretaceous stages (Maastrichtian, Turonian and Cenomanian) in 2012 had ratified GSSPs, therefore the age model for the other stages were based on selected working definitions (e.g., base of Aptian placed at base of magnetic polarity Chron M0r; base of Albian assigned to the lowest occurrence of a nannofossil in the cycle-scaled reference section) (Table 27.2 of GTS2012).

Details on the subjective merging of the spline results with cyclo- and other high-resolution stratigraphy are in the Cretaceous chapter of GTS2012, and the interested reader is kindly referred to that intricate text. That GTS2012 Cretaceous time scale model is contrasted to the GTS2020 age model later.

27.3.2 Cretaceous numerical age model of GTS2020

The GTS2020 numerical time scale for the Cretaceous follows the concept of GTS2012 with the three “primary scales”—(1) Tethyan ammonite zones of Berriasian through Barremian are calibrated to the M-sequence age model or to cyclostratigraphy in French reference sections, (2) several ammonite and microfossil zones in Aptian–Albian are calibrated to cycle stratigraphy that is constrained by radioisotopic dates, and (3) North American ammonite zones of Cenomanian through early Maastrichtian that have an abundance of interbedded bentonites with radioisotopic dates are scaled with cycle stratigraphy. This latter segment of the Cretaceous has a more mature cyclostratigraphy with more overlapping sections than the pre-Cenomanian Cretaceous. Geomathematical methodology is used for final Early and Late Cretaceous time scaling, as visualized in Figs. 27.10 and 27.11 showing the GTS2020 cubic spline fits for these chronostratigraphic intervals. This practice is new for Early Cretaceous, which for the first time now has a rather detailed and more stable dataset, as explained later.

Six Cretaceous stage boundaries now have a ratified GSSP, that is, Maastrichtian, Santonian, Turonian, Cenomanian, Albian and Hauterivian (Fig. 27.1, Table 27.1, Fig. 27.12), of which only the Hauterivian is within the geomagnetic M-sequence. Nevertheless, there is a detailed understanding of the M-sequence definition of the Berriasian through Aptian stages, as shown in Table 27.2, which also lists the definitions of

pre-Berriasian stages with M-sequence assignment and its km marine.

The Jurassic–Cretaceous boundary and base of Berriasian is in the middle of Chron M19n (Wimbledon et al., 2019, 2020), the Valanginian base is in the lower part of Chron M14r, the base of Hauterivian may be near Chron M10n and the base of Barremian is in the upper part of Chron M5n. Base Aptian is at the very end of the M-sequence at the older limit of Chron M0r at 0 km on the Hawaiian magnetic anomaly profile. The complete radioisotopic, cyclostratigraphic, and M-sequence dataset is in Table 27.2; it extends into marine magnetic anomaly M42 of potential Bajocian age to take advantage of that splined M-sequence segment also. Radioisotopic dates were reviewed earlier, with specific reference to new literature in GTS2016, and details are compiled in Appendix 2 in this book.

The critical factor for the Early Cretaceous scale in GTS2020 is that a rather high-resolution U–Pb radioisotopic, geomagnetic and cyclostratigraphic dataset is now available for the Tithonian through Barremian, not known during construction of GTS2012 (Kietzmann et al., 2018; Lena et al., 2019; Vennari et al., 2014; Aguirre-Urreta et al., 2017, 2019; Zhang et al., 2019). Important cyclostratigraphic constraints on duration of the Valanginian–Hauterivian are from Martinez et al. (2015).

The new information includes:

1. Durations of Tithonian through Barremian stages are slightly over 5 Myr per stage.
2. He et al. (2008) age near 122 Ma likely is earliest Aptian M0r or in latest Barremian M1r.
3. The Aptian Stage is about 5 Myr shorter than thought previously (see Table 27.2 for numerical details).

Together, this new dataset in Table 27.2, with emphasis on modern U–Pb dates makes it likely that the Ar/Ar age date near 146 Ma of Mahoney et al. (2005) on M18, the dates near 125 Ma on the oceanic Ontong Java Plateau and the MIT Guyot in the Pacific (Appendix 2 and Cretaceous chapter of GTS2012), and the interpretation of 62.5 long-eccentricity cycles from base-Cenomanian to top of M0r (Huang et al., 2010) should be reevaluated.

Spline-fitting as applied to Paleozoic periods in GTS2020 was also used to help obtain the GTS2020 Cretaceous time scale, as outlined in detail in Ch14A: Geomathematical and statistical procedures (this book). The resulting smoothing spline if applied only to the array of radioisotopic dates with their estimated placement relative to the Hawaiian magnetic anomaly profile, which is shown in Fig. 27.10, is approximately a straight line representing approximately constant seafloor spreading for that Hawaiian profile from Kimmeridgian through Barremian. The deviations from this spline are small.

TABLE 27.2 Stratigraphic–radioisotopic data set, aligned to the mid-km M-sequence, used for the Lower Cretaceous time scale.

Stage	radioisotopic date, 2-sigma	interpolated age with cycles	duration from 405-kyr cycles	magnetic polarity-chron assignment	mid-km M-sequence	Reference
base-Cenomanian	100.5 ± 0.14					GTS2012 and this chapter
			Albian duration 12.45 ± 0.5			
base Albian	113.10 ± 0.3					GTS2012 and this chapter
early Aptian	121.20 ± 1			several ages dates in Appendix 2		
near base Aptian	122.01 ± 0.52			no biostrat; whole M0r	minus 4.9 ± 4.9	He et al. (2008) ; this chapter
			Aptian duration 8.1 ± 0.5			
base Aptian				near Chron M0r	0 ± 2.5	
mid-Barremian	123.10 ± 0.3			upper half of M1r	55.8 ± 2.2	Zhang et al. (2019) ; this chapter
Barremian	125.45 ± 0.43			entire M1r	68.5 ± 6.1	Pringle and Duncan, (1995b)
			Barremian duration 5.00 ± 0.5			
base Barremian		126.07 ± 0.25		upper part of Chron M5n	120 ± 5	
Hauterivian	127.24 ± 0.25 (2σ approx.)			upper Hauterivian, mid-M5n	125.5 ± 5.5	Return to Agrio
Hauterivian	130.39 ± 0.25 (2σ approx.)			uppermost M10N	213.5 ± 4.6	Aguirre-Urreta et al. (2017)
			Hauterivian duration 5.93 ± 0.5			
base Hauterivian	131.29 ± 0.25			in Chron M10n	198 ± 4	Aguirre-Urreta et al. (2019)
			Valanginian duration 5.06 ± 0.5			
base Valanginian		137.05 ± 1.0		chron M14r.3	347 ± 9	Martinez et al. (2015)
Berriasian	139.24 ± 0.16			uppermost M17r	447.8 ± 9.9	Lena et al. (2019)
	139.55 ± 0.18			M17r	457.7 ± 9.9	Vennari et al. (2014)
	139.96 ± 0.17			M18n–M17r boundary interval	476.9 ± 9.3	Lena et al. (2019)
	140.34 ± 0.18			M18r–M18n boundary interval	491.8 ± 5.8	
	140.51 ± 0.16			base M18n to lower M17r	476.3 ± 19.6	Lena et al. (2019) with revised Chron Appendix 2
	142.04 ± 0.17			lower M18r	503 ± 2.1	

TABLE 27.2 (Continued)

Stage	radioisotopic date, 2-sigma	interpolated age with cycles	duration from 405-kyr cycles	magnetic polarity-chron assignment	mid-km M-sequence	Reference
	146.48 ± 1.63			M18r–M18n boundary interval	500 ± 5.1	Mahoney et al. (2005)
			Berriasian duration 5.27 ± 0.5			Kietzmann et al. (2018)
base Berriasian				mid M19n.2n	526.3 ± 14	Berriasian Working Group, ICS
Tithonian	147.11 ± 0.18			early Tithonian; upper M22r	684.7 ± 4.3	Lena et al. (2019)
			Tithonian duration 5.67 ± 0.5			Kietzmann et al. (2018)
base Tithonian				base chron M22An	701 ± 2	
base Kimmeridgian	154.1 ± 2.10			base M26r	845.2 ± 2.5	Selby et al. (2009) , GTS2016
			Kimmeridgian duration 5.20 ± 0.5			GTS2012 cycles/spreading rate
Oxfordian	155.60 ± 0.89			M24Bn–M30r	851 ± 67.7	AB4-Pell
			Oxfordian duration 5.80 ± 0.5			GTS2012 cycles/spreading rate
base Oxfordian				lower part of M36Br	1013.69 ± 1.05	GTS2012
			Callovian duration 3.00 ± 0.5			GTS2012 cycles/spreading rate
base Callovian				within M39n.3n (mid-depth scale)	1097.9	GTS2012
Bathonian	164.64 ± 0.27			M39n.3n	1097.9 ± 9.4	Kamo and Riccardi (2009)
Bajocian	168.35 ± 1.31			mid Bajocian, mid-M42-base M43r	1193 ± 18	Appendix 2
Bajocian	171.48 ± 1.22			mid Bajocian, mid-M42-base M43r	1193 ± 18	Appendix 2

Spline-fit of this data set is in [Fig. 27.10](#); for details see text.

[Kent and Gradstein \(1985\)](#) in their Cretaceous and Jurassic geochronology study for the Decade of North America Geology publications had also suggested that a constant and linear spreading of the M-sequence was a reasonable template to interpolate the Oxfordian through Barremian time scale. Despite use of few tie-points for the age versus M-sequence km plot, the Jurassic–Cretaceous boundary was interpolated by [Kent and Gradstein \(1985\)](#) at 144 Ma, only slightly older than the final estimate of

143.1 ± 0.6 Ma in GTS2020, albeit using a different definition for that system boundary.

In [Table 14A.5 of Chapter 14](#) in this book, stage durations according to the spline-curve are compared with Milankovitch-based duration estimates. Although the spline ages are probably unbiased estimates of the true ages, the Milankovitch cycle durations are probably better stage duration estimates. For a description of the technique to incorporate cycle durations in the stage age

TABLE 27.3 Stratigraphic–radioisotopic data set with cycle age and C-chron assignments, partially aligned to the mid-km C-sequence, used for the Upper Cretaceous time scale.

Stage (base)	radioisotopic date, 2-sigma	name of UK bentonite	cycle and cycle-age assignment	stratigraphy-C-chron assignment	mid-km C-sequence	Reference
Danian	66.04 ± 0.05					This chapter
Maastrichtian			66.31 ± 0.5	top of 30N	1371.84	Batenburg et al. (2012)
			69.19 ± 0.5	top of 31N	1409.56	Batenburg et al. (2012)
			70.08 ± 0.5	<i>B. clinobatus</i> Zone; mid-31R		
			70.65 ± 0.5	top of 32N	1481.12	Batenburg et al. (2012); GTS2012
			72.5 ± 0.5	<i>B. eliasi</i> Zone; mid-32N		This chapter
Campanian	74.85 ± 0.43		184.5 74.3 ± 0.5	<i>E. jenneyi</i> Zone; top 33N	1549.41	This chapter; Appendix 2
			75.92 ± 0.5	<i>R. calcarata</i> Zone; upper 33N		This chapter; Appendix 2
			76.62 ± 0.5	<i>B. scotti</i> Zone; mid-33N		This chapter; Appendix 2
			197 79.9 ± 0.5	base 33N	1732.76	This chapter
			~197 80.62 ± 0.4	<i>B. obtusus</i> Zone; beneath base 33N	1723.76	This chapter; Appendix 2
	83.27 ± 0.11		~207	<i>S. leei III</i> Zone; base 33R	1862.32	S1019 in Wang et al. (2016)
Santonian	84.43 ± 0.15			<i>D. bassleri</i> Zone		Sageman et al. (2014)
			207.5	34N		
	85.66 ± 0.19		86.08 ± 0.35	top <i>C. undulatopticatus</i> Zone		This chapter; Appendix 2
Coniacian	89.87 ± 0.18	Lewes Marl	222			Appendix 2; Gale (2019a)
Turonian	89.37 ± 0.15	Caburn Marl	224			Appendix 2; Gale (2019a)
	91.07 ± 0.28	Southerham Marls	225			
	91.15 ± 0.26	Glynde Marls	226			
	93.67 ± 0.31	Lulworth Marl	229			
	93.79 ± 0.26	C-T bentonite	232 93.65 ± 0.5			Batenburg et al. (2016)
mid-Cenomanian	96.12 ± 0.31	Thatcher Bentonite	238 96.5 ± 0.5			Batenburg et al. (2016)
Cenomanian	99.7 ± 0.3			~1 subzone above GSSP		Takashima et al. (2019)
	100.5 ± 0.14					GTS2012 and this chapter

Spline-fit for this data set is in Fig. 27.11. For details see text. GSSP, Global Boundary Stratotype Section and Point.

estimates the reader is referred to Chapter 14, Geomathematics (this book). The corrected cycle durations then can be used to estimate stage base age

estimates, combined with the constant-spreading-rate estimates for the durations of the Kimmeridgian through Callovian. These revised Callovian through Albian age

Early Cretaceous and part of Jurassic Spline Fit and Time Scale

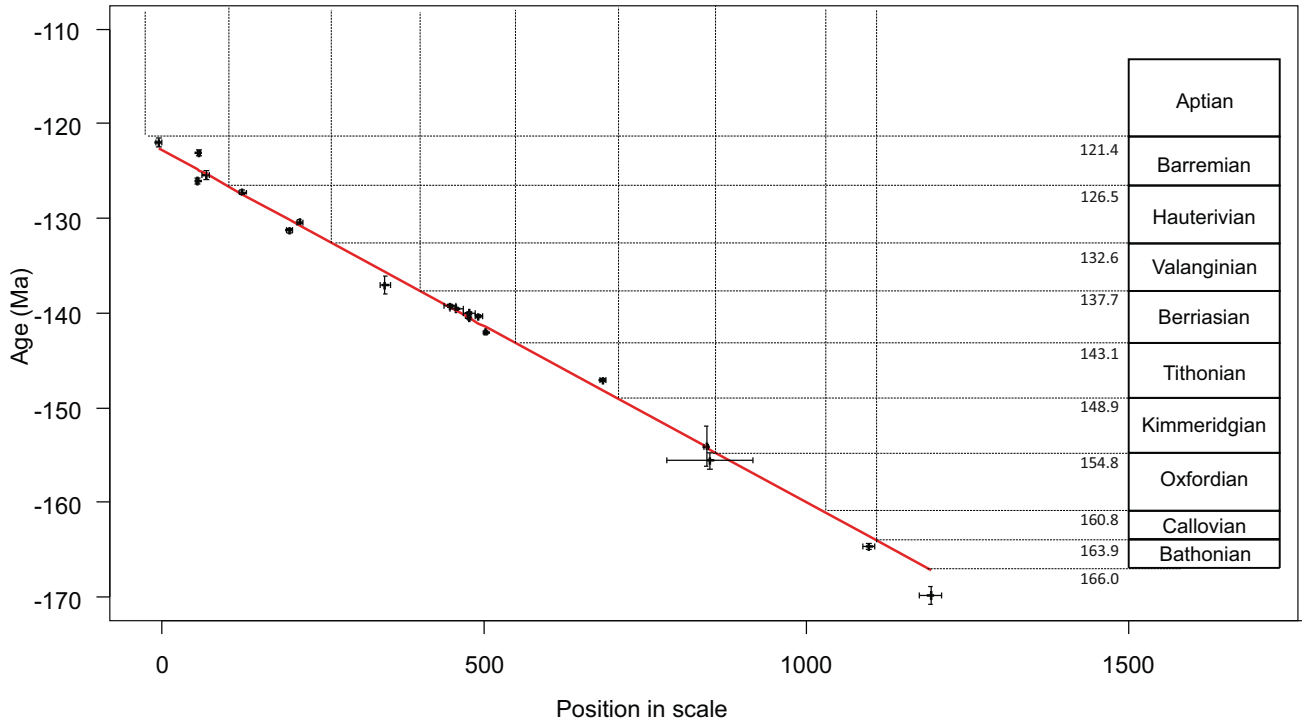


FIGURE 27.10 Early Cretaceous and Late Jurassic spline-fit and geologic time scale. Spline-fit errors are small, if present and may be invisible. For details see text in this chapter and in [Agterberg et al. \(2020, Ch. 14A: Geomathematics and statistical procedures \(this book\)\)](#). [Note that the basal ages for Jurassic stages used in GTS2020 used a different spline fit with incorporation of cyclostratigraphy (see [Hesselbo et al. \(2020, Ch. 26: The Jurassic Period, this volume\)\)](#)].

Late Cretaceous Spline Fit and Time Scale

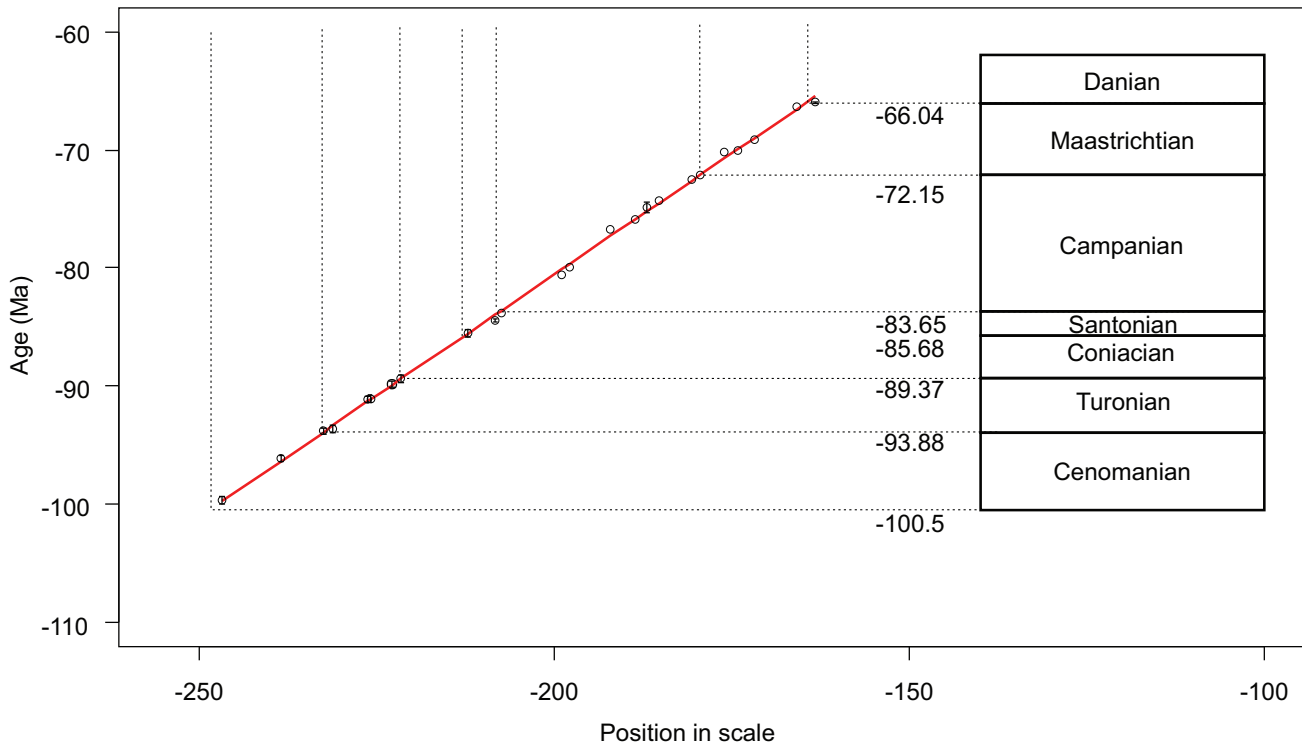


FIGURE 27.11 Late Cretaceous spline-fit and the Late Cretaceous time scale. Spline-fit uncertainties are small, if present, and may be invisible. For details see text in this chapter and in [Agterberg et al. \(2020, Ch. 14A: Geomathematics and statistical procedures, this book\)](#).

estimates are in Table 14A.6 of Chapter 14, Geomathematics, along with the original spline-based 2-sigma values. However, this incorporation of cycle-tuned durations for Berriasian through Barremian stages also implies that the spreading rates for the Hawaiian marine magnetic profile are no longer constant (discussed in Ch. 5: Geomagnetic polarity time scale, this book). Based on a further and detailed stratigraphic evaluation in this Cretaceous chapter, it was concluded that the original uncertainty used for the upper endpoint of the spline (near base Aptian) had been overestimated, also affecting nearby underlying uncertainties. Hence, uncertainty of the relevant age estimates was marginally reduced. The age of Aptian/Albian boundary in the revised spline is 113.2 ± 0.3 Ma (see Chapter 14: Geomathematics), which is in agreement with the original Selby et al. (2009) age estimate of a level slightly above this boundary.

Input values for the Late Cretaceous age determination are in Table 27.3 and include selected radioisotopic dates from Appendix 2, cycle numeration and cycle derive ages from Batenburg et al. (2012) and this chapter, stratigraphy-chron assignments and mid-km C-sequence assignments. Age determinations for the Late Cretaceous could be correlated with Milankovitch cycles, but a number of dates for which C-sequence and cycle input were available do not have reported 2-sigma values, and all dates were given equal weights for the spline-fitting. Wang et al. (2016) published U/Pb age dates on a bentonite in cored nonmarine sediments at 1019 m depth in

the Songliao Basin, China. An age of 83.27 ± 0.11 Ma was determined almost 25 m below the Chron 34n–C33r geomagnetic boundary in the core. Cyclostratigraphic analysis of the gamma record in the *single core* and applying an average sedimentation rate estimate suggests the base Campanian might be near 83.07 ± 0.15 Ma (Wang et al., 2016) or near 82.9 Ma in the middle of cycle 205 of Laskar’s notation (Wu et al., 2020). Gale and Batenburg (this study) identified the S–C Campanian boundary, using Laskar’s cycle notation at 83.75 Ma, falling within cycle 207. Kita et al. (2017) place the base of Chron 33r in the basal part of the *S. leei* III in Kansas, WI Basin, in the context of nannofossil events, thus a little younger than Sageman et al. (2014) age date. The best-fitting spline-curve is approximately a straight line with small deviations (Fig. 27.11). Details on the mathematical procedure are in Chapter 14, Geomathematics (this book); it is noted that for several input dates the error bars do not intersect the spline-curve, indicating, as also for Early Cretaceous, precision of the age determinations was probably overestimated. For this reason the uncertainty for the Santonian–Campanian age was slightly increased to overlap with the uncertainty extension of the age in the core with the Chron 34n–C33r geomagnetic boundary.

27.3.2.1 Age of stage boundaries

The base Cretaceous and base Berriasian interpolate at 143.1 ± 0.6 Ma, 1.9 Myr younger than in GTS2012, and with a smaller uncertainty (Table 27.4). The Berriasian

TABLE 27.4 The Berriasian through Maastrichtian Geologic Time Scale, compared to GTS2012.

Stages	GTS2012			GTS2020		
	Base	Uncertainty	Duration	Base	Uncertainty	Duration
Paleogene/Danian	66	0.1		66.04	0.05	
Maastrichtian	72.1	0.2	6.1	72.2	0.2	6.2
Campanian	83.6	0.3	11.6	83.7	0.5	11.5
Santonian	86.3	0.5	2.6	85.7	0.2	2
Coniacian	89.8	0.4	3.5	89.4	0.2	3.7
Turonian	93.9	0.2	4.1	93.9	0.2	4.5
Cenomanian	100.5	0.4	6.6	100.5	0.1	6.6
Albian	113	0.4	12.5	113.2	0.3	12.7
Aptian	126.3	0.4	13.3	121.4	0.6	8.2
Barremian	130.8	0.5	4.5	126.5	0.7	5.1
Hauterivian	133.9	0.6	3.1	132.6	0.6	6.1
Valanginian	140.2	0.7	6.3	137.7	0.5	5.1
Berriasian	145	0.8	4.8	143.1	0.6	5.4

Uncertainties increase in value stratigraphically downward. Below the Albian age differences are large relative to GTS2012. For details see text.

GSSPs of the Cretaceous Stages, with location and primary correlation criteria

Stage	GSSP Location	Latitude, Longitude	Boundary Level	Correlation Events	Reference
Maastrichtian	Tercis les Bains, Landes, France	43°40'46.1"N 1°06'47.9"W*	level 115.2 on platform IV of the geological site at Tercis les Bains	Mean of 12 biostratigraphic criteria of equal importance. Near ammonite FAD of <i>Pachydiscus neubergicus</i>	Episodes 24/4, 2001
Campanian	<i>candidates are in Italy and in Texas</i>			<i>Crinoid, LAD of Marsupites testudinarius or base of Chron C33r</i>	
Santonian	Olazagutia, Northern Spain	42°52'5.3"N 2°11'40"W	94.4 m in the eastern border of the Cantera de Margas quarry	Inoceramid bivalve, FAD <i>Platyceramus undulatoplicatus</i>	Episodes 37/1, 2014
Coniacian	<i>candidates are in Poland (Slupia Nadbrzenna) and Germany (Salzgitter)</i>			<i>Inoceramid bivalve, FAD of Cremnoceramus deformis erectus</i>	
Turonian	Pueblo, Colorado, USA	38°16'56"N 104°43'39"W*	base of Bed 86 of the Bridge Creek Limestone Member	Ammonite, FAD of <i>Watinoceras devonense</i>	Episodes 28/2, 2005
Cenomanian	Mont Risou, Hautes-Alpes, France	44°23'33"N 5°30'43"E	36 m below the top of the Marnes Bleues Formation on the south side of Mont Risou	Foraminifer, FAD of <i>Thalmaninella globotruncanoides</i>	Episodes 27/1, 2004
Albian	Col de Pré-Guittard Section, Drôme, France	44°29'47"N 5°18'41"E	37.4 m above the base of the Marnes Bleues Formation and 40 cm above the base of the Kilian Niveau	Foraminifer, FAD of <i>Microhedbergella renilaevis</i>	Episodes 40/3, 2017
Aptian	<i>candidate is Gorgo a Cerbara, Umbria-Marche, central Italy</i>			<i>Base of Chron M0r; near ammonite, FAD of Deshayesites oglanlensis</i>	
Barremian	<i>candidate is Río Argos near Caravaca, Murcia province, Spain</i>			<i>Ammonite, FAD of Taveraidiscus hugii</i>	
Hauterivian	La Charce Section, Drôme Province, southeast France	44°28'10"N 5°26'37.4"E	base of Bed 189 of La Charce Section	Ammonite, FAD of genus <i>Acanthodiscus</i>	
Valanginian	<i>candidate is near Caravaca (S. Spain)</i>			<i>Calpionellid, FAD of Calpionellites darderi</i>	
Berriasian	<i>Tré Maroua, SE of Gap, southeast France</i>			<i>Calpionellid, FAD of Calpionella alpina</i>	

* according to Google Earth

FIGURE 27.12 Ratified and potential GSSPs and primary correlation markers for the Cretaceous stages (status as of January 2020). Details of each GSSP are available at <http://www.stratigraphy.org>, <https://timescalefoundation.org/gssp/>, and in the *Episodes* publications. GSSP, Global Boundary Stratotype Section and Point.

Stage measures 5.4 Myr in duration, 1 Myr longer than in GTS2012. The Valanginian Stage started at 137.7 ± 0.5 Ma and lasted 5.1 Myr. In GTS2012 base Valanginian was 140.2 ± 0.7 Ma in age and lasted 6.3 Myr. The Hauterivian Stage ranges from 132.6 ± 0.6 to 126.5 ± 0.7 Ma, lasting 6.1 Myr. In GTS2012 the stage had a rather short duration of 3.1 Myr, between 133.9 and 130.8 Ma. The Barremian Stage lasted 5.1 Myr from 126.5 ± 0.7 to 121.4 ± 0.6 Ma. In GTS2012, its top was at 126.3 Ma, a large numerical difference. In GTS2012 the Aptian lasted 13.3 Myr from 126.3 until 113 Ma, being the longest stage in the Cretaceous.

With a duration of 8.2 Myr from 121.4 ± 0.6 until 113.2 ± 0.3 the GTS2020 Aptian is only the third longest stage in the Cretaceous, after the Albian with 12.7 Myr and Campanian with 11.5 Myr durations. The proposed revised interpretation of 405-kyr cycles within the Aptian (Zhang et al., 2019) yields an estimated duration of 8.1 ± 0.5 Myr, virtually identical to the current geomathematical estimate in GTS2020. The Albian lasted 12.7 Myr from 113.2 to 100.5 ± 0.1 Ma for base-Cenomanian. The 405-kyr cyclostratigraphic duration estimate for the Albian of c. 12.45 ± 0.5 Myr (Grippio et al., 2004) is close to the spline-fit result.

Base Turonian has a direct age date of 93.9 ± 0.2 , making the Cenomanian 6.6 Myr long. The Turonian Stage lasted for 4.5 Myr until base Coniacian at 89.4 ± 0.2 Ma; the latter stage lasted 3.7 Myr. The Santonian Stage ranges from 85.7 to 83.6 Ma, being the shortest Cretaceous stage with its 2.1 Myr duration. The second longest stage in the Cretaceous, the Campanian Stage lasted from 83.7 to 72.2 Ma, for a duration of 11.5 Myr. The Maastrichtian Stage started at 72.2 Ma and ended at the K/T boundary precisely dated at 66.04 Ma, with a duration of 6.2 Myr.

The Early Cretaceous stretches between 143.1 and 100.5 Ma, with a total duration of 42.6 Myr, and the Late Cretaceous ranges from 100.5 to 66.04 Ma, with a total duration of 34.5 Myr. The total duration of the Cretaceous period itself is 77.1 Myr from 143.1 to 66.04 Ma.

The GTS2020 geochronologic scale for the Cretaceous Period differs substantially from that in GTS2012 for the boundary ages of the Berriasian through Aptian stages, and much less so for the seven younger stages. Particularly for the mid-Cretaceous, the puzzling age discrepancy with oceanic basement Ar–Ar dates needs investigation.

Bibliography

- Agterberg, F.P., da Silva, A.C., and Gradstein, F.M., 2020, Chapter 14A - Geomathematical and statistical procedures. In Gradstein, F.M., Ogg, J.G., Schmitz, M.D., and Ogg, G.M. (eds), *The Geologic Time Scale 2020*. Vol. 1 (this book). Elsevier, Boston, MA.
- Aguado, R., Company, M., and Tavera, J.M., 2000, The Berriasian/Valanginian boundary in the Mediterranean region: new data from the Caravaca and Cehegin sections, SE Spain. *Cretaceous Research*, **21**: 1–21.
- Aguado, R., de Gea, G.A., and O'Dogherty, L., 2014, Integrated biostratigraphy (calcareous nannofossils, planktonic foraminifera, and radiolarians) of an uppermost Barremian–lower Aptian pelagic succession in the Subbetic Basin (southern Spain). *Cretaceous Research*, **51**: 153–173.
- Aguirre-Urreta, M.B., Rawson, P.F., Concheyro, G.A., Bown, P.R., and Ottone, E.G., 2005, Lower Cretaceous (Berriasian–Aptian) biostratigraphy of the Neuquén Basin. In Veiga, G., Spalletti, L., Howell, J. A., and Schwarz, E. (eds), *The Neuquén Basin: A Case Study in Sequence Stratigraphy and Basin Dynamics*. *Geological Society of London, Special Publication*, **252**: 57–81.
- Aguirre-Urreta, M.B., Pazos, P.J., Lazo, D.G., Fanning, C.M., and Litvak, V.D., 2008, First U/Pb SHRIMP age of the Hauterivian stage, Neuquén Basin, Argentina. *Journal of South American Earth Sciences*, **26**: 91–99.
- Aguirre-Urreta, B., Lescano, M., Schmitz, M.D., Tunik, M., Concheyro, A., Rawson, P.F., et al., 2015, Filling the gap: New precise Early Cretaceous radioisotopic ages from the Andes. *Geological Magazine*, **152** (3), 557–564.
- Aguirre-Urreta, M.B., Schmitz, M., Lescano, M., Tunik, M., Rawson, P. F., Concheyro, A., et al., 2017, A high precision U-Pb radioisotopic age for the Agrio Formation, Neuquén Basin, Argentina: implications for the chronology of the Hauterivian Stage. *Cretaceous Research*, **75**: 193–204.
- Aguirre-Urreta, M.B., Martinez, M., Schmitz, M., Lescano, M., Omarini, J., Tunik, M., et al., 2019, Interhemispheric radio-astrochronological calibration of the time scales from the Andean and the Tethyan areas in the Valanginian–Hauterivian (Early Cretaceous). *Gondwana Research*, **70**: 104–132.
- Alvarez, W., Arthur, M.A., Fischer, A.G., Lowrie, W., Napoleone, G., Premoli Silva, I., et al., 1977, Upper Cretaceous–Palaeocene magnetic stratigraphy at Gubbio, Italy—V. Type section for the Late Cretaceous–Palaeocene geomagnetic reversal time scale. *Geological Society of America Bulletin*, **88**: 383–389.
- Allemann, F., Catalano, R., Fares, F., and Remane, J., 1971, Standard calpionellid zonation (Upper Tithonian–Valanginian) of the Western Mediterranean province. *Proceedings II Planktonic Conference, Roma*, **1971**: 1337–1340.
- Amédéo, F., 1992, L'Albien du bassin Anglo-Parisien: ammonites, zonation phylétique, séquences. *Bulletin des Centres de Recherches Exploration – Production Elf-Aquitaine*, **16**: 187–233.
- Amédéo, F., and Matrimon, B., 2007, Une coupe lithologique synthétique dans l'Albien-type de l'Aube, France. *Bull. Inf. Géol. Bass. Paris*, **44**: 7–23.
- Amédéo, F., Cobban, W.A., Breton, G., and Rogron, P., 2002, *Metengonoceras teigenense* Cobban et Kennedy, 1989: une ammonite exotique d'origine Nord-Américaine dans le Cénomanién inférieur de Basse-Normandie (France). *Bulletin trimestriel de la Société géologique de Normandie et des amis du Muséum du Havre*, **87**: 5–25 5 pls (for 2000).
- Amédéo, F., Matrimon, B., Magniez-Jannin, F., and Touch, R., 2014, La limite Albien inférieur- Albien moyen dans l'Albien type de l'Aube (France): ammonites, foraminifères, séquences. *Revue de Paléobiologie*, **33**: 159–279.
- Amédéo, F., Matrimon, B., Robaszynski, F., 2018. *Stratotype Turonien*. Muséum nationale d'histoire naturelle, Biotope, Meze, Paris, p. 416 (Patrimoine géologique, 8).
- Amédéo, F., Deconinck, J.-F., and Matrimon, B., 2019, L'Albien type de l'Aube (France): Première description litho-biostratigraphique de lat totalité des Argiles tégulines de Courcelles. *Bulletin Inf. Géol. Bass. Paris*, **56** (2): 7–22.
- Amodio, S., Ferreri, V., D'Argenio, B., Weissert, H., and Sprovieri, M., 2008, Carbon-isotope stratigraphy and cyclostratigraphy of shallow-marine carbonates: the case of San Lorenzello, Lower Cretaceous of southern Italy. *Cretaceous Research*, **29**: 803–813.
- Ando, A., and Huber, B.T., 2007, Taxonomic revision of the Late Cenomanian planktonic foraminifera *Rotalipora greenhornensis* (Morow, 1934). *Journal of Foraminiferal Research*, **37**: 160–174.
- Ando, A., Huber, B.T., MacLeod, K.G., Ohta, T., and Khim, B.-K., 2009, Blake Nose stable isotopic evidence against the mid-Cenomanian glaciation hypothesis. *Geology*, **37**: 451–454, <https://doi.org/10.1130/G25580A.1>.
- Arnaud-Vanneau, A., and Bilotte, M., 1998, Larger benthic foraminifera. Columns for Jurassic chart of Mesozoic and Cenozoic sequence chronostratigraphic framework of European basins, by Hardenbol, J., Thierry, J., Farley, M.B., Jacquin, T., de Graciansky, P.-C., and Vail, P. R. (coordinators). In de Graciansky, P.-C., Hardenbol, J., Jacquin, T., and Vail, P.R. (eds), *Mesozoic–Cenozoic Sequence Stratigraphy of European Basins*. *SEPM Special Publication*, **60**: 763–781.
- Banner, F.T., Copestake, P., and White, M.R., 1993, Barremian–Aptian Praehedbergellidae of the North Sea area: a reconnaissance. *Bulletin of the Natural History Museum: Geology Series*, **49**: 1–30.
- Barron, E.J., 1983, A warm, equable Cretaceous: the nature of the problem. *Earth Science Review*, **19**: 305–338.

- Bartolucci, P., Beraldi, M., Cecca, F., Faraoni, P., Marini, A., and Pallini, G., 1992, Preliminary results on correlation between Barremian ammonites and magnetic stratigraphy in Umbria-Marche Apennines (Central Italy). *Palaeopelagos*, **2**: 63–68.
- Barbier, R., and Thieuloy, J.P., 1965, Étage Valanginien. *Mémoires du Bureau de Recherche Géologique et Minière*, **34**: 79–84.
- Batenburg, S., Sprovieri, M., Gale, A.S., Hilgen, F.J., Lirer, F., and Laskar, J., 2012, Cyclostratigraphy and astronomical tuning of the Maastrichtian at Zumaia (Basque country, northern Spain). *Earth and Planetary Science Letters*, **359**: 264–278.
- Batenburg, S., Gale, A.S., Sprovieri, M., Hilgen, F.J., Thibault, N., Boussaha, M., et al., 2014, An astronomical timescale for the Maastrichtian based on the Sopelana and Zumaia sections (Basque country, northern Spain). *Journal of the Geological Society*, **171**: 165–180.
- Batenburg, S.J., De Vleeschouwer, D., Sprovieri, M., Hilgen, F.J., Gale, A.S., Singer, B.S., et al., 2016, Orbital control on the timing of oceanic anoxia in the Late Cretaceous. *Climate of the Past*, **12**: 1195–2009. <https://doi.org/10.5194/cp-12-1995-2016>.
- Batenburg, S.J., Friedrich, O., Moriya, K., Voigt, S., Courmède, C., Moebius, I., et al., 2018, Late Maastrichtian carbon isotope stratigraphy and cyclostratigraphy of the Newfoundland Margin (Site U1403, IODP Leg 342). *Newsletters on Stratigraphy*, **51** (2), 245–260.
- Baudin, F., Faraoni, P., Marini, A., and Pallini, G., 1997, Organic matter characterization of the “Faraoni Level” from Northern Italy (Lessini Mountains and Trento Plateau): comparison with that from Umbria-Marche Apennines. *Palaeopelagos*, **7**: 41–51.
- Baudin, R., Bulot, L.G., Cecca, F., Coccioni, R., Gardin, S., and Renard, M., 1999, Un équivalent du “Niveau Faraoni” dans le Bassin du Sud-Est de la France, indice possible d’un événement anoxique fin-hauterivien étendu à la téthys méditerranéenne. *Bulletin de la Société géologique de France*, **170**: 487–498.
- Baumberger, E., 1901, *Über Facies und Transgressionen der unteren Kreide am Nordrande der mediterrano-helvetischen. Bucht im westlichen Jura*. Wissenschaftliche Beilagen Berichte Töchterschule Basel, 1–44.
- Bellier, J.P., and Moullade, M., 2002, Lower Cretaceous planktonic foraminiferal biostratigraphy of the western North Atlantic (ODP Leg 171B), and taxonomic clarification of key index species. *Revue de Micropaléontologie*, **45** (1), 9–26.
- Bengtson, P., Cobban, W.A., Dodsworth, P., Gale, A.S., Kennedy, W.J., Lamolda, M.A., et al., 1996, The Turonian stage and substage boundaries. *Bulletin de l’Institut Royal des Sciences Naturelles de Belgique, Sciences de la Terre*, **66** (Suppl.), 69–79.
- Bergen, J.A., 1994, Berriasian to early Aptian calcareous nannofossils from the Vocontian trough (SE France) and Deep Sea Drilling Site 534: new nannofossil taxa and a summary of low-latitude biostratigraphic events. *Journal of Nannoplankton Research*, **16**: 59–69.
- Bersac, S., and Bert, D., 2012, Ontogenesis, variability and evolution of the Lower Greensand Deshayesitidae (Ammonoidea, Lower Cretaceous, southern England); reinterpretation of literature data; taxonomic and biostratigraphic implications. *Annales de la Muséum d’histoire naturelle, Nice*, **27**: 197–270.
- Bice, K.L., Bralower, T.J., Duncan, R.A., Huber, B.T., Leckie, R.M., Sageman, B.B., 2002, Cretaceous climate-ocean dynamics: future directions for IODP. In: A JOI/USSSP and NSF Sponsored Workshop. Available from: <http://www.who.edu/ccod/CCOD_report.html> .
- Birkelund, T., Hancock, J.M., Hart, M.B., Rawson, P.F., Remane, J., Robaszynski, R., et al., 1984, Cretaceous stage boundaries—proposals. *Geological Society of Denmark Bulletin*, **33**: 3–20.
- Blair, S.A., and Watkins, D.K., 2009, High-resolution calcareous nannofossil biostratigraphy for the Coniacian/Santonian Stage boundary, Western Interior Basin. *Cretaceous Research*, **30**: 367–384.
- Bodin, S., Godet, A., Föllmi, K.B., Vermeulen, J., Arnaud, H., Strasser, A., et al., 2006, The late Hauterivian Faraoni oceanic anoxic event in the western Tethys: evidence from phosphorus burial rates. *Palaeogeography, Palaeoclimatology, Palaeoecology*, **235**: 245–264.
- Bornemann, A., Norris, R.D., Friedrich, O., Beckmann, B., Schouten, S., Sinninghe Damsté, J., et al., 2008, Isotopic evidence for glaciation during the Cretaceous supergreenhouse. *Science*, **319**: 189–192.
- BouDagher-Fadel, M.K., Banner, F.T., and Whittaker, J.E., 1997, *Early Evolutionary History of Planktonic Foraminifera*. Chapman & Hall, pp. 1–269.
- Bown, P.R., Rutledge, D.C., Crux, J.A., and Gallagher, L.T., 1998, Lower Cretaceous. In Bown, P.R. (ed), *Calcareous Nannofossil Biostratigraphy*. British Micropalaeontology Society Publication Series. London: Chapman & Hall, 86–131.
- Bralower, T.J., Sliter, W.V., Arthur, M.A., Leckie, R.M., Allard, D.J., and Schlanger, S.O., 1993, Dysoxic/anoxic episodes in the Aptian-Albian (Early Cretaceous). In Pringle, M.S., Sager, W.W., Sliter, W. V., and Stein, S. (eds), *The Mesozoic Pacific: Geology, Tectonics, and Volcanism*. American Geophysical Union Geophysics Monograph, **77**: 5–37.
- Bralower, T.J., Leckie, R.M., Sliter, W.V., and Thierstein, H.R., 1995, An integrated Cretaceous microfossil biostratigraphy. In Berggren, W.A., Kent, D.V., and Hardenbol, J. (eds), *Geochronology, Time Scales and Global Stratigraphic Correlations: A Unified Temporal Framework for a Historical Geology*. SEPM Special Publication, **54**: 65–79.
- Bralower, T.J., Fullagar, P.D., Paull, C.K., Dwyer, G.S., and Leckie, R.M., 1997, Mid-Cretaceous strontium-isotope stratigraphy of deep-sea sections. *Geological Society of America Bulletin*, **109**: 1421–1442.
- Bréheret, J.-G., 1988, Épisodes de sédimentation riche en matière organique dans les marnes bleues d’âge aptien et albien de la partie pélagique du bassin Vocontien. *Bulletin de la Société géologique de France*, **8** (IV), 349–356.
- Breistroffer, M., 1947, Sur les zones d’ammonites dans l’Albien de France et d’Angleterre. *Travaux du Laboratoire de Géologie de la Faculté des Sciences de l’Université de Grenoble*, **26**: 17–104.
- Bryan, S.E., and Ernst, R.E., 2008, Revised definition of Large Igneous Provinces (LIPS). *Earth-Science Reviews*, **86**: 175–202.
- Bulot, L.G., Blanc, E., Thieuloy, J.-P., and Remane, J., 1993, La limite Berriasien-Valanginien dans le Sud-Est de la France: données biostratigraphiques nouvelles. *Comptes rendus de l’Académie des Sciences, Paris, Série II. Sciences de la Terre et des Planètes*, **317**: 387–394.
- Bulot, L.G., Blanc, E., Company, M., Gardin, S., Hennig, S., Hoedemaeker, P.J., et al., 1996, The Valanginian Stage. *Bulletin de l’Institut Royal des Sciences Naturelles de Belgique, Sciences de la Terre*, **66** (Suppl.), 11–18.
- Burnett, J.A., Gallagher, L.T., and Hampton, M.J., 1998, Upper Cretaceous. In Bown, P.R. (ed), *Calcareous Nannofossil Biostratigraphy*. British Micropalaeontological Society Publication Series. London: Chapman & Hall, 132–199.
- Busnardo, R., 1965, Le Stratotype du Barrémien. 1.—Lithologie et Macrofaune, and Rapport sur l’étage Barrémien. *Mémoires du Bureau de Recherches Géologiques et Minières*, **34**: 101–116 and 161–169.
- Busnardo, R., Thieuloy, J.-P., and Moullade, M., 1979, Hypostratotype Mesogéen de l’Étage Valanginien (sud-est de la France). *Les Stratotypes Français*, **6**: 143 pp.

- Campbell, R.J., Howe, R.W., and Rexilius, J.P., 2004, Middle Campanian—lowermost Maastrichtian nannofossil and foraminiferal biostratigraphy of the northwestern Australian margin. *Cretaceous Research*, **25** (6), 827–864.
- Cande, S.C., and Kent, D.V., 1992, A new geomagnetic polarity time scale for the Late Cretaceous and Cenozoic. *Journal of Geophysical Research*, **97**: 13917–13951.
- Cande, S.C., and Kent, D.V., 1995, Revised calibration of the geomagnetic polarity timescale for the Late Cretaceous and Cenozoic. *Journal of Geophysical Research*, **100**: 6093–6095.
- Caron, M., 1966, Globotruncanidae du Crétacé supérieur du synclinal de la Gruyère (Préalpes médians, Suisse). *Revue de Micropaléontologie*, **9**: 68–93.
- Caron, M., 1983, La spéciation chez les Foraminifères planctiques: une réponse adaptée aux contraintes de l'environnement. *Zitteliana*, **10**: 671–676.
- Caron, M., 1985, Cretaceous planktonic foraminifera. In Bolli, H.M., Saunders, J.B., and Perch-Nielsen, K. (eds), *Plankton Stratigraphy*, Cambridge University Press, Cambridge, 17–86.
- Caron, M., and Homewood, P., 1983, Evolution of early planktic foraminifers. *Marine Micropaleontology*, **7** (6), 453–462.
- Casellato, C.E., 2010, Calcareous nannofossil biostratigraphy of upper Callovian-lower Berriasian successions from the Southern Alps, North Italy. *Rivista Italiana di Paleontologia e Stratigrafia*, **116**: 357–404.
- Casey, R., 1961, The stratigraphical palaeontology of the Lower Greensand. *Palaeontology*, **3**: 487–621.
- Casey, R., 1996, Lower Greensand ammonites and ammonite zonation. *Proceedings of the Geologists' Association*, **107**: 69–76.
- Casey, R., Bayliss, H.M., and Simpson, M.E., 1998, Observations on the lithostratigraphy and ammonite succession of the Aptian (Lower Cretaceous) Lower Greensand of Chale Bay, Isle of Wight, UK. *Cretaceous Research*, **19**: 511–535.
- Cecca, F., Pallini, G., Erba, E., Premoli-Silva, I., and Coccioni, R., 1994, Hauterivian-Barremian chronostratigraphy based on ammonites, nannofossils, planktonic foraminifera and magnetic chrons from the Mediterranean domain. *Cretaceous Research*, **15**: 457–467.
- Chambers, L.M., Pringle, M.S., and Fitton, J.G., 2004, Phreatomagmatic eruptions on the Ontong Java Plateau: an Aptian $^{40}\text{Ar}/^{39}\text{Ar}$ age for volcanoclastic rocks at ODP Site 1184. In Fitton, J.G., Mahoney, J.J., Wallace, P.J., and Sanders, A.D. (eds), *Origin and Evolution of the Ontong Java Plateau*. *Geological Society of London, Special Publication*, **229**: 325–331.
- Chang, S.-C., Zhang, H., Renne, P.R., and Fang, Y., 2009, High-precision $^{40}\text{Ar}/^{39}\text{Ar}$ age of the Jehol Biota. *Paleogeography, Paleoclimatology, Paleogeology*, **280**: 94–104.
- Channell, J.E.T., and Grandesso, P., 1987, A revised correlation of magnetozones and calpionellid zones based on data from Italian pelagic limestone sections. *Earth and Planetary Science Letters*, **85**: 222–240.
- Channell, J.E.T., Bralower, T.J., and Grandesso, P., 1987, Biostratigraphic correlation of M-sequence polarity chrons M1 to M22 at Capriolo and Xausa (S. Alps, Italy). *Earth and Planetary Science Letters*, **85**: 203–221.
- Channell, J.E.T., Erba, E., and Lini, A., 1993, Magnetostratigraphic calibration of the Late Valanginian carbon isotope event in pelagic limestones from Northern Italy and Switzerland. *Earth and Planetary Science Letters*, **118**: 145–166.
- Channell, J.E.T., Erba, E., Muttoni, G., and Tremolada, F., 2000, Early Cretaceous magnetic stratigraphy in the APTICORE drill core and adjacent outcrop at Cison (Southern Alps, Italy), and correlation to the proposed Barremian-Aptian boundary stratotype. *Geological Society of America Bulletin*, **112**: 1430–1443.
- Channell, J.E.T., Cecca, F., and Erba, E., 1995a, Correlations of Hauterivian and Barremian (Early Cretaceous) stage boundaries to polarity chrons. *Earth and Planetary Science Letters*, **134**: 125–140.
- Channell, J.E.T., Erba, E., Nakanishi, M., and Tamaki, K., 1995b, Late Jurassic–Early Cretaceous time scales and oceanic magnetic anomaly block models. In Berggren, W.A., Kent, D.V., and Hardenbol, J. (eds), *Geochronology, Time Scales and Global Stratigraphic Correlations: A Unified Temporal Framework for a Historical Geology*. *SEPM Special Publication*, **54**: 51–63.
- Channell, J.E.T., Casellato, C.E., Muttoni, G., and Erba, E., 2010, Magnetostratigraphy, nannofossil stratigraphy and apparent polar wander for Adria-Africa in the Jurassic–Cretaceous boundary interval. *Palaeogeography, Palaeoclimatology, Palaeoecology*, **293**: 51–75.
- Christensen, W.K., 1990, Upper Cretaceous belemnite stratigraphy of Europe. *Cretaceous Research*, **11**: 371–386.
- Christensen, W.K., 1996, A review of the Upper Campanian and Maastrichtian belemnite biostratigraphy of Europe. *Cretaceous Research*, **17**: 751–766.
- Christensen, W.K., 1997a, The Late Cretaceous belemnite family Belemnitellidae: taxonomy and evolutionary history. *Bulletin of the Geological Society of Denmark*, **44**: 59–88.
- Christensen, W.K., 1997b, Palaeobiogeography and migration in the Late Cretaceous belemnite family Belemnitellidae. *Acta Geologica Polonica*, **42**: 457–495.
- Clarke, L.J., and Jenkyns, H.C., 1999, New oxygen evidence for long-term Cretaceous climatic change in the Southern Hemisphere. *Geology*, **27**: 699–702.
- Cobban, W.A., 1993, Diversity and distribution of Late Cretaceous ammonites, Western Interior, United States. In Caldwell, W.G.E., and Kauffman, E.G. (eds), *Evolution of the Western Interior Basin*. *Geological Association of Canada Special Paper*, **39**: 435–451.
- Cobban, W.A., Walaszczyk, I., Obradovich, J.D., and McKinney, K.C., 2006, *A USGS zonal table for the Upper Cretaceous Middle Cenomanian-Maastrichtian of the Western Interior of the United States based on Ammonites, Inoceramids, and Radiometric Ages*, U.S. Geological Survey Open-File Report, 1250–2006, 45 p.
- Coccioni, R., 2003, Cretaceous anoxic events: the Italian record. Abstract volume of the Séance spécialisée de la Société géologique de France. In: *Paléocéanographie du Mésozoïque en réponse aux forçages de la paléogéographie et du paléoclimat*, 10–11 June 2003, Paris. p. 10.
- Coccioni, R., and Galeotti, S., 2003, The mid-Cenomanian Event: prelude to OAE 2. *Palaeogeography, Palaeoclimatology, Palaeoecology*, **190**: 427–440, [https://doi.org/10.1016/S0031-0182\(02\)00617-X](https://doi.org/10.1016/S0031-0182(02)00617-X).
- Coccioni, R., and Premoli Silva, I., 1994, Planktonic foraminifera from the Lower Cretaceous of Rio Argos sections (southern Spain) and biostratigraphic implications. *Cretaceous Research*, **15** (6), 645–687.
- Coccioni, R., and Premoli Silva, I., 2015, Revised Upper Albian–Maastrichtian planktonic foraminiferal biostratigraphy and magnetostratigraphy of the classical Tethyan Gubbio section (Italy). *Newsletters on Stratigraphy*, **48/1**: 47–90.
- Colin, J.-P., and Babinot, J.F., 1998, Ostracodes. Columns for Jurassic chart of Mesozoic and Cenozoic sequence chronostratigraphic framework of European basins, by Hardenbol, J., Thierry, J., Farley, M.B., Jacquin, T., de Graciansky, P.-C., and Vail, P.R. (coordinators), and chart supplements. In de Graciansky, P.-C., Hardenbol, J., Jacquin, T., and Vail, P.R. (eds), *Mesozoic-Cenozoic Sequence Stratigraphy of European Basins*. *SEPM Special Publication*, **60**: 763–781.

- Colleté, C., (ed.) 2010. *Stratotype Albien*. Musée national d'Histoire naturelle. BRGM Orle'ans. Paris, 332 p.
- Colloque sur la limite Jurassique-Crétacé, 1975, *Mémoires du Bureau de Recherches Géologiques et Minières*, **86**: 386–393 (summary).
- Combemorel, R., and Christensen, W.K., 1998, Belemnites. Columns for Jurassic chart of Mesozoic and Cenozoic sequence chronostratigraphic framework of European basins, by Hardenbol, J., Thierry, J., Farley, M.B., Jacquin, T., de Graciansky, P.-C., and Vail, P.R. (coordinators). *In de Graciansky, P.-C., Hardenbol, J., Jacquin, T., and Vail, P.R. (eds), Mesozoic-Cenozoic Sequence Stratigraphy of European Basins. SEPM Special Publication*, **60**: 763–781.
- Company, M., Sandoval, J., and Tavera, J.M., 1995, Lower Barremian ammonite biostratigraphy in the Subbetic Domain (Betic Cordillera, southern Spain). *Cretaceous Research*, **16**: 243–256.
- Conybeare, W.D., and Phillips, W., 1822, *Outlines of the Geology of England and Wales, With an Introduction Compendium of the General Principles of That Science, and Comparative Views of the Structure of Foreign Countries. Part 1*. London: William Phillips 470 p.
- Cope, J.C.W., 2007, Drawing the line: the history of the Jurassic-Cretaceous boundary. *Proceedings of the Geologists' Association*, **119**: 105–117.
- Coquand, H., 1857a, Notice sur la formation crétacée du département de la Charente. *Bulletin de la Société géologique de France, Série 2*, **14**: 55–98.
- Coquand, H., 1857b, Position des *Ostrea columba* et *biauriculata* dans le groupe de la craie inférieure. *Bulletin de la Société géologique de France, Série 2*, **14**: 745–766.
- Coquand, H., 1861, Sur la convenance d'établir dans le groupe inférieur de la formation crétacée un nouvel étage entre le Néocomien proprement dit (couches à *Toxaster complanatus* et à *Ostrea couloni*) et le Néocomien supérieur (étage Urgonien de d'Orbigny). *Mémoires de la Société d'Emulation de Provence*, **1**: 127–139.
- Coquand, H., 1871, Sur le Klippenkalk du département du Var et des Alpes-Maritimes. *Bulletin de la Société géologique de France*, **28**: 232–233.
- Corbett, M.J., Watkins, D.K., and Pospichal, J.J., 2014, Quantitative analysis of calcareous nannofossil bioevents of the Late Cretaceous (Late Cenomanian-Coniacian) Western Interior Seaway and their reliability in established zonation schemes. *Marine Micropaleontology*, **109**: 30–45, <https://doi.org/10.1016/j.marmicro.2014.04.002>.
- Cotillon, P., 1987, Bed-scale cyclicity of pelagic Cretaceous successions as a result of world-wide control. *Marine Geology*, **78**: 109–123.
- Cotillon, P., Ferry, S., Gaillard, C., Jautée, E., Latreille, G., and Rio, M., 1980, Fluctuations des paramètres du milieu marin dans le domaine vocontien (France, Sud-Est) au Crétacé inférieur: mise en évidence par l'étude des formations marno-calcaires alternantes. *Bulletin de la Société Géologique de France*, **22**: 735–744.
- Courtillot, V.E., and Renne, P.R., 2003, On the ages of flood basalt events. *Comptes Rendus Geoscience*, **335**: 113–140.
- Cramer, B.D., and Jarvis, I., 2020, Chapter 11 - Carbon isotope stratigraphy. *In Gradstein, F.M., Ogg, J.G., Schmitz, M.D., and Ogg, G.M. (eds), The Geologic Time Scale 2020. Vol. 1 (this book)*. Elsevier, Boston, MA.
- Crampton, J.S., and Gale, A.S., 2005, A plastic boomerang: speciation and intraspecific variation in the Cretaceous bivalve *Actinoceramus*. *Paleobiology*, **31**: 559–577.
- Crampton, J., and Gale, A.S., 2009, Taxonomy of the *Actinoceramus sulcatus* lineage (Late Cretaceous; Bivalvia, Inoceramidae). *Journal of Paleontology*, **83**: 89–109.
- D'Halloy, J.G.J., 1822, Observations sur un essai de cartes géologiques de la France, des Pays-Bas, et des contrées voisines. *Annales de Mines*, **7**: 353–376.
- D'Hondt, A.V., 1998, Inoceramids. Columns for Jurassic chart of Mesozoic and Cenozoic sequence chronostratigraphic framework of European basins, by Hardenbol, J., Thierry, J., Farley, M.B., Jacquin, T., de Graciansky, P.-C., and Vail, P.R. (coordinators). *In de Graciansky, P.-C., Hardenbol, J., Jacquin, T., and Vail, P.R. (eds), Mesozoic-Cenozoic Sequence Stratigraphy of European Basins. SEPM Special Publication*, **60**: 763–781.
- D'Hondt, A.V., Lamolda, M.A., and Pons, J.M., 2007, Stratigraphy of the Coniacian-Santonian transition, meeting organised by the Santonian Working Group of the Subcommittee on Cretaceous Stratigraphy (coordinators) *Cretaceous Research*, **28** (1), 142.
- d'Omalius d'Halloy, J.G.J., 1822, Observations sur un essai de cartes géologiques de la France, des Pays-Bas, et des contrées voisines. *Annales de Mines*, **7**: 353–376.
- d'Orbigny, A., 1840, *Paléontologie française. Terrains crétacés. 1. Céphalopodes*. Paris, 622 p.
- d'Orbigny, A., 1842, *Paléontologie française. Terrains crétacés. 2. Gastropodes*. Paris: Masson 456 p.
- d'Orbigny, A., 1847, *Paléontologie française. Terrains crétacés. 4. Brachiopodes*. Paris: Masson 390 p.
- d'Orbigny, A., 1849–1850, *Paléontologie française. Terrains jurassique. 1. Céphalopodes*. Paris: Bertrand.
- d'Orbigny, A., 1852, *Cours élémentaire de paléontologie et de géologie stratigraphique*, Vol. 2. Paris: Masson, pp. 383–847.
- De Grossouvre, A., 1901, *Recherches sur la Craie supérieure. Partie 1: stratigraphie générale. Mémoires pour servir à l'explication de la carte géologique détaillée de la France*. Paris: Imprimerie Nationale 1013 p.
- De Wever, P., 1998, Radiolarians columns for Jurassic chart of Mesozoic and Cenozoic sequence chronostratigraphic framework of European basins, by Hardenbol, J., Thierry, J., Farley, M.B., Jacquin, T., de Graciansky, P.-C., and Vail, P.R. (coordinators). *In de Graciansky, P.-C., Hardenbol, J., Jacquin, T., and Vail, P.R. (eds), Mesozoic-Cenozoic Sequence Stratigraphy of European Basins. SEPM Special Publication*, **60**: 763–781.
- Desor, E., 1854, Quelques mots sur l'étage inférieur du groupe néocomien (étage Valanginien). *Bulletin de la Société des Sciences Naturelles de Neuchâtel*, **3**: 172–180.
- Desor, E., and Gressly, A., 1859, Études géologiques sur le Jura neuchâtelois. *Bulletin de la Société des Sciences Naturelles de Neuchâtel*, **4**: 1–159.
- Douglas, R.G., and Savin, S.M., 1975, Oxygen and carbon isotope analyses of Tertiary and Cretaceous microfossils from Shatsky Rise and other sites in the North Pacific Ocean. *Initial Reports of the Deep Sea Drilling Project*, **32**: 509–520.
- Dumont, A., 1849, Rapport sur la carte géologique du Royaume. *Bulletin de l'Académie royal des Sciences, des Lettres et des Beaux-Arts de Belgique*, **16**: 351–373.
- Dzyuba, O.S., Izokh, O.P., and Shurygin, B.N., 2013, Carbon isotope excursions in Boreal Jurassic–Cretaceous boundary sections and their correlation potential. *Palaeogeography, Palaeoclimatology, Palaeoecology*, **381–382**: 33–46.
- Earth Impact Database, 2018. Maintained by the Planetary and Space Science Centre, University of New Brunswick. Available from: < www.passc.net/EarthImpactDatabase/ > .

- Elamri, Z., and Zaghib-Turki, D., 2014, Santonian-Campanian biostratigraphy of the Kalaat Senan area (west-central Tunisia). *Turkish Journal of Earth Sciences*, **23** (2), 184–203.
- Eldrett, J.S., Ma, C., Bergman, S.C., Lutz, B., Gregory, F.J., Dodsworth, P., et al., 2015, An astronomically calibrated stratigraphy of the Cenomanian, Turonian and earliest Coniacian from the Cretaceous Western Interior Seaway, USA: implications for global chronostratigraphy. *Cretaceous Research*, **56**: 316–344.
- Erba, E., 1994, Nannofossils and superplumes: the Early Aptian nannocoid crisis. *Paleoceanography*, **9**: 483–501.
- Erba, E., 2004, Calcareous nannofossils and Mesozoic oceanic anoxic events. *Marine Micropaleontology*, **52**: 85–106.
- Erba, E., 2006, The first 150 million years history of calcareous nannoplankton: biosphere–geosphere interactions. *Palaeoecography, Palaoclimatology, Palaeoecology*, **232**: 237–250.
- Erba, E., Aguaro, R., Avram, E., Barboschkin, E.J., Bergen, J., Bralower, T.J., et al., 1996, The Aptian Stage. *Bulletin de l'Institut Royal des Sciences Naturelles de Belgique, Sciences de la Terre*, **66** (Suppl.), 31–43.
- Erba, E., Channell, J.E.T., Claps, M., Jones, C., Larson, R., Opdyke, B., et al., 1999, Integrated stratigraphy of the Cismon Apticore (southern Alps, Italy): a “reference section” for the Barremian-Aptian interval at low latitudes. *Journal of Foraminiferal Research*, **29**: 371–391.
- Erba, E., Bartolini, A., and Larson, R.I., 2004, Valanginian Weissert oceanic event. *Geology*, **32**: 149–152.
- Erbacher, J., Thurow, J., and Litke, R., 1996, Evolution patterns of radiolaria and organic matter variations: a new approach to identify sea-level changes in mid-Cretaceous pelagic environments. *Geology*, **24**: 499–502.
- Ernst, R.E., and Buchan, K.L., 2001, Large mafic magmatic events through time and links to mantle plume-heads. In Ernst, R.E., and Buchan, K.L. (eds), *Mantle Plumes: Their Identification Through Time. Geological Society of America Special Paper*, **352**: 483–575.
- Falzone, F., Petrizzo, M.P., Jenkyns, H.C., Gale, A.S., and Tsikos, H., 2016, Planktonic foraminiferal biostratigraphy and assemblage composition across the Cenomanian-Turonian boundary interval at Clot Chevalier (Vocontian Basin, SE France). *Cretaceous Research*, **59**: 69–97.
- Fiet, N., 2000, Calibrage temporal de l’Aptien et des sous-étages associés par une approche cyclostratigraphique appliquée à la série pélagique de Marches-Ombrie (Italie centrale). *Bulletin de la Société géologique de France*, **171**: 103–113.
- Fiet, N., and Gorin, G., 2000, Lithological expression of Milankovitch cyclicity in carbonate-dominated, pelagic, Barremian deposits in central Italy. *Cretaceous Research*, **21**: 457–467.
- Fiet, N., Beaudoin, B., and Parize, O., 2001, Lithostratigraphic analysis of Milankovitch cyclicity in pelagic Albian deposits of central Italy: implications for the duration of the stage and substages. *Cretaceous Research*, **22**: 265–275.
- Fiet, N., Quidelleur, X., Parize, O., Bulot, L.G., and Gillot, P.Y., 2006, Lower Cretaceous stage durations combining radiometric data and orbital chronology: towards a more stable relative time scale? *Earth and Planetary Science Letters*, **246**: 407–417.
- Föllmi, K.B., Godet, A., Bodin, S., and Linder, P., 2006, Interactions between environmental change and shallow water carbonate buildup along the northern Tethyan margin and their impact on the Early Cretaceous carbon isotope record. *Paleoceanography*, **21**: article #PA4211, 16 pp, <https://doi.org/10.1029/2006PA001313>.
- Frau, C., Bulot, L.G., Réhaková, D., and Wimbledon, W.A.P., 2016, The revision of the ammonite index species *Berriasella jacobi* Mazenot, 1939 and its consequences for the biostratigraphy of the Berriasian Stage. *Cretaceous Research*, **66**: 94–114.
- Frau, C., Bulot, L.G., Delanoy, G., Moreno-Bedmar, J.A., Masse, J.-P., Tendil, A.J.-B., and Lanteaume, C., 2018, The Aptian GSSP candidate at Gorgo a Cerbara (central Italy): an alternative explanation of the bio-, litho- and chemostratigraphic markers. *Newsletters in Stratigraphy*, **51**: 311–326.
- Galbrun, B., 1984, Magnétostratigraphie de la limite Jurassique-Crétacé. Proposition d’une échelle de polarité à partir du stratotype du Berriasien (Berrias, Ardèche, France) et la Sierra de Lugar (Province de Murcie, Espagne). *Mémoires des Sciences della Terre*, **38**: 95 p.
- Gale, A.S., 1995, Cyclostratigraphy and correlation of the Cenomanian Stage in Western Europe. In House, M.R., and Gale, A.S. (eds), *Orbital Forcing Timescales and Cyclostratigraphy. Geological Society Special Publication*, **85**: 177–197.
- Gale, A.S., 2016, Roveacrinida (Crinoidea, Articulata) from the Santonian-Maastrichtian (Upper Cretaceous) of England, the US Gulf Coast (Texas, Mississippi) and southern Sweden. *Papers in Palaeontology*, **2**: 489532, <https://doi.org/10.1002/spp2.1050>.
- Gale, A.S., 2017, An integrated microcrinoid zonation for the Lower Campanian chalk of southern England, and its implications for correlation. *Cretaceous Research*, **87**: 312352, <https://doi.org/10.1016/j.cretres.2017.02.002>.
- Gale, A.S., 2019a, Correlation, age and significance of Turonian Chalk Hardgrounds in southern England and northern France: the roles of tectonics, eustasy and condensation. *Cretaceous Research*, **1103**: article #104164, <https://doi.org/10.1016/j.cretres.2019.06.010>.
- Gale, A.S., 2019b, Microcrinoids (Echinodermata: Articulata: Roveacrinida) from the Cenomanian-Santonian chalk of the Anglo-Paris Basin: taxonomy and biostratigraphy. *Revue de Paléobiologie*, **38**: 379–533.
- Gale, A.S., Montgomery, P., Kennedy, W.J., Hancock, J.M., Burnett, J. A., and McArthur, J.M., 1995, Definition and global correlation of the Santonian-Campanian boundary. *Terra Nova*, **7**: 611–622.
- Gale, A.S., Kennedy, W.J., Burnett, J.A., Caron, M., and Kidd, B.E., 1996, The Late Albian to Early Cenomanian succession at Mont Risou near Rosans (Drôme, SE France): an integrated study (ammonites, inoceramids, planktonic foraminifera, nannofossils, oxygen and carbon isotopes). *Cretaceous Research*, **17**: 515–606.
- Gale, A.S., Young, J.R., Shackleton, N.J., Crowhurst, S.J., and Wray, D. S., 1999, Orbital tuning of Cenomanian marly chalk successions: towards a Milankovitch time-scale for the Late Cretaceous. *Philosophical Transactions of the Royal Society of London, Series A*, **357**: 1815–1829.
- Gale, A.S., Hardenbol, J., Hathway, B., Kennedy, W.J., Young, J.R., and Phansalkar, V., 2002, Global correlation of Cenomanian (Upper Cretaceous) sequences: evidence for Milankovitch control on sea level. *Geology*, **30**: 291–294.
- Gale, A.S., Kennedy, J.W., Lees, J.A., Petrizzo, M.R., and Walaszczyk, I., 2007, An integrated study (inoceramid bivalves, ammonites, calcareous nannofossils, planktonic foraminifera, stable carbon isotopes) of the Ten Mile Creek section, Lancaster, Dallas County, north Texas, a candidate Global boundary Stratotype Section and Point for the base of the Santonian Stage. *Acta Geologica Polonica*, **57**: 113–160.
- Gale, A.S., Hancock, J.M., Kennedy, W.J., Petrizzo, M.R., Lees, J.A., Walaszczyk, I., et al., 2008, An integrated study (geochemistry, stable oxygen and carbon isotopes, nannofossils, planktonic foraminifera, inoceramid bivalves, ammonites and crinoids) of the Waxahachie Dam Spillway section, north Texas, a possible

- boundary stratotype for the base of the Campanian Stage. *Cretaceous Research*, **29**: 131–167.
- Gale, A.S., Bown, P., Caron, M., Crampton, J., Crowhurst, S.J., Kennedy, W.J., et al., 2011, The uppermost Middle and Upper Albian succession at the Col de Palluel, Hautes-Alpes, France: an integrated study (ammonites, inoceramid bivalves, planktonic foraminifera, nannofossils, geochemistry, stable oxygen and carbon isotopes, cyclostratigraphy). *Cretaceous Research*, **32**: 59–130.
- Gale, A.S., Jenkyns, H.C., Tsikos, H., van Breugel, Y., Bottini, C., Erba, E., et al., 2019a, High-resolution bio- and chemostratigraphy of an expanded record of Oceanic Anoxic Event 2 (Late Cenomanian–Early Turonian) at Clot Chevalier, near Barrême, SE France (Vocontian Basin, SE France). *Newsletters on Stratigraphy*, **52**: 97–129, <https://doi.org/10.1127/nos/2018/0445>.
- Gale, A.S., Kennedy, W.J., and Walaszczyk, I., 2019b, Upper Albian, Cenomanian and Lower Turonian stratigraphy, ammonite and inoceramid bivalve faunas from the Cauvery Basin, Tamil Nadu, South India. *Acta Geologica Polonica*, **69**: 161–338.
- Gale, A.S., and Christensen, W.K., 1995, Occurrence of the belemnite *Actinocamax plenus* (Blainville) in the Cenomanian of SE France and its significance. *Bulletin of the Geological Society of Denmark*, **43**: 68–77.
- Gambacorta, G., Jenkyns, H.C., Russo, F., Tsikos, H., Wilson, P.A., Faucher, G., et al., 2015, Carbon- and oxygen-isotope records of mid-Cretaceous Tethyan pelagic sequences from the Umbria-Marche and Belluno Basins (Italy). *Newsletters on Stratigraphy*, **48/3**: 299–323.
- Gambacorta, G., Malinverno, A., and Erba, E., 2019, Orbital forcing of carbonate versus siliceous productivity in the late Albian-late Cenomanian (Umbria-Marche Basin, central Italy). *Newsletters on Stratigraphy*, **52/2**: 197–220.
- Gerasimov, P.A., and Mikhailov, N.R., 1966, Volgian Stage and general stratigraphic scale of the Upper Series of the Jurassic System. *Isvestia Akademia Nauka, S.S.S.R., Geology Series*, **2**: 118–138 [In Russian].
- Ghirardi, J., Deconinck, J.-F., Pellenard, P., Martinez, M., Bruneau, L., Amiotte-Suchet, P., and Pucéat, E., 2014, Multi-proxy orbital chronology in the aftermath of the Aptian Ocean Anoxic Event 1a: Palaeoceanographic implications (Serre Chaitieu section, Vocontian Basin, SE France). *Newsletters in Stratigraphy*, **47/3**: 247–262.
- Gibson, F., 2006, Timescales of Plume-Lithosphere Interactions in LIPs: $^{40}\text{Ar}/^{39}\text{Ar}$ Geochronology of Alkaline Igneous Rocks From the Paraná-Etendeka Large Igneous Province. Available from: <www.largeigneousprovinces.org/06nov.html> .
- Gibson, S.A., Thompson, R.N., and Day, J.A., 2006, Timescales and mechanisms of plume–lithosphere interactions: $^{40}\text{Ar}/^{39}\text{Ar}$ geochronology and geochemistry of alkaline igneous rocks from the Paraná–Etendeka large igneous province. *Earth and Planetary Science Letters*, **256**: 1–17.
- Gilder, S., Chen, Y., Cogne, J.P., Tan, X.D., Courtillot, V., Sun, D.J., et al., 2003, Paleomagnetism of Upper Jurassic to Lower Cretaceous volcanic and sedimentary rocks from the western Tarim basin and implications for inclination shallowing and absolute dating of the M-0 (ISEA?) chron. *Earth and Planetary Science Letters*, **206**: 587–600.
- Giraud, F., 1995, Recherche des périodicités astronomiques et des fluctuations du niveau marin à partir de l'étude du signal carbonaté des séries pélagiques alternantes. *Documents des Laboratoires de Géologie Lyon*, **134**: 279 p.
- Giraud, F., Beaufort, L., and Cotillon, P., 1995, Periodicities of carbonate cycles in the Valanginian of the Vocontian Trough: a strong obliquity control. In House, M.R., and Gale, A.S. (eds), *Orbital Forcing Timescales and Cyclostratigraphy. Geological Society Special Publication*, **85**: 143–164.
- González-Donoso, J.M., Linares, D., and Robaszynski, F., 2007, The rotaliporids, a polyphyletic group of Albian-Cenomanian planktonic foraminifera: emendation of genera. *Journal of Foraminiferal Research*, **37** (2), 175–186.
- Gorbachik, T.N., 1986, *Jurassic and Early Cretaceous planktonic foraminifera of the south of the USSR* (in Russian). AN SSSR, “Nauka”, pp. 1–239. (*Jurskie i Rammelovye planktonye foraminifery Juga SSSR. Akademia NAUK SSSR. Moskovskoi Oschestvo Prirody*).
- Graciansky, P.-C., Hardenbol, J., Jacquin, T., and Vail, P.R. (eds.), 1998, *Mesozoic-Cenozoic Sequence Stratigraphy of European Basins*. SEPM Special Publication, **60**: 786 pp.
- Gradstein, F.M., Ogg, J.G., and Smith, A.G., 2004, (coordinators) *A Geologic Time Scale 2004*. Cambridge: Cambridge University Press 589 p.
- Gradstein, F.M., Ogg, J.G., Schmitz, M.D. and Ogg, G.M. (eds.), 2012, *The Geologic Time Scale 2012*. Elsevier Publ. Co., 1144 pp.
- Gradstein, F.M., Gale, A., Kopaevich, L., Waskowska, A., Grigelis, A., Glinkikh, L., et al., 2017, The planktonic foraminifera of the Jurassic. Part II: Stratigraphy, palaeoecology and palaeobiogeography. *Swiss Journal of Paleontology*, **136**: 259–271.
- Grant, S.F., Coe, A.L., and Armstrong, H.A., 1999, Sequence stratigraphy of the Coniacian succession of the Anglo-Paris Basin. *Geological Magazine*, **136**: 17–38.
- Graciansky, P.-C., Hardenbol, J., Jacquin, T., and Vail, P.R. (eds), 1998, *Mesozoic-Cenozoic Sequence Stratigraphy of European Basins*. p. 786.
- Green, K.A., and Brecher, A., 1974, Preliminary paleomagnetic results for sediments from Site 263, Leg 27. *Initial Reports, Deep Sea Drilling Project*, **27**: 405–413.
- Grippo, A., Fischer, A.G., Hinnov, L.A., Herbert, T.M., and Premoli Silva, I., 2004, Cyclostratigraphy and chronology of the Albian stage (Piobbico core, Italy). In D’Argenio, B., Fischer, A.G., Premoli Silva, I., Weissert, H., and Ferreri, V. (eds), *Cyclostratigraphy: Approaches and Case Histories. SEPM Special Publication*, **81**: 57–81.
- Grossman, E.L., and Joachimski, M.M., 2020, Chapter 10 - Oxygen isotope stratigraphy. In Gradstein, F.M., Ogg, J.G., Schmitz, M.D., and Ogg, G.M. (eds), *The Geologic Time Scale 2020*. Vol. 1 (this book). Elsevier, Boston, MA.
- Hailwood, E.A., 1979, Paleomagnetism of Late Mesozoic to Holocene sediments from the Bay of Biscay and Rockall Plateau, drilled on IPOD Leg 48. *Initial Reports, Deep Sea Drilling Project*, **48**: 305–339.
- Hancock, J.M., 1991, Ammonite scales for the Cretaceous System. *Cretaceous Research*, **12**: 259–291.
- Hancock, J.M., 2001, A proposal for a new position for the Aptian/Albian boundary. *Cretaceous Research*, **22**: 677–683.
- Hancock, J.M., and Gale, A.S., 1996, The Campanian Stage. *Bulletin de l’Institut Royal des Sciences Naturelles de Belgique, Sciences de la Terre*, **66** (Suppl.), 103–109.
- Hancock, J.M., Peake, N.B., Burnett, J., Dhondt, A.V., Kennedy, W.J., and Stokes, R., 1993, High Cretaceous biostratigraphy at Tercis, SW France. *Bulletin de l’Institut Royal des Sciences Naturelles de Belgique, Sciences de la Terre*, **63**: 133–148.

- Haq, B.U., 2014, Cretaceous eustasy revisited. *Global and Planetary Change*, **113**: 44–58.
- Hardenbol, J., Thierry, J., Farley, M.B., Jacquin, T., de Graciansky, P.-C., Vail, P.R., et al., 1998, Mesozoic and Cenozoic sequence chronostratigraphic framework of European basins, 763–781, and chart supplements. In de Graciansky, P.-C., Hardenbol, J., Jacquin, T., and Vail, P.R. (eds), *Mesozoic-Cenozoic Sequence Stratigraphy of European Basins*. *SEPM Special Publication*, **60**: 3–13.
- Harding, I.C., Smith, G.A., Riding, J.B., and Wimbledon, W.A.P., 2011, Inter-regional correlation of Jurassic/Cretaceous boundary strata based on the Tithonian-Valanginian dinoflagellate cyst biostratigraphy of the Volga Basin, western Russia. *Review of Palaeobotany and Palynology*, **167** (1–2), 82–116.
- Harland, W.B., Armstrong, R.L., Cox, A.V., Craig, L.E., Smith, A.G., and Smith, D.G., 1990, *A Geologic Time Scale 1989*. Cambridge: Cambridge University Press 263 p.
- Hart, M.B., 1980, A water depth model for the evolution of the planktonic Foraminifera. *Nature*, **286**: 252–254.
- Hart, M.B., 1999, The evolution and biodiversity of Cretaceous planktonic Foraminifera. *Geobios*, **32** (2), 247–255.
- Hart, M., Amédéo, F., and Owen, H., 1996, The Albian stage and substage boundaries. *Bulletin de l'Institut Royal des Sciences Naturelles de Belgique, Sciences de la Terre*, **66** (Suppl.), 45–56.
- Haynes, S.J., Huber, B.T., and Macleod, K.G., 2015, Evolution and phylogeny of mid-Cretaceous (Albian–Coniacian) biserial planktic foraminifera. *Journal of Foraminiferal Research*, **45** (1), 42–81.
- He, H.Y., Pan, Y.X., Tauxe, L., Qin, H.F., and Zhu, R.X., 2008, Toward age determination of the M0r (Barremian–Aptian boundary) of the Early Cretaceous. *Physics of the Earth and Planetary Interiors*, **169**: 41–48.
- Hennebert, M., Robaszynski, F., and Goolaerts, S., 2009, Cyclostratigraphy and chronometric scale in the Campanian – Lower Maastrichtian – the Abiod Formation at Ellès, central Tunisia. *Cretaceous Research*, **30**: 325–338.
- Herbert, T.D., 1992, Paleomagnetic calibration of Milankovitch cyclicity in Lower Cretaceous sediments. *Earth and Planetary Science Letters*, **112**: 15–28.
- Herbert, T.D., D'Hondt, S.L., Premoli-Silva, I., Erba, E., and Fischer, A. G., 1995, Orbital chronology of Cretaceous–Early Palaeocene marine sediments. In Berggren, W.A., Kent, D.V., and Hardenbol, J. (eds), *Geochronology, Time Scales and Global Stratigraphic Correlations: A Unified Temporal Framework for a Historical Geology*. *SEPM Special Publication*, **54**: 81–94.
- Herrle, J.O., and Mutterlose, J., 2003, Calcareous nannofossils from the Aptian-Lower Albian of southeast France: palaeoecological and biostratigraphic implications. *Cretaceous Research*, **24**: 1–22.
- Herrle, J.O., Kössler, P., Friedrich, O., Erlenkeuser, H., and Hemleben, C., 2004, High-resolution carbon isotope records of the Aptian to Lower Albian from SE France and the Mazagan Plateau (DSDP Site 545): a stratigraphic tool for paleoceanographic and paleobiologic reconstruction. *Earth and Planetary Science Letters*, **218**: 149–161.
- Herrle, J.O., Schroder-Adams, C.J., Davis, W., Pugh, A.T., Galloway, J. M., and Fath, J., 2015, Mid-Cretaceous High Arctic stratigraphy, climate, and Oceanic Anoxic Events. *Geology*, **43**: 403–406.
- Hesselbo, S.P., Coe, A.L., and Jenkyns, H.C., 1990, Recognition and documentation of depositional sequences from outcrop: an example from the Aptian and Albian on the eastern margin of the Wessex Basin. *Journal of the Geological Society*, **147**: 549–559.
- Hesselbo, S.P., Ogg, J.G., and Ruhl, M., 2020, Chapter 26 – The Jurassic Period. In Gradstein, F.M., Ogg, J.G., Schmitz, M.D., and Ogg, G.M. (eds), *The Geologic Time Scale 2020*. Vol. **2** (this book). Elsevier, Boston, MA.
- Hicks, J.F., and Obradovich, J.D., 1995, Isotopic age calibration of the GRTS from C33N to C31N: Late Cretaceous Pierre Shale, Red Bird section, Wyoming, USA. *Geological Society of America, Abstracts with Programs*, **27**: A174.
- Hicks, J.F., Obradovich, J.D., and Tauxe, L., 1995, A new calibration point for the Late Cretaceous time scale: the $^{40}\text{Ar}/^{39}\text{Ar}$ isotopic age of the C33r/C33n geomagnetic reversal from the Judith River Formation (Upper Cretaceous), Elk Basin, Wyoming, USA. *Journal of Geology*, **103**: 243–256.
- Hicks, J.F., Obradovich, J.D., and Tauxe, L., 1999, Magnetostratigraphy, isotopic age calibration and intercontinental correlation of the Red Bird section of the Pierre Shale, Niobrara County, Wyoming, USA. *Cretaceous Research*, **20**: 1–27.
- Hilgen, F.J., Hinnov, L.A., Aziz, H.A., Abels, H.A., Batenburg, S., Bosmans, J.H.C., et al., 2014, Stratigraphic continuity and fragmentary sedimentation: the success of cyclostratigraphy as part of integrated stratigraphy. In Smith, D.G., Bailey, R.J., Burgess, P.M., and Fraser, A.J. (eds), *Strata and Time: Probing the Gaps in Our Understanding*. Geological Society of London, Special Publication, p. 404.
- Hochuli, P.A., Menegatti, A.P., Weissert, H., Riva, A., Erba, E., and Premoli Silva, I., 1999, Episodes of high productivity and cooling in the early Aptian Alpine Tethys. *Geology*, **27**: 657–660.
- Hoedemaeker, P.J., and Leereveld, H., 1995, Biostratigraphy and sequence stratigraphy of the Berriasian-lowest Aptian (Lower Cretaceous) of the Río Argos succession, Caravaca, SE Spain. *Cretaceous Research*, **16**: 195–230.
- Hoedemaeker, P.J., Company, M.R., Aguirre Urreta, M.B., Avram, E., Bogdanova, T.N., Bujtor, L., et al., 1993, Ammonite zonation for the Lower Cretaceous of the Mediterranean region; basis for the stratigraphic correlation within IGCP, Project 262. *Revista Española de Paleontología*, **8**: 117–120.
- Hoedemaeker, P.J., Reboulet, S., Aguirre-Urreta, M.B., Alsen, P., Atrops, F., Barragan, R., et al., 2003, Report on the 1st international workshop of the IUGS Lower Cretaceous Ammonite Working Group, the 'Kilian Group' (Lyon, 11 July 2002). *Cretaceous Research*, **24**: 89–94.
- Houša, V., Pruner, P., Zakharov, V.A., Kostak, M., Chadima, M., Rogov, M.A., et al., 2007, Boreal–Tethyan correlation of the Jurassic–Cretaceous boundary interval by magneto- and biostratigraphy. *Stratigraphy and Geological Correlation*, **15** (3), 297–309.
- Huang, C., 2018, Astronomical timescale for the Mesozoic. *Stratigraphy Timescales*, **3**: 1–70.
- Huang, Z., Ogg, J.G., and Gradstein, F.M., 1993, A quantitative study of Lower Cretaceous cyclic sequences from the Atlantic Ocean and the Vocontian Basin (SE France). *Paleoceanography*, **8**: 275–291.
- Huang, C., Hinnov, L.A., Fischer, A.G., Grippo, A., and Herbert, T., 2010, Astronomical tuning of the Aptian Stage from Italian reference sections. *Geology*, **38**: 899–902.
- Huber, B.T., 1992, Paleobiogeography of Campanian-Maastrichtian foraminifera in the southern high latitudes. *Palaeogeography, Palaeoclimatology, Palaeoecology*, **92** (3–4), 325–360.
- Huber, B.T., and Leckie, R.M., 2011, Planktic foraminiferal species turnover across deep-sea Aptian/Albian boundary sections. *Journal of Foraminiferal Research*, **41**: 53–95.

- Huber, B.T., and Petrizzo, M.R., 2014, Evolution and taxonomic study of the Cretaceous planktonic foraminifer genus *Helvetoglobotruncana* Reiss, 1957. *Journal of Foraminiferal Research*, **44**: 40–57.
- Huber, B.T., Hodell, D.A., and Hamilton, C.P., 1995, Middle-Late Cretaceous climate of the southern high latitudes: stable isotopic evidence for minimal equator-to-pole thermal gradients. *Geological Society of America Bulletin*, **107**: 1164–1191.
- Huber, B.T., Norris, R.D., and MacLeod, K.G., 2002, Deep sea paleotemperature record of extreme warmth during the Cretaceous. *Geology*, **30**: 123–126.
- Huber, B.T., MacLeod, K.G., and Tur, N.A., 2008, Chronostratigraphic framework for Upper Campanian-Maastrichtian sediments on the Blake Nose (subtropical North Atlantic). *Journal of Foraminiferal Research*, **38**: 162–182.
- Huber, B.T., Petrizzo, M.R., Young, J.R., Falzoni, F., Gilardoni, S.E., Bown, P.R., et al., 2016, Pforams@mikrotax: a new online taxonomic database for planktonic foraminifera. *Micropaleontology*, **62** (6), 429–438.
- Huber, B.T., Petrizzo, M.R., Watkins, D.K., Haynes, S.J., and MacLeod, K.G., 2017, Correlation of Turonian continental margin and deep-sea sequences in the subtropical Indian Ocean sediments by integrated planktonic foraminiferal and calcareous nannofossil biostratigraphy. *Newsletters on Stratigraphy*, **50**: 141–185.
- Husson, D., Galbrun, B., Laskar, J., Hinnov, L.A., Thibault, N., Gardin, S., et al., 2011, Astronomical calibration of the Maastrichtian. *Earth and Planetary Science Letters*, **305**: 328–340.
- Ingle, S., and Coffin, M.F., 2004, Impact origin for the greater Ontong Java Plateau? *Earth and Planetary Science Letters*, **218**: 123–134.
- Jacquin, T., and de Graciansky, P.-C., 1998, Major transgressive-regressive cycles: the stratigraphic signature of European basin development. In de Graciansky, P.-C., Hardenbol, J., Jacquin, T., and Vail, P.R. (eds), *Mesozoic-Cenozoic Sequence Stratigraphy of European Basins*. *SEPM Special Publication*, **60**: 15–29.
- Janasi, V.A., Freitas, V.A., and Heaman, L.H., 2011, The onset of flood basalt volcanism, Northern Paraná Basin, Brazil: a precise U–Pb baddeleyite/zircon age for a Chapecó-type dacite. *Earth and Planetary Science Letters*, **302**: 147–153.
- Jarrard, R.D., 1974, Paleomagnetism of some Leg 27 sediment cores. *Initial Reports, Deep Sea Drilling Project*, **27**: 415–423.
- Jarvis, I., Gale, A.S., Jenkyns, H.C., and Pearce, M.A., 2006, Secular variation in Late Cretaceous carbon isotopes: a new $\delta^{13}\text{C}$ carbonate reference curve for the Cenomanian–Campanian (99.6–70.6 Ma). *Geological Magazine*, **143**: 561–608.
- Jarvis, I., Lignum, J.S., Gröcke, D.R., Jenkyns, H.C., and Pearce, M.A., 2011, Black shale deposition, atmospheric CO_2 drawdown, and cooling during the Cenomanian-Turonian Oceanic Anoxic Event. *Paleoceanography*, **26**: PA3201, <https://doi.org/10.1029/2010PA002081>.
- Jenkyns, H.C., 1999, Mesozoic anoxic events and palaeoclimate. *Zentralblatt für Geologie und Paläontologie, Teil I*, **7–9**: 943–949.
- Jenkyns, H.C., 2010, Geochemistry of oceanic anoxic events. *Geochemistry, Geophysics, Geosystems*, **11**: article # Q03004, <https://doi.org/10.1029/2009GC002788>.
- Jenkyns, H.C., 2017, Transient cooling episodes during Cretaceous Oceanic Anoxic Events with special reference to OAE1a (Early Aptian). *Philosophical Transactions of the Royal Society*, **A376**: 20170073.
- Jenkyns, H.C., Gale, A.S., and Corfield, R.M., 1994, Carbon- and oxygen-isotope stratigraphy of the English Chalk and the Italian Scaglia and its palaeoclimatic significance. *Geological Magazine*, **131**: 1–34.
- Jinnah, Z.A., Roberts, E.M., Deino, A.L., Larsen, J.S., Link, P.K., and Fanning, C.M., 2009, New $^{40}\text{Ar}/^{39}\text{Ar}$ and detrital zircon U–Pb ages for the Upper Cretaceous Wahweap and Kaiparowits formations on the Kaiparowits Plateau, Utah: implications for regional correlation, provenance, and biostratigraphy. *Cretaceous Research*, **30**: 287–299.
- Jones, C.E., and Jenkyns, H.C., 2001, Seawater strontium isotopes, oceanic anoxic events, and seafloor hydrothermal activity in the Jurassic and Cretaceous. *American Journal of Science*, **301**: 112–149.
- Joo, Y.J., and Sageman, B.G., 2014, Cenomanian to Campanian carbon isotope chemostratigraphy from the Western Interior Basin, USA. *Journal of Sedimentary Research*, **84**: 529–542.
- Jourdan, F., Renne, P.R., and Reimold, W.U., 2009, An appraisal of the ages of terrestrial impact structures. *Earth and Planetary Science Letters*, **286**: 1–13.
- Kamo, S.L., and Riccardi, A.C., 2009, A new U–Pb zircon age for an ash layer at the Bathonian–Callovian boundary, Argentina. *GFF*, **131**: 177–182.
- Kennedy, W.J., and Gale, A.S., 2017b, The Ammonoidea of the Lower Chalk. Part 7. *Palaeontographical Society (Monograph)*, 461–571.
- Kietzmann, D.A., Iglesia Llanos, M.P., and Kohan Martínez, M., 2018, Astronomical calibration of the Tithonian-Berriasian in the Neuquén Basin, Argentina: A contribution from the Southern Hemisphere to the geologic time scale. In Montenari, M. (ed), *Stratigraphy and Timescales*. **3**: 327–355.
- Kolodny, Y., and Raab, M., 1988, Oxygen isotopes in phosphatic fish remains from Israel; paleothermometry of tropical Cretaceous and Tertiary shelf waters. *Palaeogeography, Palaeoclimatology, Palaeoecology*, **64**: 59–67.
- Kuiper, K.F., Deino, A., Hilgen, F.J., Krijgsman, W., Renne, P.R., and Wijbrans, J.R., 2008, Synchronizing rock clocks of Earth history. *Science*, **320**: 500–504.
- Kauffman, E.J., Kennedy, W.J., and Wood, C.J., 1996, The Coniacian stage and substage boundaries. *Bulletin de l'Institut Royal des Sciences Naturelles de Belgique, Sciences de la Terre*, **66** (Suppl.), 81–94.
- Keating, B.H., and Helsley, C.E., 1978a, Magnetostratigraphic studies of Cretaceous age sediments from Sites 361, 363, and 364. *Initial Reports, Deep Sea Drilling Project*, **40**: 459–467.
- Keating, B.H., and Helsley, C.E., 1978b, Magnetostratigraphic studies of Cretaceous sediments from DSDP Site 369. *Initial Reports, Deep Sea Drilling Project*, **41** (Suppl.), 983–986.
- Keating, B.H., and Helsley, C.E., 1978c, Paleomagnetic results from DSDP Hole 391C and the magnetostratigraphy of Cretaceous sediments from the Atlantic Ocean floor. *Initial Reports, Deep Sea Drilling Project*, **44**: 523–528.
- Kemp, T.S., 2005, *The Origin and Evolution of Mammals*. Oxford: Oxford University Press 342 pp.
- Kemper, E., Rawson, P.F., and Thieuloy, J.P., 1981, Ammonites of Tethyan ancestry in the early Lower Cretaceous of north-west Europe. *Palaeontology*, **24**: 251–311.
- Kennedy, W.J., 1984, Ammonite faunas and the 'standard zones' of the Cenomanian to Maastrichtian Stages in their type areas, with some proposals for the definition of the stage boundaries by ammonites. *Geological Society of Denmark Bulletin*, **33**: 147–161.
- Kennedy, W.J., 2019, The Ammonoidea of the Upper Chalk. Part 1. *Monographs of the Palaeontographical Society*, **173**: 112 pp.

- Kennedy, W.J., and Cobban, W.A., 1991, Stratigraphy and inter-regional correlation of the Cenomanian-Turonian transition in the Western Interior of the United States near Pueblo, Colorado. A potential boundary stratotype for the base of the Turonian Stage. *Newsletters on Stratigraphy*, **24**: 1–33.
- Kennedy, W.J., and Gale, A.S., 2015, Ammonites from the Albian and Cenomanian (Cretaceous) of Djebel Mhrila, Tunisia. *Revue de Paléobiologie*, **34** (2), 235–361.
- Kennedy, W.J., and Gale, A.S., 2016, Late Turonian ammonites from northwestern Aquitaine, France. *Cretaceous Research*, **58**: 265–296.
- Kennedy, W.J., and Gale, A.S., 2017a, Trans-Tethyan correlation of the Lower-Middle Cenomanian boundary interval; southern England (Southerham, near Lewes Sussex) and Douar el Khiana, northeastern Algeria. *Acta Geologica Polonica*, **67**: 75–108.
- Kennedy, W.J., Juignet, P., and Girard, J., 1990, *Budaiceras hyatti* (Shattuck, 1903), a North American index ammonite from the Lower Cenomanian of Haute Normandie, France. *Neues Jahrbuch für Geologie und Paläontologie Abhandlungen*, **1990**: 525–535.
- Kennedy, W.J., Christensen, W.K., Hancock, J.M., 1995. Defining the base of the Maastrichtian and its substages. Internal report for the Maastrichtian Working Group. In: *Second International Symposium on Cretaceous Boundaries, Brussels, 8–16 September 1995*, 13 p. [Unpublished].
- Kennedy, W.J., Gale, A.S., Bown, P.R., Caron, M., Davey, R.J., Gröcke, D., et al., 2000a, Integrated stratigraphy across the Aptian-Albian boundary in the Marnes Bleues at the Col de Pré-Guittard, Arnayon (Brôme), and at Tartonne (Alpes-de-Haute-Provence), France: a candidate Global Boundary Stratotype Section and Boundary Point for the base of the Albian Stage. *Cretaceous Research*, **21**: 591–720.
- Kennedy, W.J., Walaszczyk, I., and Cobban, W.A., 2000b, Pueblo, Colorado, USA, candidate Global Boundary Stratotype Section and Point for the base of the Turonian Stage of the Cretaceous and for the Middle Turonian substage, with a revision of the Inoceramidae (Bivalve). *Acta Geologica Polonica*, **50**: 295–334.
- Kennedy, W.J., Gale, A.S., Lees, J.A., and Caron, M., 2004, Definition of a Global Boundary Stratotype Section and Point (GSSP) for the base of the Cenomanian Stage, Mont Risou, Hautes-Alpes, France. *Episodes*, **27**: 21–32.
- Kennedy, W.J., Walaszczyk, I., and Cobban, W.A., 2005, The Global Boundary Stratotype Section and Point for the base of the Turonian Stage of the Cretaceous: Pueblo, Colorado, U.S.A. *Episodes*, **28** (2), 93–104.
- Kennedy, W.J., Gale, A.S., Huber, B., Petrizzo, M.R., and Jenkyns, H.C., 2014, Integrated stratigraphy across the Aptian-Albian boundary in the Marnes Bleue, at the Col de Pre-Guittard, Arnayon (Drome) revisited, a candidate Global Boundary Stratotype Section and new proposal of a Boundary Point for the base of the Albian Stage: the first occurrence of the planktic foraminiferan *Microhedbergella renilaevis* Huber and Leckie, 2011. *Cretaceous Research*, **51**: 248–259.
- Kennedy, W.J., Gale, A.S., Huber, B.T., Petrizzo, M.R., Bown, P., and Jenkyns, H.C., 2017, The Global Boundary Stratotype Section and Point (GSSP) for the base of the Albian Stage, of the Cretaceous, the Col de Palluel section, Arnayon, Drôme, France. *Episodes*, **40**: 177–188.
- Kent, D.V., and Gradstein, F.M., 1985, A Cretaceous and Jurassic geochronology. *Bulletin of the Geological Society of America*, **96**: 1419–1427.
- Kerr, A.C., 1998, Oceanic plateau formation: a cause of mass extinction and black shale deposition around the Cenomanian-Turonian boundary? *Journal of the Geological Society*, **155**: 619–626.
- Kietzmann, D.A., Palma, R.M., and Iglesia Llanos, M.P., 2015, Cyclostratigraphy of an orbitally-driven Tithonian–Valanginian carbonate ramp succession, Southern Mendoza, Argentina: implications for the Jurassic–Cretaceous boundary in the Neuquén Basin. *Sedimentary Geology*, **315**: 29–46.
- Kilian, W., 1888, *Description Géologique de la Montagne de Lure (Basses-Alpes)*. Paris: Université Masson, These de Doctorat 458 pp.
- Kita, Z.A., Watkins, D.K., and Sageman, B.S., 2017, High-resolution calcareous nannofossil biostratigraphy of the Santonian/Campanian Stage boundary, Western Interior Basin, USA. *Cretaceous Research*, **69**: 49–55.
- Koeberl, C., Armstrong, R.A., and Reimold, W.U., 1997, Morokweng, South Africa: a large impact structure of Jurassic–Cretaceous boundary age. *Geology*, **25**: 731–734.
- Kuhnt, W., and Moullade, M., 2007, The Gargasian (middle Aptian) of La Marcouline section at Cassis–La Bédoule (SE France): stable isotope record and orbital cyclicity. *Carnets de Géologie*, **2007** (02), 1–9.
- Kuhnt, W., Holbourn, A., Gale, A., Chellai, E.H., and Kennedy, W.J., 2009, Cenomanian sequence stratigraphy and sea-level fluctuations in the Tarfaya Basin (SW Morocco). *Geological Society of America Bulletin*, **121**: 1695–1710.
- Lamolda, M.A., and Paul, C.R.C., 2007, Carbon and Oxygen Stable Isotopes across the Coniacian-Santonian boundary at Olazagutia (Navarra Province), Spain. *Cretaceous Research*, **28**: 18–29.
- Lamolda, M.A., Hancock, J.M., Burnett, J.A., Collom, C.J., Christensen, W.K., Dhondt, A.V., et al., 1996, The Santonian Stage and sub-stages. *Bulletin de l'Institut Royal des Sciences Naturelles de Belgique, Sciences de la Terre*, **66** (Suppl.), 95–102.
- Lamolda, M.A., Peryt, D., and Ion, J., 2007, Planktonic foraminiferal bioevents in the Coniacian/Santonian boundary interval at Olazagutia, Navarra province, Spain. *Cretaceous Research*, **28** (1), 18–29.
- Lamolda, M.A., Paul, C.R.C., and Peryt, D., 2014, The Global Boundary Stratotype and Section Point for the base of the Santonian Stage, “Cantera de Margas”, Olazagutia, northern Spain. *Episodes*, **37**: 2–13.
- Landman, N.H., and Waage, K.M., 1993, Scaphitid ammonites of the Upper Cretaceous (Maastrichtian) Fox Hills Formation in South Dakota and Wyoming. *Bulletin of the American Museum of Natural History*, **215**: 257.
- Large Igneous Provinces Commission (of the International Association of Volcanology and Chemistry of the Earth’s Interior), 2011. LIP Record. Available from: <<http://largeigneousprovinces.org/record>> [and subpages].
- Larson, R.L., 1991, Latest pulse of the Earth: evidence for a mid Cretaceous super plume. *Geology*, **19**: 547–550.
- Larson, R.L., and Erba, E., 1999, Onset of the mid-Cretaceous greenhouse in the Barremian-Aptian: igneous events and the biological, sedimentary, and geochemical responses. *Paleoceanography*, **14**: 663–678.
- Laskar, J., Fienga, A., Gastineau, M., and Manche, H., 2011, La2010: a new orbital solution for the long-term motion of the Earth. *Astronomy Astrophysics*, **532**: A89.
- Leckie, R.M., Bralower, T.J., and Cashman, R., 2002, Oceanic anoxic events and plankton evolution: biotic response to tectonic forcing during the mid-Cretaceous. *Paleoceanography*, **17**: 1041, <https://doi.org/10.1029/2001PA000623>.

- Leereveld, H., 1995, Dinoflagellate cysts from the Lower Cretaceous Río Argos succession (SE Spain). *LPP Contributions Series*, 2: 175.
- Lena, L., López-Martínez, R., Lescano, M., Aguirre-Urreta, B., Concheyro, A., Vennari, V., et al., 2019, High-precision U–Pb ages in the early Tithonian to early Berriasian and implications for the numerical age of the Jurassic–Cretaceous boundary. *Solid Earth*, **10**: 1–14.
- Lerbekmo, J.F., 1989, The stratigraphic position of the 33-33r (Campanian) polarity chron boundary in southeastern Alberta. *Bulletin of Canadian Petroleum Geology*, **37**: 43–47.
- Lerbekmo, J.F., and Braman, D.R., 2002, Magnetostratigraphic and biostratigraphic correlation of late Campanian and Maastrichtian marine and continental strata from the Red Deer River Valley to the Cypress Hills, Alberta, Canada. *Canadian Journal of Earth Sciences*, **39**: 539–557.
- Li, L., Keller, G., and Stinnesbeck, W., 1999, The Late Campanian and Maastrichtian in northwestern Tunisia: palaeoenvironmental inferences from lithology, macrofauna and benthic foraminifera. *Cretaceous Research*, **20** (2), 231–252.
- Li, X., Jenkyns, H.C., Wang, C., Hu, X., Chen, X., Wei, Y., et al., 2006, Upper Cretaceous carbon- and oxygen-isotope stratigraphy of hemipelagic carbonate facies, southern Tibet, China. *Journal of the Geological Society*, **163**: 375–382.
- Li, X., Bralower, T.J., Montañez, I.P., Osleger, D.A., Arthur, M.A., Bice, D.M., et al., 2008, Toward an orbital chronology for the early Aptian Oceanic Anoxic Event (OAE1a, ~120 Ma). *Earth and Planetary Science Letters*, **271**: 88–100.
- Lini, A., Weissert, H., and Erba, E., 1992, The Valanginian carbon isotope event: a first episode of greenhouse climate conditions during the Cretaceous. *Terra Nova*, **4**: 374–384.
- Locklair, R.E., and Sageman, B.B., 2008, Cyclostratigraphy of the Upper Cretaceous Niobrara Formation, Western Interior, U.S.A.: a Coniacian–Santonian orbital timescale. *Earth and Planetary Science Letters*, **269**: 539–552.
- Longoria, J.F., 1977, Bioestratigrafía del Cretácico Inferior basada en microfósiles planctónicos. *Boletín de la Sociedad Geológica Mexicana*, **38/1**: 2–17.
- López-Martínez, R., Aguirre-Urreta, B., Lescano, M., Concheyro, A., Vennari, V., and Ramos, V.A., 2017, Tethyan calpionellids in the Neuquén Basin (Argentine Andes), their significance in defining the Jurassic/Cretaceous boundary and pathways for Tethyan-Eastern Pacific connections. *Journal of South American Earth Sciences*, **78**: 116–125.
- Lowrie, W., and Alvarez, W., 1977, Late Cretaceous geomagnetic polarity sequence: detailed rock and palaeomagnetic studies of the Scaglia Rossa limestone at Gubbio, Italy. *Geophysics Journal of the Royal Astronomical Society*, **51**: 561–581.
- Lowrie, W., Alvarez, W., Premoli-Silva, I., and Monechi, S., 1980, Lower Cretaceous magnetic stratigraphy in Umbrian pelagic carbonate rocks. *Geophysical Journal, Royal Astronomical Society*, **60**: 263–281.
- Luber, T.L., Bulot, L.G., Redfern, J., Frau, C., Arantegui, A., and Masrour, M., 2017, A revised ammonoid biostratigraphy for the Aptian of NW Africa: Essaouira-Agadir Basin, Morocco. *Cretaceous Research*, **79**: 12–34.
- Luber, T.L., Bulot, L.G., Redfern, J., Nahim, M., Jeremiah, J., Simmons, M., et al., 2019, A revised chronostratigraphic framework for the Aptian of the Essaouira-Agadir Basin, a candidate type section for the NW African Atlantic Margin. *Cretaceous Research*, **93**: 292–317.
- Lucas, S.G., 1997, *Dinosaurs, the Textbook*, Second ed. Dubuque, IA: Wm. C. Brown Publishers: 336 pp.
- Lucas, S.G., Kirkland, J.I., and Estep, J.W. (eds), 1998, Lower and Middle Cretaceous terrestrial ecosystems. *New Mexico Museum of Natural History and Science Bulletin* **14**: 330 pp.
- Lucas, S.G., Sullivan, R.M., and Spielmann, J.A., 2012, Cretaceous vertebrate biochronology, North American Western Interior. *Journal of Stratigraphy*, **36** (2), 426–461.
- Ma, C., Meyers, S.R., Sageman, B.B., Singer, B.S., and Jicha, B.R., 2014, Testing the astronomical timescale for oceanic anoxic event 2, and its extension into Cenomanian strata of the Western Interior Basin, USA. *Bulletin of the Geological Society of America*, **126**: 974–989.
- Ma, C., Myers, S.R., and Sageman, B.B., 2019, Testing Late Cretaceous astronomical solutions in a 15 million year astrochronological record from North America. *Earth and Planetary Science Letters*, <https://doi.org/10.1016/j.epsl.2019.01.053>.
- Magniez-Jannin, F., 1995, Cretaceous stratigraphic scales based on benthic foraminifera in West Europe (biochronohorizons). *Bulletin de la Société géologique de France*, **166**: 565–572.
- Mahoney, J.J., Storey, M., Duncan, R.A., Spencer, K.J., and Pringle, M. S., 1993, Geochemistry and age of the Ontong Java Plateau. In Pringle, M.S. (ed), *The Mesozoic Pacific: Geology, Tectonics, and Volcanism. American Geophysical Union Geophysical Monographs*, **77**: 233–262.
- Mahoney, J.J., Fitton, J.G., Wallace, P.J., et al., 2001, Basement drilling of the Ontong Java Plateau Sites 1183–1187. *Proceedings of the Ocean Drilling Program, Initial Reports*, **192**: College Station, TX (Ocean Drilling Program) http://www-odp.tamu.edu/publications/192_IR/192ir.htm.
- Mahoney, J.J., Duncan, R.A., Tejada, M.L.G., Sager, W.W., and Bralower, T.J., 2005, Jurassic-Cretaceous boundary age and mid-ocean-ridge-type mantle source for Shatsky Rise. *Geology*, **33**: 185–188.
- Malinverno, A., Erba, E., and Herbert, T.D., 2010, Orbital tuning as an inverse problem: chronology of the early Aptian oceanic anoxic event 1a (Selli Level) in the Cismonte APTICORE. *Paleoceanography*, **25**: article #PA2203, <https://doi.org/10.1029/2009PA001769>.
- Malinverno, A., Hildebrandt, J., Tominaga, M., and Channell, J.E., 2012, M-sequence geomagnetic polarity time scale (MHTC12) that steadies global spreading rates and incorporates astrochronology constraints. *Journal of Geophysical Research: Solid Earth*, **117** (B6), article #B06104, 17 pp, <https://doi.org/10.1029/2012JB009260>.
- Martínez, M., Pellenard, P., Deconinck, J.-F., Monna, F., Riquier, L., Boulila, S., et al., 2012, An orbital floating time scale of the Hauterivian/Barremian GSSP from a magnetic susceptibility signal (Rio Argos, Spain). *Cretaceous Research*, **36**: 106–115.
- Martínez, M., Deconinck, J.F., Pellenard, P., Reboulet, S., and Riquier, L., 2013, Astrochronology of the Valanginian stage from reference sections (Vocontian Basin, France) and palaeoenvironmental implications for the Weissert Event. *Palaeogeography, Palaeoclimatology, Palaeoecology*, **376**: 91–102.
- Martínez, M., Deconinck, J.F., Pellenard, P., Riquier, L., Company, M., Reboulet, S., et al., 2015, Astrochronology of the Valanginian–Hauterivian stages (Early Cretaceous): chronological relationships between the Paraná–Etendeka large igneous province and the Weissert and the Faraoni events. *Cretaceous Research*, **131**: 158–173.

- Martinez, M., Aguado, R., Company, M., Sandoval, J., and O'Dogherty, L., 2020, Integrated astrochronology of the Barremian Stage (Early Cretaceous) and its biostratigraphic subdivisions. EGU General Assembly, Online 4–8 May 2020: https://presentations.copernicus.org/EGU2020/EGU2020-8923_presentation.pdf.
- Masse, J.-P., 1998, Calcareous algae. Columns for Jurassic chart of Mesozoic and Cenozoic sequence chronostratigraphic framework of European basins, by Hardenbol, J., Thierry, J., Farley, M.B., Jacquin, T., de Graciansky, P.-C., and Vail, P.R. (coordinators). In de Graciansky, P.-C., Hardenbol, J., Jacquin, T., and Vail, P.R. (eds), *Mesozoic-Cenozoic Sequence Stratigraphy of European Basins. SEPM Special Publication*, **60**: 763–781.
- Masse, J.-P., and Philip, J., 1998, Rudists. Columns for Jurassic chart of Mesozoic and Cenozoic sequence chronostratigraphic framework of European basins, by Hardenbol, J., Thierry, J., Farley, M.B., Jacquin, T., de Graciansky, P.-C., and Vail, P.R. (coordinators). In de Graciansky, P.-C., Hardenbol, J., Jacquin, T., and Vail, P.R. (eds), *Mesozoic-Cenozoic Sequence Stratigraphy of European Basins. SEPM Special Publication*, **60**: 763–781.
- Masters, B.A., 1977, Mesozoic planktonic foraminifera. A world-wide review and analysis. *Oceanic Micropaleontology*, **1**: 301–731.
- McArthur, J.M., Kennedy, W.J., Gale, A.S., Thirlwall, M.F., Chen, M., Burnett, J., et al., 1992, Strontium isotope stratigraphy in the late Cretaceous: international correlation of the Campanian/Maastrichtian boundary. *Terra Nova*, **4**: 332–345.
- McArthur, J.M., Thirlwall, M.F., Chen, M., Gale, A.S., and Kennedy, W.J., 1993, Strontium isotope stratigraphy in the late Cretaceous: numerical calibration of the Sr isotope curve, and international correlation for the Campanian. *Paleoceanography*, **8**: 859–873.
- McArthur, J.M., Kennedy, W.J., Chen, M., Thirlwall, M.F., and Gale, A.S., 1994, Strontium isotope stratigraphy for the Late Cretaceous: direct numerical age calibration of the Sr-isotope curve for the U.S. Western Interior Seaway. *Palaeogeography, Palaeoclimatology, Palaeoecology*, **108**: 95–119.
- McArthur, J.M., Janssen, N.M.M., Reboulet, S., Leng, M.J., Thirlwall, M.F., and van de Schootbrugge, B., 2007, Palaeotemperatures, polar ice-volume, and isotope stratigraphy (Mg/Ca, $\delta^{18}\text{O}$, $\delta^{13}\text{C}$, $^{87}\text{Sr}/^{86}\text{Sr}$): the Early Cretaceous (Berriasian, Valanginian, Hauterivian). *Palaeogeography, Palaeoclimatology, Palaeoecology*, **248**: 391–430.
- McArthur, J.M., Howarth, R.J., Shields, G.A., and Zhou, Y., 2020, Chapter 7 - Strontium isotope stratigraphy. In Gradstein, F.M., Ogg, J.G., Schmitz, M.D., and Ogg, G.M. (eds), *The Geologic Time Scale 2020*. Vol. 1 (this book). Elsevier, Boston, MA.
- Meissner, P., Mutterlose, J., and Bodin, S., 2015, Latitudinal temperature trends in the northern hemisphere during the Early Cretaceous (Valanginian-Hauterivian). *Palaeogeography, Palaeoclimatology, Palaeoecology*, **424**: 17–39.
- Mena, M., Orgeira, M.J., and Lagorioi, S., 2006, Paleomagnetism, rock-magnetism and geochemical aspects of early Cretaceous basalts of the Paraná Magmatic Province, Misiones, Argentina. *Earth Planets Space*, **58**: 1283–1293.
- Menegatti, A.P., Weissert, H., Brown, R.S., Tyson, R.V., Farrimond, P., Strasser, A., et al., 1998, High-resolution $\delta^{13}\text{C}$ stratigraphy through the early Aptian “Livello Selli” of the Alpine Tethys. *Paleoceanography*, **13**: 530–545.
- Mesozoic Planktonic Foraminiferal Working Group (Huber, B.T., coordinator), 2006. Mesozoic Planktonic Foraminiferal Taxonomic Dictionary. [Unpublished.].
- Meyers, S.R., Siewert, S.E., Singer, B.S., Sageman, B.B., Condon, D., Obradovich, J.D., et al., 2010, Reducing error bars through the intercalibration of radioisotopic and astrochronologic time scales for the Cenomanian/Turonian Boundary Interval, Western Interior Basin, USA. In: *American Geological Union Fall Meeting, San Francisco, CA, 13–17 December 2010, Abstract*. Available from: <<http://www.agu.org/meetings/fm10/waisfm10.html>> .
- Meyers, S.R., Siewert, S.E., Singer, B.S., Sageman, B.B., Condon, D., Obradovich, J.D., et al., 2012, Intercalibration of radioisotopic and astrochronologic time scales for the Cenomanian-Turonian Boundary interval, Western Interior Basin, USA. *Geology*, **40**: 7–10.
- Midtkandal, I., Svensen, H.H., Planke, S., Corfu, F., Polteau, S., Torsvik, T.H., et al., 2016, The Aptian (Early Cretaceous) anoxic event (OAE1a) in Svalbard, Barents Sea and the absolute age of the Barremian-Aptian boundary. *Palaeogeography, Palaeoclimatology, Palaeoecology*, **463**: 126–135, <https://doi.org/10.1016/j.palaeo.2016.09.023>.
- Miller, K.G., Barrera, E., Olsson, R.K., Sugarman, P.J., and Savin, S.M., 1999, Does ice drive early Maastrichtian eustasy? *Geology*, **27**: 783–786.
- Miller, K.G., Sugarman, P.J., Browning, J.V., Kominz, M.A., Hernández, J.C., Olsson, R.K., et al., 2003, Late Cretaceous chronology of large, rapid sea-level changes: glacioeustasy during the greenhouse world. *Geology*, **31**: 585–588.
- Miller, K.G., Sugarman, P.J., Browning, J.V., Kominz, M.A., Olsson, R., K., Feigenson, M.D., et al., 2004, Upper Cretaceous sequences and sea-level history, New Jersey coastal plain. *Geological Society of America Bulletin*, **116**: 368–393.
- Mitchell, R.N., Bice, D.M., Montanari, A., Cleaveland, L.C., Christianson, K.T., Coccioni, R., et al., 2008, Oceanic anoxic cycles? Orbital prelude to the Bonarelli Level (OAE 2). *Earth and Planetary Science Letters*, **267**: 1–16.
- Möller, C., Mutterlose, J., and Alsen, P., 2015, Integrated stratigraphy of Lower Cretaceous sediments (Ryazanian-Hauterivian) from North-East Greenland. *Palaeogeography, Palaeoclimatology, Palaeoecology*, **437**: 85–97.
- Monteil, E., and Foucher, J.-C., 1998, Dinoflagellate cysts. Columns for Jurassic chart of Mesozoic and Cenozoic sequence chronostratigraphic framework of European basins, by Hardenbol, J., Thierry, J., Farley, M.B., Jacquin, T., de Graciansky, P.-C., and Vail, P.R. (coordinators). In de Graciansky, P.-C., Hardenbol, J., Jacquin, T., and Vail, P.R. (eds), *Mesozoic-Cenozoic Sequence Stratigraphy of European Basins. SEPM Special Publication*, **60**: 763–781.
- Montgomery, P., Hailwood, E.A., Gale, A.S., and Burnett, J.A., 1998, The magnetostratigraphy of Coniacian-Late Campanian chalk sequences in southern England. *Earth and Planetary Science Letters*, **156**: 209–224.
- Morel, N. (ed), 2015. *Stratotype Cénomaniens*. Muséum National d'Histoire Naturelle. Biotope, Meze, BRGM Orléans. Paris, 384 p.
- Moullade, M., 1966, Etude stratigraphique et micropaléontologique du Crétacé inférieur de la «Fosse Vocontienne». *Documents des Laboratoires de Géologie de Lyon*, **15**: 1–369.
- Moullade, M., Tronchetti, G., and Masse, J.-P. (eds), 1998a. Le stratotype historique de l'Aptien inférieur (Bédoulien) dans la région de Cassis-La Bédoule (S.E. France). *Géologie Méditerranéenne XXV* (3–4), 298.

- Moullade, M., Masse, J.-P., Tronchetti, G., Kuhnt, W., Ropolo, P., Bergen, J.A., et al., 1998b, Le stratotype historique de l'Aptien (région de Cassis-La Bédoule, SE France): synthèse stratigraphique. *Géologie Méditerranéenne*, **XXV** (3–4), 289–298.
- Moullade, M., Tronchetti, G., Kuhnt, W., Renard, M., and Bellier, J.-P., 2004, The Gargasian (Middle Aptian) of Cassis-La Bédoule (Lower Aptian historical stratotype, SE France): geographic location and lithostratigraphic correlations. *Carnets de Géologie Notebooks on Geology*, Letter, 2004/02, 24 p. Available from, http://paleopolis.rediris.es/cg/CG2004_L02_MM_etat/index_v1.html.
- Moullade, M., Tronchetti, G., and Bellier, J.-P., 2005, The Gargasian (Middle Aptian) strata from Cassis-La Bédoule (Lower Aptian historical stratotype, SE France): planktonic and benthic foraminiferal assemblages and biostratigraphy. *Carnets de Géologie Notebooks on Geology*, Article, **2005/02**, 20 p. Available from, http://paleopolis.rediris.es/cg/CG2005_A02/index.html.
- Moullade, M., Granier, B., and Tronchetti, G., 2011, The Aptian Stage: back to fundamentals. *Episodes*, **34**: 148–156.
- Mutterlose, J., and Böckel, B., 1998, The Barremian-Aptian interval in NW Germany: a review. *Cretaceous Research*, **19**: 539–568.
- Mutterlose, J., Autran, G., Baraboschkin, E.J., Cecca, F., Erba, E., Gardin, S., et al., 1996, The Hauterivian Stage. *Bulletin de l'Institut Royal des Sciences Naturelles de Belgique, Sciences de la Terre*, **66** (Suppl.), 19–24.
- Mutterlose, J., Bomemann, A., Luppold, F.W., Owen, H.G., Ruffell, A., Weiss, W., et al., 2003, The Vöhrum section (northwest Germany) and the Aptian/Albian boundary. *Cretaceous Research*, **24**: 203–252.
- Mutterlose, J., Bodin, S., and Fähnrich, W., 2014, Strontium-isotope stratigraphy of the Early Cretaceous (Valanginian–Barremian): implications for Boreal–Tethys correlation and paleoclimate. *Cretaceous Research*, **50**: 252–263.
- Mutterlose, J., Rawson, P.F., Reboulet, S., Baudin, F., Bulot, L., Emmanuel, L., et al., in press. The Global Boundary Stratotype Section and Point (GSSP) for the base of the Hauterivian Stage (Lower Cretaceous), La Charce, southeast France. *Episodes*. <https://doi.org/10.18814/epiiugs/2020/020072>.
- Myers, S.R., Siewert, S.E., Singer, B.S., Sageman, B.B., Condon, D.J., Obradovich, J.D., et al., 2012, Integration of radioisotopic and astrochronologic timescales for the Cenomanian-Turonian boundary, Western Interior Basin, USA. *Geology*, **40**: 7–10.
- Nederbragt, A.J., 1990. *Biostratigraphy and Paleoceanographic Potential of the Cretaceous Planktic Foraminifera Heterohelicidae* (Doctoral dissertation). Centrale Huisdrukkerij Vrije Universiteit.
- Niebuhr, B., 2005, Geochemistry and time-series analyses of orbitally forced Upper Cretaceous marl–limestone rhythmites (Lehrte West Syncline, northern Germany). *Geological Magazine*, **142**: 31–55.
- Nikitin, S.N., 1881, Jurassic Deposits between Rybinsk, Mologa, and Myshkin. *Materialy dlya geologii Rossii*, **X**: 201–331 [In Russian].
- Oboh-Ikuenobe, F.E., Benson, D.G., Scott, R.W., Holbrook, J.M., Evetts, M.J., and Erbacher, J., 2007, Re-evaluation of the Albian-Cenomanian boundary in the U.S. Western Interior based on dinoflagellate cysts. *Review of Palaeobotany and Palynology*, **144**: 77–97.
- Oboh-Ikuenobe, F.E., Holbrook, J.M., Scott, R.W., Akins, S.L., Evetts, M.J., Benson, D.G., et al., 2008, Anatomy of epicontinental flooding: late Albian-early Cenomanian of the southern U.S. Western Interior Basin. In Pratt, B.R., and Homden, C. (eds), Dynamics of Epeiric Seas. *Geological Association of Canada Special Publication*, **48**: 201–227.
- Obradovich, J.D., 1993, A Cretaceous time scale. In Caldwell, W.G.E., and Kauffman, E.G. (eds), Evolution of the Western Interior Basin. *Geological Association of Canada Special Paper*, **39**: 379–396.
- Obradovich, J.D., Matsumoto, T., Nishida, T., and Inoue, Y., 2002, Integrated biostratigraphic and radiometric scale on the Lower Cenomanian (Cretaceous) of Hokkaido, Japan. *Proceedings of the Japan Academy, Series B-Physical and Biological Sciences*, **78** (6), 149–153.
- O'Brien, C.L., Robinson, S.A., Pancost, R.D., Damste, J.S.S., Schouten, S., Lunt, D.J., et al., 2017, Cretaceous sea-surface temperature evolution: constraints from TEX₈₆ and planktonic foraminiferal oxygen isotopes. *Earth-Science Reviews*, **172**: 224–247.
- O'Connor, L.K., Batenburg, S.J., Robinson, S.A., Jenkyns, H.C., 2020. An orbitally paced, near-complete record of Campanian climate and sedimentation in the Mississippi embayment, USA. *Newsletters on Stratigraphy*, article #534, <https://doi.org/10.1127/nos/2020/0534>.
- O'Connor, L.K., Remmelzwaal, S., Robinson, S.A., Batenburg, S.J., Jenkyns, H.C., Parkinson, I., et al., in press. Deconstructing the Plenus Cold Event (Cenomanian, Cretaceous). *Paleoceanography*.
- Odin, G.S., 1996, Le site de Tercis (Landes). Observations stratigraphiques sur le Maastrichtien. Arguments pour la localisation et la corrélation du Point Stratotype Global de la limite Campanien – Maastrichtien. *Bulletin de la Société géologique de France*, **167**: 637–643.
- Odin, G.S., Hancock, J.M., Antonescu, E., Bonnemaïson, M., Caron, M., Cobban, W.A., et al., 1996, Definition of a Global Boundary Stratotype Section and point for the Campanian/Maastrichtian boundary. *Bulletin de l'Institut Royal des Sciences Naturelles de Belgique, Sciences de la Terre*, **66** (Suppl.), 111–117.
- Odin, G.S., (ed.), 2001. *The Campanian-Maastrichtian Stage Boundary: Characterization at Tercis les Bains (France) and Correlation with Europe and other Continents*. Development in Paleontology and Stratigraphy, **19**: 881 pp.
- Odin, G.S., and Lamaurelle, M.A., 2001, The global Campanian-Maastrichtian Stage boundary. *Episodes*, **24**: 229–238.
- Ogg, J.G., Ogg, G.M., and Gradstein, F.M., 2016, *A Concise Geologic Time Scale 2016*, 234p. Elsevier.
- Ogg, J.G., 1987, Early Cretaceous magnetic polarity time scale and the magnetostratigraphy of DSDP Sites 603 and 534, western Central Atlantic. *Initial Reports of the Deep Sea Drilling Project*, **93**: 849–888.
- Ogg, J.G., 1988, Early Cretaceous and Tithonian magnetostratigraphy of the Galicia margin (Ocean Drilling Program Leg 103). *Proceedings of the Ocean Drilling Program, Scientific Results*, **103**: 659–682.
- Ogg, J.G., 2020, Chapter 5 - Geomagnetic polarity time scale. In Gradstein, F.M., Ogg, J.G., Schmitz, M.D., and Ogg, G.M. (eds), *The Geologic Time Scale 2020*. Vol. **1** (this book). Elsevier, Boston, MA.
- Ogg, J.G., Bardot, L., 2001. Aptian through Eocene magnetostratigraphic correlation of the Blake Nose Transect (Leg 171B), Florida Continental Margin. *Proceedings of the Ocean Drilling Program, Scientific Results*, **171B**. 59 p. Available from: <http://www-odp.tamu.edu/publications/171B_SR/chap_09/chap_09.htm> .
- Ogg, J.G., and Lowrie, W., 1986, Magnetostratigraphy of the Jurassic-Cretaceous boundary. *Geology*, **14**: 547–550.
- Ogg, J.G., and Smith, A.G., 2004, In Gradstein, F.M., Ogg, J.G., and Smith, A.G. (eds), *A Geologic Time Scale 2004*. Cambridge: Cambridge University Press, p. 589.
- Ogg, J.G., Steiner, M.B., Oloriz, F., and Tavera, J.M., 1984, Jurassic magnetostratigraphy, 1. Kimmeridgian-Tithonian of Sierra Gorda

- and Carcabuey, southern Spain. *Earth and Planetary Science Letters*, **71**: 147–162.
- Ogg, J.G., Steiner, M.B., Company, M., and Tavera, J.M., 1988, Magnetostratigraphy across the Berriasian-Valanginian stage boundary (Early Cretaceous) at Cehegin (Murcia Province, southern Spain). *Earth and Planetary Science Letters*, **87**: 205–215.
- Ogg, J.G., Hasenyager II, R.W., Wimbledon, W.A., Channell, J.E.T., and Bralower, T.J., 1991, Magnetostratigraphy of the Jurassic–Cretaceous boundary interval—Tethyan and English faunal realms. *Cretaceous Research*, **12**: 455–482.
- Ogg, J.G., Kodama, K., and Wallick, B.P., 1992, Lower Cretaceous magnetostratigraphy and paleolatitudes off northwest Australia, ODP Site 765 and DSDP Site 261, Argo Abyssal Plain, and ODP Site 766, Gascoyne Abyssal Plain. *Proceedings of the Ocean Drilling Program, Scientific Results*, **123**: 523–548.
- Ogg, J.G., Hasenyager II, R.W., and Wimbledon, W.A., 1994, Jurassic–Cretaceous boundary: Portland-Purbeck magnetostratigraphy and possible correlation to the Tethyan faunal realm. *Géobios, Mémoire Spécial*, **17**: 519–527.
- Ogg, J.G., Ogg, G., and Gradstein, F.M., 2008, *The Concise Geologic Time Scale*. Cambridge: Cambridge University Press 177 pp.
- Ogg, J.G., Hinnov, L.A., and Huang, C., 2012, Cretaceous. In Gradstein, F.M., Ogg, J.G., Schmitz, M., and Ogg, G. (eds), *The Geologic Time Scale 2012*. Elsevier, 793–853.
- Ogg, J.G., Ogg, G.M., and Gradstein, F.M., 2016. *A Concise Geologic Time Scale 2016*. Elsevier, 234 p.
- Oosting, A.M., Leereveld, H., Dickens, G.R., Henderson, R.A., and Brinkhuis, 2006, Correlation of Barremian-Aptian (mid-Cretaceous) dinoflagellate cyst assemblages between the Tethyan and Austral realms. *Cretaceous Research*, **27**: 762–813.
- Oppel, C.A., 1865, Die Tithonische Etage. *Zeitschrift der Deutschen Geologischen Gesellschaft, Jahrgang*, **17**: 535–558.
- Owen, H.G., 1996a, Boreal and Tethyan late Aptian to late Albian ammonite zonation and palaeobiogeography. In: Spaeth, C. (ed), Jost Wiedmann Memorial Volume, Proceedings of the 4th International Cretaceous Symposium, Hamburg, 1992. *Mitteilung aus dem Geologisch-Paläontologischen Institut der Universität Hamburg*, vol. 77. pp. 461–481.
- Owen, H.G., 1996b, “Uppermost Wealden facies and Lower Greensand Group (Lower Cretaceous) in Dorset, southern England: correlation and palaeoenvironment” by Ruffell & Batten (1994) and “The Sandgate Formation of the M20 Motorway near Ashford, Kent and its correlation” by Ruffell & Owen (1995)”: reply. *Proceedings of the Geologists’ Association*, **107**: 74–76.
- Owen, H.G., 2002, The base of the Albian Stage; comments on recent proposals. *Cretaceous Research*, **23**: 1–13.
- Paul, C.R.C., Lamolda, M.A., Mitchell, S.F., Vaziri, M.R., Gorostidi, A., and Marshall, J.D., 1999, The Cenomanian-Turonian boundary at Eastbourne (Sussex, UK): a proposed European reference section. *Palaeogeography, Palaeoclimatology, Palaeoecology*, **150**: 83–121.
- Pearson, P.N., 2012, Oxygen isotopes in Foraminifera: an overview and historical review. In Ivany, L.C., and Huber, B.T. (eds), *Reconstructing Earth’s Deep Time Climate. The Paleontological Society Papers*, **18**: 1–38.
- Pearson, P.N., Ditchfield, P.W., Singano, J., Harcourt-Brown, K.G., Nicholas, C.J., Olsson, R.K., et al., 2001, Warm tropical sea surface temperatures in the Late Cretaceous and Eocene epochs. *Nature*, **413**: 481–487.
- Pechersky, D.M., and Khramov, A.N., 1973, Mesozoic paleomagnetic scale of the U.S.S.R. *Nature*, **244**: 499–501.
- Pérez-Rodríguez, I., Lees, J.A., Larrasoña, J.C., Arz, J.A., and Arenillas, I., 2012, Planktonic foraminiferal and calcareous nannofossil biostratigraphy and magnetostratigraphy of the uppermost Campanian and Maastrichtian at Zumaia, northern Spain. *Cretaceous Research*, **37**: 100–126.
- Pessagno, E.A., 1967, Upper Cretaceous planktonic foraminifera from the western Gulf Coastal Plain. *Palaeontographica Americana*, **5**: 245–445.
- Petrizzo, M.R., 2000, Upper Turonian–lower Campanian planktonic foraminifera from southern mid–high latitudes (Exmouth Plateau, NW Australia): biostratigraphy and taxonomic notes. *Cretaceous Research*, **21** (4), 479–505.
- Petrizzo, M.R., 2001, Late Cretaceous planktonic foraminifera from Kerguelen Plateau (ODP Leg 183): new data to improve the Southern Ocean biozonation. *Cretaceous Research*, **22** (6), 829–855.
- Petrizzo, M.R., 2003, Late Cretaceous planktonic foraminiferal bioevents in the Tethys and in the Southern Ocean record: an overview. *Journal of Foraminiferal Research*, **33** (4), 330–337.
- Petrizzo, M.R., 2019, A critical evaluation of planktonic foraminiferal biostratigraphy across the Coniacian-Santonian boundary interval in Spain, Texas, and Tanzania, *Geologic Problem Solving with Microfossils IV*, SEPM Special Publication, **111**: 186–198, <http://dx.doi.org/10.2110/sepmsp.111.04>.
- Petrizzo, M.R., and Huber, B.T., 2006, Biostratigraphy and taxonomy of late Albian planktonic foraminifera from ODP Leg 171B (western North Atlantic Ocean). *Journal of Foraminiferal Research*, **36** (2), 166–190.
- Petrizzo, M.R., Falzoni, F., and Premoli Silva, I., 2011, Identification of the base of the lower-to-middle Campanian *Globotruncana ventricosa* Zone: comments on reliability and global correlations. *Cretaceous Research*, **32**: 387–405.
- Petrizzo, M.R., Huber, B.T., Gale, A.S., Barchetta, A., and Jenkyns, H. C., 2012, Abrupt planktonic foraminiferal turnover across the Niveau Kilian at Col de Pré-Guittard (Vocontian Basin, southeast France): new criteria for defining the Aptian/Albian boundary. *Newsletters on Stratigraphy*, **45**: 55–74.
- Petrizzo, M.R., Huber, B.T., Gale, A.S., Barchetta, A., and Jenkyns, H. C., 2013, Erratum. Abrupt planktonic foraminiferal turnover across the Niveau Kilian at Col de Pré-Guittard (Vocontian Basin, southeast France): new criteria for defining the Aptian/Albian boundary. *Newsletters on Stratigraphy*, **46** (1), 93.
- Petrizzo, M.R., Caron, M., and Premoli-Silva, I., 2015, Remarks on the identification of the Albian/Cenomanian boundary and taxonomic clarification of the planktonic foraminifera index species *globotruncanoides, brotzeni* and *tehamaensis*. *Geological Magazine*, **152**: 521–536.
- Petrizzo, M.R., Jiménez Berrocoso, Á., Falzoni, F., Huber, B.T., and Macleod, K.G., 2017, The Coniacian–Santonian sedimentary record in southern Tanzania (Ruvuma Basin, East Africa): planktonic foraminiferal evolutionary, geochemical and palaeoceanographic patterns. *Sedimentology*, **64** (1), 252–285.
- Premoli Silva, I., and Sliter, W.V., 1995, Cretaceous planktonic foraminiferal biostratigraphy and evolutionary trends from the Bottaccione section, Gubbio, Italy. *Palaeontographia Italica*, **82**: 1–89.
- Premoli Silva, I., and Sliter, W.V., 1999, Cretaceous paleoceanography: evidence from planktonic foaminiferal evolution. In Barrera, E., and Johnson, C.C. (eds), *Evolution of the Cretaceous Ocean-Climate System. Geological Society of America Special Paper*, **332**: 301–328.

- Premoli Silva, I., Soldan, D.M., and Petrizzo, M.R., 2018, Upper Hauterivian-upper Barremian planktonic foraminiferal assemblages from the Arroyo Gilico section (Southern Spain). *Journal of Foraminiferal Research*, **48** (4), 314–355.
- Price, G.D., 1999, The evidence for and implications of polar ice during the Mesozoic. *Earth Science Reviews*, **48**: 183–210.
- Pringle, M.S., and Duncan, R.A., 1995a, Radiometric ages of basaltic lavas recovered sites 865, 866, and 869. *Proceedings of the Ocean Drilling Program, Scientific Results*, **143**: 277–283.
- Pringle, M.S., and Duncan, R.A., 1995b, Radiometric ages of basaltic lavas recovered at Lo-En, Wodejebato, MIT, and Takuyo-Daisan Guyots, northwestern Pacific Ocean. *Proceedings of the Ocean Drilling Program, Scientific Results*, **144**: 547–557.
- Pringle, M.S., Chambers, L., Ogg, J.G., 2003. Synchronicity of volcanism on Ontong Java and Manihiki plateaux with global oceanographic events? In: American Geophysical Union and European Union of Geophysics Conference, Nice, France, May 2003, Abstract.
- Pruner, P., Houša, V., Olóriz, F., Košťak, M., Krs, M., Man, O., et al., 2010, High-resolution magnetostratigraphy and the biostratigraphic zonation of the Jurassic/Cretaceous boundary strata in the Puerto Escaño section (southern Spain). *Cretaceous Research*, **31**: 192–206.
- Pucéat, E., Lécuyer, C., Sheppard, S.M.F., Dromart, G., Reboulet, S., and Grandjean, P., 2003, Thermal evolution of Cretaceous Tethyan marine waters inferred from oxygen isotope composition of fish tooth enamels. *Paleoceanography*, **18**: 1029, <https://doi.org/10.1029/2002PA00823>.
- Quidelleur, X., Paquette, J.L., Fiet, N., Takashima, R., Tiepolo, M., Desmares, D., et al., 2011, New U-Pb (ID-TIMS and LA-ICPMS) and $^{40}\text{Ar}/^{39}\text{Ar}$ geochronological constraints of the Cretaceous geologic time scale calibration from Hokkaido (Japan). *Chemical Geology*, **286**: 72–83.
- Rawson, P.F., 1983, The Valanginian to Aptian Stages—current definitions and outstanding problems. *Zitteliana*, **10**: 493–500.
- Rawson, P.F., 1990, Event stratigraphy and the Jurassic-Cretaceous boundary. *Transactions of the Institute of Geology and Geophysics, Academy Sciences USSR, Siberian Branch*, **699**: 48–52 [In Russian with English summary].
- Rawson, P.F., Curry, D., Dille, F.C., Hancock, J.M., Kennedy, W.J., Neale, J.W., et al., 1978, A correlation of Cretaceous rocks in the British Isles. *Geological Society of London Special Report*, **9**: 70.
- Rawson, P.F., Avram, E., Baraboshkin, E.J., Cecca, F., Company, M., and Delanoy, G., 1996a, The Barremian Stage. *Bulletin de l'Institut Royal des Sciences Naturelles de Belgique, Sciences de la Terre*, **66** (Suppl.), 25–30.
- Rawson, P.F., D'Hondt, A.V., Hancock, J.M., and Kennedy, W.J. (eds), 1996b. Proceedings of the second international symposium on Cretaceous Stage Boundaries, Brussels, 8–16 September 1995. *Bulletin de l'Institut Royal des Sciences Naturelles de Belgique, Sciences de la Terre* **66** (Suppl.), 117 p.
- Ray, D.C., van Buchem, F.S.P., Baines, G., Davies, A., Gréselle, B., Simmons, M.D., et al., 2019, The magnitude and cause of short-term eustatic Cretaceous sea-level change: a synthesis. *Earth Science Reviews*, **197**: article #102901: 20 pp, <https://doi.org/10.1016/j.earscirev.2019.102901>.
- Reboulet, S., 1996, L'évolution des ammonites du Valanginien-Hauterivien inférieur du bassin vocontien et de la plate-forme provençale (sud-est de la France): relations avec la stratigraphie séquentielle et implications biostratigraphiques. *Documents des Laboratoires de Géologie Lyon*, **137**: 370 p.
- Reboulet, S., 2001, Limiting factors on shell growth, mode of life and segregation of Valanginian ammonoid populations: evidence from adult-size variations. *Geobios*, **34**: 423–435.
- Reboulet, S., and Atrops, F., 1999, Comments and proposals about the Valanginian-Lower Hauterivian ammonite zonation of south-eastern France. *Ecologiae Geologicae Helveticae*, **92**: 183–197.
- Reboulet, S., Mattioli, E., Pittet, B., Baudin, B., Olivero, D., and Proux, O., 2003, Ammonoid and nannoplankton abundance in Valanginian (early Cretaceous) limestone-marl alternations from the southeast France Basin: carbonate dilution or productivity? *Palaeogeography, Palaeoclimatology, Palaeoecology*, **201**: 113–139.
- Reboulet, S., Hoedemaeker, P.J., Aguirre-Urreta, M.B., Alsen, P., Atrops, F., Baraboshkin, E.Y., et al., 2006, Report on the 2nd international meeting of the IUGS Lower Cretaceous ammonite working group, the “Kilian Group”, Neuchâtel, Switzerland, 8 September 2005. *Cretaceous Research*, **27**: 712–715.
- Reboulet, S., Klein, J., Barragán, R., Company, M., González-Arreola, C., Lukeneder, A., et al., 2009, Report on the 3rd international meeting of the IUGS Lower Cretaceous Ammonite Working Group, the “Kilian Group”, Vienna, Austria, 15th April 2008. *Cretaceous Research*, **30**: 496–502.
- Reboulet, S., Rawson, P.F., Moreno-Bedmar, J.A., Aguirre-Urreta, M.B., Barragán, R., Bogomolov, Y., et al., 2011, Report on the 4th international meeting of the IUGS Lower Cretaceous Ammonite Working Group, the “Kilian Group” (Dijon, France, 30th August, 2010). *Cretaceous Research*, **32**: 786–793.
- Reboulet, S., Szives (reporters), O., Aguirre-Urreta, B., Barragán, R., Company, M., Frau, C., et al., 2018, Report on the 6th international meeting of the IUGS Lower Cretaceous Ammonite Working Group, the Kilian Group (Vienna, Austria, 20th August 2017). *Cretaceous Research*, **91**: 100–110.
- Reimond, W.U., Koeberl, C., Brandstätter, F., Kruger, F.J., Armstrong, R.A., and Bootsman, C., 1999, Morokweng impact structure, South Africa: geologic, petrographic, and isotopic results, and implications for the size of the structure. In Dressler, B.O., and Sharpton, V.L. (eds), Large Meteorite Impacts and Planetary Evolution II. *Geological Society of America Special Paper*, **339**: 61–90.
- Remane, J., 1985, Calpionellids. In Bolli, H.M., Saunders, J.B., and Perch Nielsen, K. (eds), *Plankton Stratigraphy*. Cambridge: Cambridge University Press, 555–572.
- Remane, J., 1991, The Jurassic-Cretaceous boundary: problems of definition and procedure. *Cretaceous Research*, **12**: 447–453.
- Remane, J., 1998, Calpionellids. Columns for Jurassic chart of Mesozoic and Cenozoic sequence chronostratigraphic framework of European basins, by Hardenbol, J., Thierry, J., Farley, M.B., Jacquin, T., de Graciansky, P.-C., and Vail, P.R. (coordinators). In de Graciansky, P.-C., Hardenbol, J., Jacquin, T., and Vail, P.R. (eds), Mesozoic-Cenozoic Sequence Stratigraphy of European Basins. *SEPM Special Publication*, **60**: 763–781.
- Remane, J., Bakalova-Ivanova, D., Borza, K., Knauer, J., Nagy, I., Pop, G., et al., 1986, Agreement on the subdivision of the Standard Calpionellid Zones defined at the IInd Planktonic Conference Roma 1971. *Acta Geologica Hungarica*, **29**: 5–14.
- Renard, M., de Rafélis, M., Emmanuel, L., Moullade, M., Masse, J.-P., Kuhnt, W., et al., 2005. Early Aptian $\delta^{13}\text{C}$ and manganese anomalies

- from the historical Cassis-La Bédoule stratotype sections (S.E. France): relationship with a methane hydrate dissociation event and stratigraphic implications. In: Carnets de Géologie/Notebooks on Geology, Article, 2005/04, 18 p. Available from: <http://paleopolis.rediris.es/cg/CG2005_A04/index.html> .
- Renevier, E., 1874, Tableau des terrains sédimentaires formés pendant les époques de la phase organique du globe terrestre avec leurs représentants en Suisse et dans les régions classiques, leurs synonymes et les principaux fossiles de chaque étage. *Bulletin de la Société vaudoise des Sciences naturelles*, **13**: 218–252.
- Renne, P.R., Mundil, M., Balco, G., Min, K., and Ludwig, K.R., 2010, Joint determination of ^{40}K decay constants and $^{40}\text{Ar}^*/^{40}\text{K}$ for the Fish Canyon sanidine standard, and improved accuracy for $^{40}\text{Ar}/^{39}\text{Ar}$ geochronology. *Geochimica et Cosmochimica Acta*, **74**: 5349–5367.
- Renne, P.R., Deino, A.L., Hilgen, F.J., Kuiper, K.F., Mark, D.F., Mitchell, W.S., et al., 2013, Time scales of critical events around the Cretaceous-Paleogene Boundary. *Science*, **339**: 684, <https://doi.org/10.1126/science.1230492>.
- Riveline, J., 1998, Charophytes. Columns for Jurassic chart of Mesozoic and Cenozoic sequence chronostratigraphic framework of European basins, by Hardenbol, J., Thierry, J., Farley, M.B., Jacquin, T., de Graciansky, P.-C., and Vail, P.R. (coordinators). In de Graciansky, P.-C., Hardenbol, J., Jacquin, T., and Vail, P.R. (eds), Mesozoic-Cenozoic Sequence Stratigraphy of European Basins. *SEPM Special Publication*, **60**: 763–781.
- Robaszynski, F., 1998, Planktonic foraminifera. Columns for Jurassic chart of Mesozoic and Cenozoic sequence chronostratigraphic framework of European basins, by Hardenbol, J., Thierry, J., Farley, M.B., Jacquin, T., de Graciansky, P.-C., and Vail, P.R. (coordinators). In de Graciansky, P.-C., Hardenbol, J., Jacquin, T., and Vail, P.R. (eds), Mesozoic-Cenozoic Sequence Stratigraphy of European Basins. *SEPM Special Publication*, **60**: 763–781.
- Robaszynski, F., and Caron, M.C., 1979, Atlas of mid-Cretaceous planktonic foraminifera (Boreal Sea and Tethys). *Cahiers de Micropaléontologie*, **1**: 1–185.
- Robaszynski, F., and Caron, M., 1995, Foraminifères planctoniques du crétacé: commentaire de la zonation Europe-Méditerranée. *Bulletin de la Société géologique de France*, **166**: 681–692.
- Robaszynski, F., Caron, M., Gonzalez Donoso, J.M., and Wonders, A.H., 1984, The European working group on Planktonic Foraminifera, Atlas of Late Cretaceous globotruncanids. *Revue de Micropaléontologie*, **26**: 145–305.
- Robaszynski, F., Caron, M., Dupuis, C., Amédéo, F., Gonzalez-Donoso, J.M., Linares, D., et al., 1990, A tentative integrated stratigraphy in the Turonian of Central Tunisia: formations, zones and sequential stratigraphy in the Kalaat Senan area. *Bulletin des Centres Recherches Exploration-Production Elf-Aquitaine*, **14**: 213–384.
- Robaszynski, F., Gonzalez Donoso, J.M., Linares, D., Amédéo, F., Caron, M., Dupuis, C., et al., 2000, Le Crétacé supérieur de la région de Kalaat Senan, Tunisie Centrale. Litho-biostratigraphie intégrée: zones d'ammonites, de foraminifères planctoniques et de nanfossiles du Turonien supérieur au Maastrichtien. *Bulletin des Centres de Recherche et d'Exploration-Production d'Elf-Aquitaine*, **22**: 359–490.
- Robaszynski, F., Amédéo, F., Devalque, C., Matrimon, B., 2014, Le Turonien des Massifs d'Uchaux et de la Ceze (S.E. France). *Memoires de la Classe des Sciences Academie Royale de Belgique*, Brussels. 197 p. 48 pls.
- Röhl, U., and Ogg, J.G., 1996, Aptian-Albian sea level history from guyots in the western Pacific. *Paleoceanography*, **11**: 595–624.
- Ropolo, P., Conte, G., Gonnet, R., Masse, J.-P., and Moullade, M., 1998, Les faunes d'ammonites du Barrémien supérieur/Aptien inférieur (Bédoulien) dans la région stratotypique de Cassis-La Bédoule (S.E. France): état des connaissances et propositions pour une zonation par ammonites du Bédoulien type. *Géologie Méditerranéenne*, **25**: 167–175.
- Roth, P.H., 1989, Ocean circulation and calcareous nannoplankton evolution during the Jurassic and Cretaceous. *Palaeogeography, Palaeoclimatology, Palaeoecology*, **74**: 111–126.
- Round, F.E., Crawford, R.M., and Mann, D.G., 1990, *The Diatoms: Biology and Morphology of the Genera*. Cambridge: Cambridge University Press, 747 p.
- Ryan, W.B.F., Bolli, H.M., Foss, G.N., Natland, J.H., Hottman, W.E., and Foresman, J.B., 1978, Objectives, principal results, operations, and explanatory notes of Leg 40, South Atlantic. *Initial Reports, Deep Sea Drilling Project*, **40**: 5–20.
- Sageman, B.B., Meyers, S.R., and Arthur, M.A., 2006, Orbital time scale and new C-isotope record for Cenomanian-Turonian boundary stratotype. *Geology*, **34**: 125–128.
- Sageman, B.B., Singer, B.S., Meyers, S.R., Walaszczyk, I., Seiwert, S.E., Condon, D.J., et al., 2014, Integrating $^{40}\text{Ar}/^{39}\text{Ar}$, U-Pb, and astronomical clocks in the Cretaceous Niobrara Formation, Western Interior Basin, USA. *Bulletin of the Geological Society of America*, **126**: 956–973, <https://doi.org/10.1130/B30929.1>.
- Salaj, J., 1984, Foraminifera and detailed microbiostratigraphy of the boundary beds of the Lower Cretaceous stages in the Tunisian Atlas. *Geologicky Zbornik*, **35**: 583–599.
- Sazonov, N.T., 1951, On some little-known ammonites of the Lower Cretaceous. *Byulleten' Moskovskogo Obshchestva Ispytatelei Prirody*, **56**: 1–176 [In Russian].
- Scaife, J.D., Ruhl, M., Dickson, J.A., Mather, T.A., Jenkyns, H.C., Percival, L.M.E., et al., 2017, Sedimentary mercury enrichments as a marker for submarine large igneous province volcanism? Evidence from the Mid-Cenomanian event and Oceanic Anoxic Event 2 (Late Cretaceous). *Geochemistry, Geophysics, Geosystems*, **18**: 4253–4275, <https://doi.org/10.1002/2017GC007153>.
- Schlanger, S.O., and Jenkyns, H.C., 1976, Cretaceous oceanic anoxic events: causes and consequences. *Geology en Mijnbouw*, **55**: 179–184.
- Schlanger, S.O., Arthur, M.A., Jenkyns, H.C., and Scholle, P.A., 1987, The Cenomanian-Turonian oceanic anoxic event, I. Stratigraphy and distribution of organic carbon-rich beds and the marine ^{13}C excursion. In Brooks, J., and Fleet, A.J. (eds), Marine Petroleum Source Rocks. *Geological Society of London, Special Publication*, **26**: 371–399.
- Schnabl, P., Pruner, P., and Wimbledon, W.A.P., 2015, A review of magnetostratigraphic results in the Tithonian-Berriasian of Nordvik (Siberia) and possible biostratigraphic constraints. *Geologica Carpathica*, **66**: 489–498.
- Scholle, P.A., and Arthur, M., 1980, Carbon isotope fluctuations in Cretaceous pelagic limestones: potential stratigraphic and petroleum exploration tool. *Bulletin of the American Association of Petroleum Geologists*, **64**: 67–87.
- Schönfeld, J., Schulz, M.-G., McArthur, J.M., Burnett, J., Gale, A., Hambach, U., et al., 1996, New results on biostratigraphy, geochemistry and correlation from the standard section for the Upper Cretaceous

- white chalk of northern Germany (Lägerdorf–Kronsmoor–Hemmoor). In: Spaeth, C. (ed), *Jost Wiedmann Memorial Volume; Proceedings of the 4th International Cretaceous Symposium, Hamburg, 1992*. Mitteilung aus dem Geologisch-Paläontologischen Institut der Universität Hamburg, vol. 77. pp. 545–575.
- Scotese, C.R., 2014. *Atlas of Late Cretaceous Paleogeographic Maps, PALEOMAP Atlas for ArcGIS, Volume 2, The Cretaceous, Maps 16–22, Mollweide Projection*, PALEOMAP Project, Evanston, IL.
- Scott, R.W., 2007, Calibration of the Albian/Cenomanian boundary by ammonite biostratigraphy: U.S. Western Interior. *Acta Geologica Sinica*, **81**: 940–948.
- Scott, R.W., 2009, Uppermost Albian biostratigraphy and chronostratigraphy. *Carnets de Géologie/Notebooks on Geology, Article*, **2009** (03), 15.
- Scott, R.W., 2011. CRET1 Chronostratigraphic Database. Available from: <<http://precisionstratigraphy.com>> .
- Scott, R.W., Oboh-Ikuenobe, F.E., Benson, D.G., and Holbrook, J.M., 2009, Numerical age calibration of the Albian/Cenomanian boundary. *Stratigraphy*, **6**: 17–32.
- Selby, D., Mutterlose, J., and Condon, D.J., 2009, U-Pb and Re-Os Geochronology of the Aptian/Albian and Cenomanian/Turonian stage boundaries: implications for timescale calibration, osmium isotope seawater composition and Re-Os systematics in organic-rich sediments. *Chemical Geology*, **265**: 394–409.
- Séronie-Vivien, M., 1972, Contribution à l'étude de Sénonien en Aquitaine septentrionale, ses stratotypes: Coniacien, Santonien, Campanien. *Les Stratotypes Français*, **2**: 195.
- Sharland, P.R., Archer, R., Casey, D.M., Davies, R.B., Hall, S.H., Heward, A.P., et al., 2001, Arabian Plate Sequence Stratigraphy. *GeoArabia Special Publication*, **2**: 372.
- Sharland, P.R., Casey, D.M., Davies, R.B., Simmons, M.D., and Sutcliffe, O.E., 2004, Arabian Plate sequence stratigraphy. *GeoArabia: Middle East Petroleum Geosciences*, **9** (2), 199–214.
- Shimokawa, A., 2010, *Zircon U-Pb Geochronology of the Great Valley Group: Recalibrating the Lower Cretaceous Time Scale* (M.S. thesis). University of North Carolina at Chapel Hill. 46 p. [See also: Shimokawa, A., Coleman, D.S., Bralower, T.J., 2010. Recalibrating the Lower Cretaceous time scale with U-Pb zircon ages from the Great Valley Group. *Geological Society of America Abstracts with Programs*. Vol. **42**, No. 5, p. 393. <https://gsa.confex.com/gsa/2010AM/webprogram/Paper182413.html>].
- Shipboard Scientific Party, 1998, Site 1049: paleomagnetism section (authored by Ogg, J.G., Bardot, L., and Foster, J.). In: *Proceedings Ocean Drilling Program, Initial Reports*, **171B**. pp. 70–75.
- Shipboard Scientific Party, 2004, Explanatory notes: biostratigraphy. In: *Proceedings of the Ocean Drilling Program, Initial Reports*, **207**. Available from: <http://www-odp.tamu.edu/publications/207_IR> .
- Siewert, S.E., 2011, *Integrating ⁴⁰Ar/³⁹Ar, U-Pb and Astronomical Clocks in the Cretaceous Niobrara Formation*. M.S. thesis, University of Wisconsin at Madison, 74 pp.
- Sigal, J., 1977, Essai de zonation du Crétacé méditerranéen à l'aide des foraminifères planctoniques. *Géologie Méditerranéenne*, **4/2**: 99–108.
- Sikora, P., and Bergen, J., 2004, Lower Cretaceous Biostratigraphy of Ontong Java sites from DSDP Leg 30 and ODP Leg 192. In Fitton, J.G., Mahoney, J.J., Wallace, P.J., and Sanders, A.D. (eds), *Origin and Evolution of the Ontong Java Plateau*. *Geological Society of London, Special Publication*, **229**: 83–111.
- Simmons, M.D., Sharland, P.R., Casey, D.M., Davies, R.B., and Sutcliffe, O.E., 2007, Arabian Plate sequence stratigraphy: potential implications for global chronostratigraphy. *GeoArabia: Middle East Petroleum Geosciences*, **12** (4), 101–130.
- Simmons, M.S., Miller, K.G., Ray, D.C., Davies, A., van Buchem, F.S.P., and Gréselle, B., 2020, Chapter 13 - Phanerozoic eustasy. In Gradstein, F.M., Ogg, J.G., Schmitz, M.D., and Ogg, G.M. (eds), *The Geologic Time Scale 2020*. Vol. **1** (this book). Elsevier, Boston, MA.
- Sinninghe Damsté, J.S., Muyzer, G., Abbas, B., Rampen, S.W., Massé, G., Allard, W.G., et al., 2004, The rise of rhizosolenid diatoms. *Science*, **304**: 584–587.
- Smelror, M., Kelley, S.R.A., Dypvik, H., Mørk, A., Nagy, J., and Tsikalas, F., 2001, Mjølner (Barents Sea) meteorite impact ejecta offers a Volgian–Ryazanian boundary marker. *Newsletters on Stratigraphy*, **38**: 129–140.
- Smith, W., 1815. A Delineation of the Strata of England and Wales, With Parts of Scotland.
- Speijer, R.P., Pälke, H., Hollis, C.J., Hooker, J.J., and Ogg, J.G., 2020, Chapter 28 – The Paleogene Period. In Gradstein, F.M., Ogg, J.G., Schmitz, M.D., and Ogg, G.M. (eds), *The Geologic Time Scale 2020*. Vol. **2** (this book). Elsevier, Boston, MA.
- Speranza, F., Satolli, S., Mattioli, E., and Calamita, F., 2005, Magnetic stratigraphy of Kimmeridgian–Aptian sections from Umbria-Marche (Italy): new details on the M-polarity sequence. *Journal of Geophysical Research*, **110**: B12109, <https://doi.org/10.1029/2005JB003884>.
- Sprenger, A., and ten Kate, W.G., 1993, Orbital forcing of calcilutite-marl cycles in southeast Spain and an estimate for the duration of the Berriasian Stage. *Geological Society of America Bulletin*, **105**: 807–818.
- Sprovieri, M., Coccioni, R., Lirer, F., Pelosi, N., and Lozar, F., 2006, Orbital tuning of a lower Cretaceous composite record (Maiolica Formation, central Italy). *Paleoceanography*, **21**: PA4212, <https://doi.org/10.1029/2005PA001224>.
- Sprovieri, M., Sabatino, N., Pelosi, N., Batenburg, S.J., Coccioni, R., Iavarone, M., et al., 2013, Late Cretaceous orbitally-paced carbon isotope stratigraphy from the Bottaccione Gorge (Italy). *Palaeogeography, Palaeoclimatology, Palaeoecology*, **379–380**: 81–94.
- Steuber, T., Scott, R.W., Mitchell, S.F., and Skelton, P.S., 2016, Part N, revised, volume 1, Chapter 26C: stratigraphy and diversity dynamics of Jurassic–Cretaceous Hippuritida (rudist bivalves). *Treatise Online*, **81**: 1–17 7 g., 1 table.
- Stewart, K., Turner, S., Kelley, S., Hawkesworth, C., Kirstein, L., and Mantovani, M., 1996, 3-D ⁴⁰Ar–³⁹Ar geochronology in the Parana continental flood basalt province. *Earth and Planetary Science Letters*, **143**: 95–109.
- Stoll, H.M., and Schrag, D.P., 2000, High-resolution stable isotope records from the Upper Cretaceous rocks of Italy and Spain: Glacial episodes in a greenhouse planet? *Geological Society of America Bulletin*, **112**: 308–319.
- Strasser, A., Hillgartner, H., and Pasquier, J.B., 2004, Cyclostratigraphic timing of sedimentary processes: an example from the Berriasian of the Swiss and French Jura Mountains. In D'Argenio, B., Fischer, A.G., Premoli Silva, I., Weissert, H., and Ferreri, V. (eds), *Cyclostratigraphy: Approaches and Case Histories*. *SEPM Special Publication*, **81**: 135–151.

- Stratotype Albien. Muséum national d'Histoire naturelle. In Colleté, C. (ed), Paris: Biotope, Meze, BRGM OrléansBiotope, Meze, BRGM Orléans. Paris, 332 p.
- Subcommission on Cretaceous Stratigraphy, 2009. Annual Report 2009. 12 p. Available from: <http://www2.mnhn.fr/hdt203/media/ISCS/ICS2009_Report_Creta.pdf>.
- Surlyk, F., 1984, The Maastrichtian Stage in NW Europe and its brachiopod zonation. *Bulletin of the Geological Society of Denmark*, **33**: 217–223.
- Swisher III, C.C., Wang, Y.Q., Wang, X.L., Xu, X., and Wang, Y., 1999, Cretaceous age for the feathered dinosaurs of Liaoning, China. *Nature*, **400**: 58–61.
- Takashima, R., Nishi, H., Yamanaka, T., Orihashi, Y., Tsujino, Y., Quidelleur, X., et al., 2019, Establishment of Upper Cretaceous bio- and carbon-isotope stratigraphy in the northwest Pacific Ocean and radiometric ages around the Albian/Cenomanian, Coniacian/Santonian and Santonian/Campanian boundaries. *Newsletters on Stratigraphy*, <https://doi.org/10.1127/nos/2019/0472>.
- Takashima, R., Nishi, H., Hayashi, K., Okada, H., Kawahata, H., Yamanaka, T., Fernando, A.G., and Mampuku, M., 2009, Litho-, bio- and chemostratigraphy across the Cenomanian–Turonian boundary (OAE 2) in the Vocontian Basin of southeastern France. *Palaeogeography, Palaeoclimatology, Palaeoecology*, **273**: 61–74.
- Tarduno, J.A., 1990, A brief reversed polarity interval during the Cretaceous Normal Polarity Superchron. *Geology*, **18**: 638–686.
- Tarduno, J.A., Sliter, W.V., Bralower, T.J., McWilliams, M., Premoli-Silva, I., and Ogg, J.G., 1989, M-sequence reversals recorded in DSDP Sediment Cores from the Western Mid-Pacific Mountains and Magellan Rise. *Geological Society of America Bulletin*, **101**: 1306–1319.
- Tarduno, J.A., Sliter, W.V., Kroenke, L., Leckie, R.M., Mayer, H., Mahoney, J.J., et al., 1991, Rapid formation of Ontong Java Plateau by Aptian mantle volcanism. *Science*, **254**: 399–403.
- Tarduno, J.A., Lowrie, W., Sliter, W.V., Bralower, T.J., and Heller, F., 1992, Reversed polarity characteristic magnetizations in the Albian Contessa Section, Umbrian Apennines, Italy: implications for the existence of a Mid-Cretaceous Mixed Polarity Interval. *Journal of Geophysical Research*, **97** (B1), 241–271.
- Tavera, J.M., Aguado, R., Company, M., Oloriz, F., 1994. Integrated biostratigraphy of the Durangites and Jacobi zones (J/K boundary) at the Puerto Escano section in southern Spain (Province of Cordoba). In: Cariou, E., Hantzpergue, P. (eds), *Third International Symposium on Jurassic Stratigraphy, Poitiers, France, 22–29 September 1991*. Geobios, Mémoire Spécial, **17** (1): 469–476.
- Thierry, J., 1998, Ammonites. Columns for Jurassic chart of Mesozoic and Cenozoic sequence chronostratigraphic framework of European basins, by Hardenbol, J., Thierry, J., Farley, M.B., Jacquin, T., de Graciansky, P.-C., and Vail, P.R. (coordinators). In de Graciansky, P.-C., Hardenbol, J., Jacquin, T., and Vail, P.R. (eds), *Mesozoic–Cenozoic Sequence Stratigraphy of European Basins. SEPM Special Publication*, **60**: 776–777.
- Thibault, N., Husson, D., Harlou, R., Gardin, S., Galbrun, B., Huret, E., et al., 2012, Astronomical calibration of upper Campanian–Maastrichtian carbon isotope events and calcareous plankton biostratigraphy in the Indian Ocean (ODP Hole 762C): implication for the age of the Campanian–Maastrichtian boundary. *Palaeogeography, Palaeoclimatology, Palaeoecology*, **377–378**: 52–71.
- Thibault, N., Jarvis, I., Voigt, S., Gale, A.S., Attree, K., and Jenkyns, H. C., 2016, Astronomical calibration and global correlation of the Santonian (Cretaceous) based on the marine carbon isotope record. *Paleoceanography* article #PA002941, **31**: 847–865, <https://doi.org/10.1002/2016PA002941>.
- Thieuloy, J.-P., 1977, La zone à Callidiscus du Valanginien supérieur vocontien (Sud-Est de la France). Lithostratigraphie, ammonitofaune, limite Valanginien-Hauterivien, corrélations. *Géologie Alpine*, **53**: 83–143.
- Thurmann, J., 1836, Lettre à ME de Beaumont. *Bulletin de la société géologique de France, Serie I*, **7**: 207–211.
- Tröger, K.-A., and Kennedy, W.J., 1996, The Cenomanian Stage. *Bulletin de l'Institut Royal des Sciences Naturelles de Belgique, Sciences de la Terre*, **66** (Suppl.), 57–68.
- Tsikalas, F., 2005. Mjøltnir Impact Crater. Geophysics Research Group, Department of Geology, University of Oslo. Available from: <<http://folk.uio.no/ftsikala/mjolnir/>>.
- Tur, N.A., Smirnov, J.P., and Huber, B.T., 2001, Late Albian–Coniacian planktic foraminifera and biostratigraphy of the northeastern Caucasus. *Cretaceous Research*, **22**: 719–734.
- van Buchem, F.S.P., Simmons, M.D., Droste, H.J., and Davies, R.B., 2011, Late Aptian to Turonian stratigraphy of the eastern Arabian Plate – depositional sequences and lithostratigraphic nomenclature. *Petroleum Geosciences*, **17**: 211–222.
- VandenBerg, J., Klootwijk, C.T., and Wonders, A.A.H., 1978, Late Mesozoic and Cenozoic movements of the Italian peninsula: further paleomagnetic data from the Umbrian sequence. *Geological Society of America Bulletin*, **89**: 133–150.
- VandenBerg, J., and Wonders, A.A.H., 1980, Paleomagnetism of Late Mesozoic pelagic limestones from the Southern Alps. *Journal of Geophysical Research*, **85**: 3623–3627.
- van Hinte, J.E., 1965, The type Campanian and its planktonic Foraminifera. *Proceedings of the Koninklijke Nederlandse Akademie van Wetenschappen, Series B*, **68**: 8–28.
- Vennari, V.V., Lescano, M., Naipauer, M., Aguirre-Urreta, B., Concheyro, A., Schaltegger, U., et al., 2014, New constraints on the Jurassic–Cretaceous boundary in the High Andes using high-precision U–Pb data. *Gondwana Research*, **26**: 374–385.
- Voigt, S., and Schonfeld, J., 2010, Cyclostratigraphy of the reference section for the Cretaceous white chalk of northern Germany, Lägerdorf–Kronsmoor – a late Campanian–early Maastrichtian orbital time scale. *Palaeogeography, Palaeoclimatology, Palaeoecology*, **287**: 67–80.
- Voigt, S., Erbacher, J., Mutterlose, J., Weiss, W., Westerhold, T., Wiese, F., et al., 2008, The Cenomanian – Turonian of the Wunstorf section – (North Germany): global stratigraphic reference section and new orbital time scale for Oceanic Anoxic Event 2. *Newsletters on Stratigraphy*, **43**: 65–89.
- Voigt, S., Friedrich, O., Norris, R.D., and Schönfeld, J., 2010, Campanian–Maastrichtian carbon isotope stratigraphy: shelf-ocean correlation between the European shelf sea and the tropical Pacific Ocean. *Newsletters on Stratigraphy*, **44**: 57–72.
- Voigt, S., Gale, A.S., Jung, C., and Jenkyns, H.C., 2012, Global correlation of Upper Campanian–Maastrichtian successions using carbon-isotope stratigraphy: development of a new Maastrichtian timescale. *Newsletters on Stratigraphy*, **45**: 25–53.
- von Salis, K., 1998, Calcareous nannofossils. Columns for Jurassic chart of Mesozoic and Cenozoic sequence chronostratigraphic framework

- of European basins, by Hardenbol, J., Thierry, J., Farley, M.B., Jacquin, T., de Graciansky, P.-C., and Vail, P.R. (coordinators). In de Graciansky, P.-C., Hardenbol, J., Jacquin, T., and Vail, P.R. (eds), *Mesozoic-Cenozoic Sequence Stratigraphy of European Basins. SEPM Special Publication*, **60**: 763–781.
- Wagerich, M., 2012, “OAE3”-regional Atlantic organic carbon burial during the Coniacian-Santonian. *Climate of the Past*, **8**: 1447–1455, <https://doi.org/10.5194/cp-8-1447-2012>.
- Walaszczyk, I., and Cobban, W.A., 2007, Inoceramid fauna and biostratigraphy of the upper Middle Coniacian–lower Middle Santonian of the Pueblo Section (SE Colorado, US Western Interior). *Cretaceous Research*, **28**: 132–142.
- Walaszczyk, I., and Cobban, W.A., 2016, Inoceramid bivalves and biostratigraphy of the upper Albian and Cenomanian of the United States Western Interior Basin. *Cretaceous Research*, **59**: 30–68.
- Walaszczyk, I., and Wood, C.J., 1998, Inoceramid and biostratigraphy at the Turonian/Coniacian boundary; based on the Salzgitter-Salder Quarry, Lower Saxony, Germany, and the Słupia Nadbrzeżna section, Central Poland. *Acta Geologica Polonica*, **48**: 395–434.
- Walaszczyk, I., and Wood, C.J., 2018, Inoceramid bivalves from the Coniacian (Upper Cretaceous) of the Staffhorst shaft (Lower Saxony, Germany) – stratigraphical significance of a unique section. *Cretaceous Research*, **87**: 226–240, <http://dx.doi.org/10.1016/j.cretres.2017.07.001>.
- Walaszczyk, I., Odin, G.S., and Dhondt, A.V., 2002, Inoceramids from the Upper Campanian and Lower Maastrichtian of the Tercis section (SW France), the Global Stratotype Section and Point for the Campanian – Maastrichtian boundary; taxonomy, biostratigraphy and correlation potential. *Acta Geologica Polonica*, **52**: 269–305.
- Walaszczyk, I., Wood, C.J., Lees, J.A., Peryt, D., Voigt, S., and Wiese, F., 2010, The Salzgitter-Salder Quarry (Lower Saxony, Germany) and Słupia Nadbrzeżna river cliff section (central Poland): a proposed candidate composite Global Boundary Stratotype Section and Point for the base of the Coniacian Stage (Upper Cretaceous). *Acta Geologica Polonica*, **60**: 445–477.
- Walaszczyk, I., Dubicka, Z., Olszewska-Nejbert, D., and Remin, Z., 2016, Integrated biostratigraphy of the Santonian through Maastrichtian (Upper Cretaceous) of Poland. *Acta Geologica Polonica*, **66**: 313–350.
- Walaszczyk, I., and Cobban, W.A., 2000, Inoceramid faunas and biostratigraphy of the Upper Turonian – Lower Coniacian of the Western Interior of the United States. *Special Papers in Palaeontology*, **64**: 1–118.
- Walaszczyk, I., Cobban, W.A., and Harries, P.J., 2001, Inoceramids and inoceramid biostratigraphy of the Campanian and Maastrichtian of the United States Western Interior Basin. *Revue de Paléobiologie*, **20**: 117–234.
- Wang, T.T., Ramezani, J., Wang, C.S., Wu, H.C., He, H.Y., and Bowring, S.A., 2016, High-precision U–Pb geochronologic constraints on the Late Cretaceous terrestrial cyclostratigraphy and geomagnetic polarity from the Songliao Basin, Northeast China. *Earth and Planetary Science Letters*, **446**: 37–44.
- Weissert, H., and Bréheret, J.G., 1991, A carbonate-isotope record from Aptian-Albian sediments of the Vocontian Trough (SE France). *Bulletin de la Société géologique de France*, **162**: 1133–1140.
- Weissert, H., and Lini, A., 1991, Ice Age interludes during the time of Cretaceous greenhouse climate? In Muller, D.W., McKenzie, J.A., and Weissert, H. (eds), *Controversies in Modern Geology*. London: Academic Press, 173–191.
- Weissert, H., Lini, A., Föllmi, K.B., and Kuhn, O., 1998, Correlation of Early Cretaceous carbon isotope stratigraphy and platform drowning events: a possible link? *Palaeogeography, Palaeoclimatology, Palaeoecology*, **137**: 189–203.
- Wendler, I., 2013, A critical evaluation of carbon isotope stratigraphy and biostratigraphic implications for Late Cretaceous global correlation. *Earth Science Reviews*, **126**: 116–146.
- Wendler, I., Wendler, J., Grafe, K.-U., Lehmann, J., and Willems, H., 2009, Turonian to Santonian carbon isotope data from the Tethys Himalaya, southern Tibet. *Cretaceous Research*, **30**: 961–979.
- Wendler, I., Willems, H., Grafe, K.-U., Ding, L., and Luo, H., 2011, Upper Cretaceous inter-hemispheric correlation between the Southern Tethys and the Boreal: chemo- and biostratigraphy and paleoclimatic reconstructions from a new section in the Tethys Himalaya, S-Tibet. *Newsletters on Stratigraphy*, **44/2**: 137–171.
- Wierzbowski, H., Anczkiewicz, R., Pawlak, J., Rogov, M.A., and Kuznetsov, A.B., 2017, Revised Middle–Upper Jurassic strontium isotope stratigraphy. *Chemical Geology*, **466**: 239–255.
- Wiese, F., 1999, Stable isotope data (^{13}C , ^{18}O) from the Middle and Upper Turonian (Upper Cretaceous) of Liencres (Cantabria, northern Spain) with a comparison to northern Germany (Söhle & Salzgitter-Salder). *Newsletters on Stratigraphy*, **37**: 37–62.
- Wiese, F., and Kaplan, U., 2001, The potential of the Lengerich section (Münster Basin, northern Germany) as a possible candidate Global boundary Stratotype Section and Point (GSSP) for the Middle/Upper Turonian boundary. *Cretaceous Research*, **22**: 549–563.
- Wignall, P.B., 2001, Large igneous provinces and mass extinctions. *Earth-Science Reviews*, **53**: 1–33.
- Wilson, P.A., Norris, R.D., and Cooper, M.J., 2002, Testing the Cretaceous greenhouse hypothesis using glassy foraminiferal calcite from the core of the Turonian tropics on Demerara Rise. *Geology*, **30**: 607–610.
- Wimbledon, W.A.P., 2017, Developments with fixing a Tithonian/Berriasian (J/K) boundary. *Volumina Jurassica*, **XV**: 181–186.
- Wimbledon, W.A.P., Casellato, C.E., Reháková, D., Bulot, L.G., Erba, E., Gardin, S., et al., 2011, Fixing a basal Berriasian and Jurassic-Cretaceous (J-K) boundary – is there perhaps some light at the end of the tunnel? *Rivista Italiana di Paleontologia e Stratigrafia*, **117**: 295–307.
- Wimbledon, W.A.P., et al., 2019, Proposal of Tré Maroua as the GSSP for the Berriasian Stage (Cretaceous System), Made on Behalf of the Berriasian Working Group of the International Subcommittee on Cretaceous Stratigraphy (ICS). 81 p. 24 Figures.
- Wimbledon, W.A.P., Reháková, D., Svobodová, A., Schnabl, P., Pruner, P., Elbra, T., et al., 2020, Fixing a J/K boundary: a comparative account of key Tithonian-Berriasian profiles in the departments of Drôme and Hautes-Alpes, France. *Geologica Carpathica*, **71**: 24–46.
- Wissler, L., Weissert, H., Buoncunto, F.P., Ferreri, V., and D’Argenio, B., 2004, Calibration of the Early Cretaceous time scale; a combined chemostratigraphic and cyclostratigraphic approach to the Barremian–Aptian interval, Campania Apennines and Southern Alps (Italy). In D’Argenio, B., Fischer, A.G., Premoli Silva, I., Weissert, H., and Ferreri, V. (eds), *Cyclostratigraphy: Approaches and Case Histories. SEPM Special Publication*, **81**: 123–133.
- Wonders, A.A.H., 1980, Middle and Late Cretaceous Planktonic Foraminifera of the Western Mediterranean Area (Doctoral dissertation). Utrecht University.
- Woodburne, M.O., 2004, *Late Cretaceous and Cenozoic Mammals of North America: Biostratigraphy and Geochronology*. New York: Columbia University Press 376 p.

- Wortmann, U.G., Herrle, J.O., and Weissert, H., 2004, Altered carbon cycling and coupled changes in Early Cretaceous weathering patterns: evidence from integrated carbon isotope and sandstone records of the western Tethys. *Earth and Planetary Science Letters*, **220**: 69–82.
- Wright, C.W., Kennedy, W.J., and Gale, A.S., 2017, The Ammonoidea of the Lower Chalk. Part 7. *Palaeontographical Society (Monograph)*, **171**: 461–571.
- Wu, H.C., Zhang, S.H., Hinnov, L.A., Jiang, G.Q., Yang, T.S., Li, H.H., et al., 2014, Cyclostratigraphy and orbital tuning of the terrestrial Upper Santonian-Lower Danian in Songliao Basin, northeastern China. *Earth and Planetary Science Letters*, **407**: 82–95.
- Wu, H.C., Hinnov, L.A., Zhang, S.H., Jiang, G.Q., Chu, R., Yang, T.S., et al., 2020. Continental geological evidence for two Solar System chaotic events in the Late Cretaceous. *Proceedings of the National Academy of Sciences (USA)*, in press.
- Young, J.Y., Gale, A.S., Knight, R.I., and Smith, A.B. (eds), 2010. *Fossils of the Gault Clay*. p. 342.
- Zaborski, P.M.P., 1985, Upper Cretaceous ammonites from the Calabar region, south-east Nigeria. *Bulletin of the British Museum (Natural History), Geology Series*, **39**: 72.
- Zakharov, V.A., Bown, P., and Rawson, P.F., 1996, The Berriasian Stage and the Jurassic-Cretaceous boundary. *Bulletin de l'Institut Royal des Sciences Naturelles de Belgique, Sciences de la Terre*, **66** (Suppl.), 7–10.
- Zeebe, R.E., 2017, Numerical solutions for the orbital motion of the solar system over the past 100 Myr: limits and new results. *The Astronomical Journal*, **154** (5), 193.
- Zhang, Y., Ogg, J.G., Minguéz, D.A., Hounslow, M., Olausen, S., Gradstein, F.M., and Esmeray-Senlet, S., 2019, Magnetostratigraphy of U/Pb-dated boreholes in Svalbard, Norway, implies that the Barremian–Aptian Boundary (beginning of Chron M0r) is 121.2 ± 0.4 Ma. In: AGU Annual Meeting (San Francisco, 9–13 December 2019). #GP44A-06. <<https://agu.confex.com/agu/fm19/meetingapp.cgi/Paper/577991>> .
- Zheng, X.-Y., Jenkyns, H.C., Gale, A.S., Henderson, G., and Ward, D.J., 2013, Nd-isotope evidence for changes in ocean circulation associated with transient cooling in the European shelf sea during OAE 2 (Cenomanian–Turonian). *Earth and Planetary Science Letters*, **375**: 338–348.
- Zheng, X.-Y., Jenkyns, H.C., Gale, A.S., Ward, D.J., and Henderson, G.M., 2016, Recurrent climate-driven reorganizations of ocean circulation in the European epicontinental sea during the mid-Cretaceous; evidence from Nd isotopes. *Geology*, **44**: 151–154.